

Volume II - Final Report

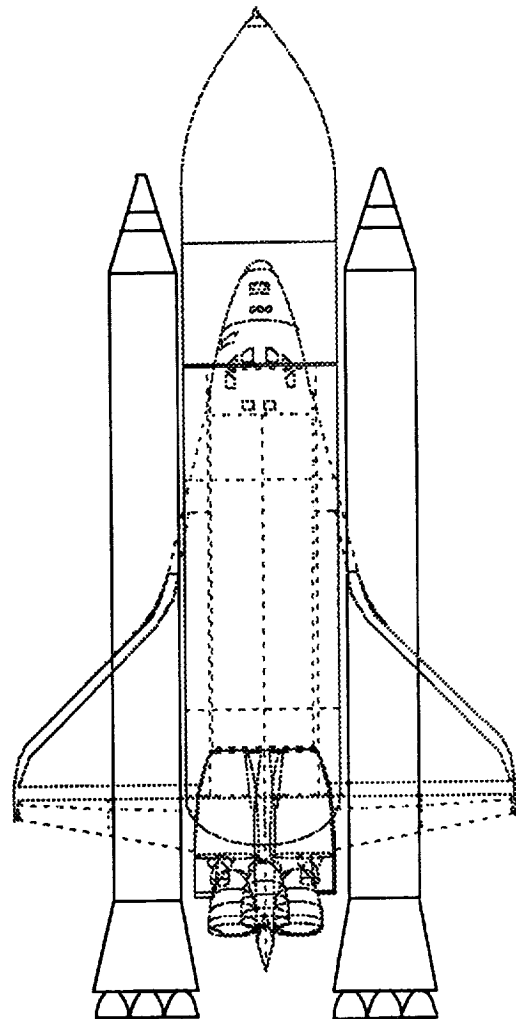
February 1990

Addendum 1

Liquid Rocket Booster (LRB) for the Space Transportation System (STS) Systems Study

(0) (2)
CN22
TURNER J/PUBLICATION
MARSHALL SPACE FLIGHT CENTER
HUNTSVILLE AL.

RETURN ADDRESS CN220



MARTIN MARIETTA
MANNED SPACE SYSTEMS

(NASA-CR-184128) LIQUID ROCKET BOOSTER
(LRB) FOR THE SPACE TRANSPORTATION SYSTEM
(STS) SYSTEMS STUDY. VOLUME 2: ADDENDUM 1
Final Report (Martin Marietta Aerospace)
100 p

N91-22366

Unclas
CSCL 21H G3/20 0002650

FOREWORD

This document provides the Final Report, Volume II, Addendum 1, for the Liquid Rocket Booster (LRB) for Space Transportation System (STS) Study performed under the NASA Contract NAS8-37136. The report was prepared by Manned Space Systems, Martin Marietta Corporation, New Orleans, Louisiana, for the NASA/Marshall Space Flight Center (MSFC).

The MSFC Contracting Officer Representative is Uwe Hueter. The Martin Marietta Study Manager is Thomas B. Mobley.

ACRONYMS AND ABBREVIATIONS

ACC	Aft Cargo Carrier
ALS	Advanced Launch System
ARS	Advanced Recovery System
BA	Booster Acceleration
BRM	Booster Reference Mission
C_dA	Coefficient of Drag Area
cg	Center of Gravity
DDT&E	Design, Development, Test , and Evaluation
ET	External Tank
GO2	Gaseous Oxygen
GR-EP	Graphite-Epoxy
GLOW	Gross Liftoff Weight
HABP	Hypersonic Arbitrary Body Program
High Q	High Dynamic Pressure
ICD	Interface Control Document
IVBC	Integrated Vehicle Baseline Configuration
kips	Thousand Pounds per Second
LCC	Life Cycle Cost
LH2	Liquid Helium
LO2	Liquid Oxygen
LRB	Liquid Rocket Booster
MAX	Peak Dynamic Loads Not Time Consistent
MLP	Mobile Launch Platform
NASA	National Aeronautics and Space Administration
NASTRAN	National Aeronautics and Space Administration Structural Analysis
NCFI	North Carolina Foam Industries
P/A	Propulsion Avionics
PAL	Protuberance Air Loads
ROM	Rough Order of Magnitude
RP-1	Kerosene
RSRB	Redesigned Solid Rocket Booster
SRB	Solid Rocket Booster
SSME	Space Shuttle Main Engine
STA	Structural Test Article

STBE	Space Transportation Booster Engine
STS	Space Transportation System
TDDP	Trajectory Design Data Package
TPS	Thermal Protection System
TWT	Transonic Wind Tunnel Test
VAB	Vehicle Assembly Building

TABLE OF CONTENTS

<u>Section</u>	<u>Title</u>	<u>Page</u>
Task 1 -	External Tank Impacts for the Optimum STS LO2/LH2 Liquid Rocket Booster	
1.0	Study Overview.....	1-1
1.1	Study Objectives	1-1
1.2	ET Impacts Results Summary.....	1-1
2.0	STS Configuration With LO2/LH2 Boosters.....	1-4
2.1	General Arrangement.....	1-4
2.2	Mass Properties.....	1.4
2.3	Vehicle Performance.....	1.10
3.0	Loads and Dynamic Analysis.....	1-10
3.1	Rigid Body ET Interface Loads-Ultimate	1-10
3.2	Transient Response Analysis of LO2/LH2 LRB.....	1-14
3.3	Transient Loads Results.....	1-18
4.0	Stress Analysis.....	1-21
4.1	ET Loads	1-21
4.2	Assessment Methodology.....	1-21
4.3	Prelaunch Assessment Results	1-23
4.4	Liftoff Assessment Results	1-23
4.5	Max Booster Acceleration Assessment Results	1-28
4.6	Additional Assessment Results.....	1-28
4.7	ET Assessment Conclusions	1-30
4.8	Cryogenic Shrinkage at the Aft ET Attachment	1-30
5.0	Aerodynamic Impacts	1-33
5.1	Shockwave Impingement.....	1-33
5.2	Future Wind Tunnel Work.....	1-36
6.0	Thermal Impacts on ET	1-36
7.0	Cost Impacts.....	1-36
Task 2 -	Recoverable Propulsion Avionics Module for a LO2/LH2 Liquid Rocket Booster Using Modified Space Shuttle Main Engines (SSME-35)	
1.0	Study Overview.....	2-1

<u>Section</u>	<u>Title</u>	<u>Page</u>
1.1	Background.....	2-1
1.2	Groundrules and Assumptions.....	2-1
1.3	Study Results Summary	2-1
2.0	P/A Module Configuration.....	2-2
2.1	General Arrangement.....	2-2
2.2	Structural Details.....	2-2
2.2.1	Holddown Loads and Fittings.....	2-2
2.2.2	Thrust Beams.....	2-6
2.2.3	Nose Cap	2-10
2.2.4	Shell Details	2-10
2.3	P/A Module Interfaces.....	2-14
2.3.1	LRB Interfaces	2-14
2.3.2	Ground Interfaces.....	2-18
2.4	Recovery System	2-18
3.0	Vehicle Analysis	2-18
3.1	Aerodynamic Analysis	2-18
3.1.1	Aerodynamic Characteristics	2-18
3.1.2	Aerodynamic Loads	2-21
3.2	Aerothermal Analysis.....	2-21
3.3	Thermal Analysis	2-30
3.4	Recovery.....	2-30
3.5	Mass Properties	2-33
3.5.1	LRB P/A Module Weight Statement.....	2-33
3.5.2	LRB Weight Impact	2-35
3.6	Flight Performance	2-35
4.0	Cost Analysis.....	2-37
4.1	Ground Rules, Assumptions, and Results.....	2-37
4.2	Recovery Cost Sensitivities.....	2-45
4.2.1	STE Cost Growth Sensitivities.....	2-45
4.2.2	LCC Sensitivity Service Life	2-47
4.2.3	LCC Sensitivity Refurbishment Factors	2-47
4.2.4	Attrition Sensitivity	2-47
4.3	Cost Summary	2-49

FIGURES

<u>Figure</u>	<u>Title</u>	<u>Page</u>
Task 1 - External Tank Impacts for the Optimum STS LO2/LH2 Liquid Rocket Booster		
1.1-1	Shared NSTS/ALS LCC Estimates.....	1-2
2.1-1	STS Configuration with LO2/LH2 Boosters	1-6
2.1-2	STS Configuration with LO2/LH2 Boosters Dimensions	1-7
2.1-3	Pump-Fed Engine LO2/LH2 - Option 2.....	1-8
3.1-1	ET Interface Loads - Ultimate	1-13
3.2-1	LO2/LH2 LRB Base Bending Moment	1-17
3.2-2	LO2/LH2 LRB ET cg Z Deflection	1-17
3.3-1	ET LO2 Tank Bottom Pressure	1-20
4.2-1	ET Interface Loads Convention	1-22
4.4-1	Liftoff Booster Loads Comparison	1-24
4.4-2	Required 985 Frame Web Stiffeners	1-26
4.4-3	Liftoff Orbiter Loads Comparison	1-27
4.5-1	Max Booster Acceleration (BA) Loads Comparison.....	1-29
4.8-1	ET/LRB Aft Attachment Shrinkage and Interface Loads.....	1-31
4.8-2	LRB Math Model and Data	1-32
5.1-1	LO2/LH2 LRB Aerodynamic Impact.....	1-34
5.1-2	XY Plane ET Pressure Coefficient Distribution.....	1-35
6.0-1	Comparison of SRB vs LRB Heating.....	1-37
Task 2 - Recoverable Propulsion Avionics Module for a LO2/LH2 Liquid Rocket Booster Using Modified Space Shuttle Main Engines (SSME-35)		
2.1-1	LRB P/A Module General Arrangement	2-3
2.1-2	LRB P/A Module Overall Dimensions	2-4
2.1-3	LRB P/A Module Configuration	2-5
2.2.1-1	LRB P/A Module "X" Axis Holddown Loads	2-7
2.2.1-2	LRB P/A Module Holddown Longerons	2-8
2.2.2-1	LRB P/A Module Thrust Beams	2-9
2.2.3-1	Water Impact Loads	2-11
2.2.3-2	LRB P/A Module Nose Cap Geometry	2-12
2.2.4-1	LRB P/A Module Frame and Shell Details.....	2-13

<u>Figure</u>	<u>Title</u>	<u>Page</u>
2.3.1-1	LRB P/A Module Interfaces	2-15
2.3.1-2	Explosive Nut-Thruster Concept.....	2-16
2.4-1	Recovery System Arrangement	2-19
2.4-2	Flotation Bags.....	2-20
3.1.1-1	Stability Margin and Trim Conditions.....	2-22
3.1.1-2	Aerodynamic Characteristics-Normal Force.....	2-23
3.1.1-3	Aerodynamic Characteristics-Axial Force.....	2-23
3.1.1-4	Aerodynamic Characteristics-Pitching Moment	2-24
3.1.1-5	Aerodynamic Characteristics-L/D Ratio.....	2-24
3.1.2-1	Aerodynamic Loads	2-25
3.2-1	Ascent and Recovery Heating Rates- BP1	2-26
3.2-2	Ascent and Recovery Heating Rates-BP2A.....	2-27
3.2-3	Ascent and Recovery Heating Rates-BP3.....	2-28
3.2-4	Ascent and Recovery Heating Rates-BP4.....	2-29
3.3-1	Structural Parametric Sizing	2-31
3.3-2	TPS Thickness Requirement	2-32
3.4-1	Recovery Events Sequence	2-34
4.1-1	LRB LH2 Booster LCC.....	2-42
4.2.1-1	LRB LH2 Booster Expendable vs. Reusable LCC	2-46
4.2.2-1	Service Life.....	2-48
4.2.3-1	Refurbishment.....	2-48
4.2.4-1	Attrition of Reusable Hardware	2-50

TABLES

<u>Table</u>	<u>Title</u>	<u>Page</u>
Task 1 - External Tank Impacts for the Optimum STS LO2/LH2 Liquid Rocket Booster		
1.1-1	Potential ET Impacts.....	1-3
1.2-1	ET Impacts Summary	1-5
2.2-1	LO2/LH2 Pump-Fed Dry Weight Mass Properties	1-9
2.3-1	LRB Reference Mission Payload Requirement.....	1-11
2.3-2	LRB LO2/LH2 Pump-Fed Optimum Performance	1-12
3.2-1	Modeled LO2/LH2 Mass and cg	1-15
3.3-1	ET Loads Due to Launch Transient.....	1-19
 Task 2 - Recoverable Propulsion Avionics Module for a LO2/LH2 Liquid Rocket Booster Using Modified Space Shuttle Main Engines (SSME-35)		
2.4-1	Recovery System Characteristics	2-20
3.5.2-1	LRB P/A Module Weight Summary.....	2-36
3.6-1	LRB Reference Mission Payload Requirement.....	2-36
3.6-2	LO2/LH2 LRB Performance Summary with P/A Module	2-38
4.1-1	Programmatic Cost Groundrules and Assumptions	2-39
4.1-2	LH2 LRB P/A Module Recovery Assumptions.....	2-40
4.1-3	LH2 LRB P/A Module Average Unit Cost Per Flight.....	2-44

VOLUME II ADDENDUM 1

TASK 1

EXTERNAL TANK IMPACTS FOR THE OPTIMUM STS LO₂/LH₂ LIQUID ROCKET BOOSTER

1.0 STUDY OVERVIEW

1.1 STUDY OBJECTIVES

Part 3 of the Liquid Rocket Booster (LRB) study evaluated the potential of a common LRB design for use with both the Space Transportation System (STS) and the Advanced Launch System (ALS). A goal of the ALS program is to have a common Liquid Oxygen/Liquid Hydrogen (LO2/LH2) engine developed for both the ALS booster and the core stage. The LO2/LH2 LRB option for the STS was evaluated to identify potential LRB program cost reductions due to joint participation of NASA and the Air Force in the development of a common liquid rocket booster. The analysis results indicated that there was no significant life cycle cost (LCC) savings for the two programs as a result of the development of a common LO2/LH2 engine (option 3). The Design, Development, Test, and Evaluation (DDT&E) costs for the common engine showed potential up-front program cost savings (Figure 1.1-1). However, the scope of the analysis did not include the identification of impacts on the shuttle external tank (ET) due to the increased size of the LO2/LH2 LRB compared to the LO2/RP-1 option. Therefore, potential costs associated with ET modifications were not included in cost analyses.

The objectives of this task (LRB Study, Part 4, Task 1) was to identify the structural impacts to the ET, and to determine if any significant ET re-development costs are required as a result of the larger LO2/LH2 LRB. The potential ET impacts evaluated are presented in Table 1.1-1.

1.2 ET IMPACTS RESULTS SUMMARY

The two major concerns with the LO2/LH2 booster were the surface area and mass of the LO2 tank forward of the ET LRB attachment and the induced loads from the LRB LH2 tank cryo shrinking.

The 174 ft length of the LO2/LH2 LRB results in increased aero loads on the ET LO2 tank and increased ET/LRB forward attachment interface loads in the "y" direction. However, because the LO2/LH2 LRB gross liftoff weight (GLOW) is significantly less than the Solid Rocket Booster (SRB) and the LO2/RP-1, the required booster thrust is reduced. As a result of the reduced thrust, the "x" direction interface loads are reduced. This reduced "x" load provides additional margins for the forward ET/LRB fitting and crossbeam to help offset the increased "y" loads. A negative result of the decreased LRB thrust is that the ratio of Space Shuttle Main Engine (SSME) thrust to booster thrust

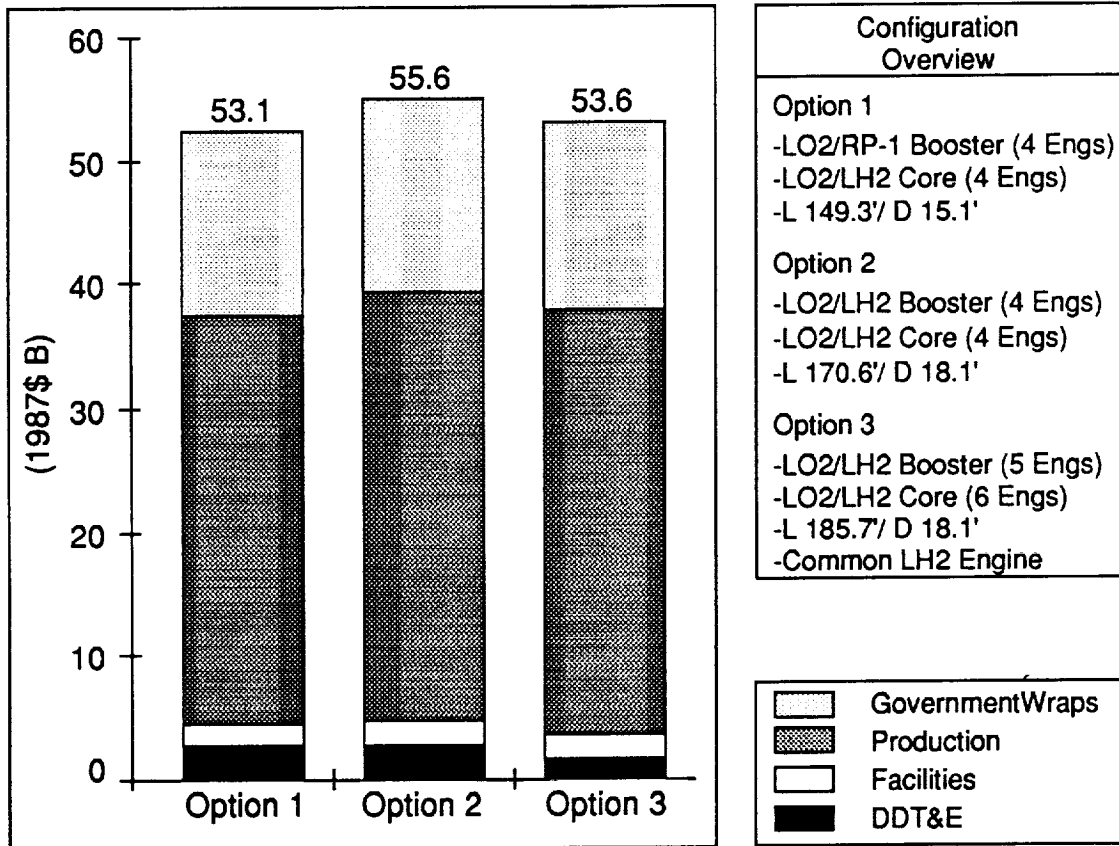


Figure 1.1-1 Shared NSTS/ALS LCC Estimates

Structure	2058 Ring Frame ET/LRB Aft Attach Hardware Fwd SRB Beam Intertank
Interfaces	LRB Attach Hardware Additional ET/LRB & ET/Orbiter Electrical Interfaces
TPS	Additional LO2 Tank TPS Attach Hardware TPS Range Safety System (Antenna & LSC) Protruberance TPS Debris Limits
Performance	Trajectory

(Reference - ET CEI CPT01-M09A NSTS 07700 Vol X)

Table 1.1-1 Potential ET Impacts

increases. The increased ratio of SSME thrust results in an increased compression load in the ET LH2 tank barrel panels.

The impacts of the increased aero loads and the change in ET/LRB/Orbiter interface loads is summarized in Table 1.2-1. These impacts will not require significant structural modifications to the ET design. No major structural test is necessary, and the ET redevelopment costs and increased unit costs as a result of the impacts are not considered a discriminator between the LO2/LH2 LRB and other propellant options.

2.0 STS CONFIGURATION WITH LO2/LH2 BOOSTERS

2.1 GENERAL ARRANGEMENT

The option 2 LO2/LH2 LRB concept evaluated in the STS/ALS commonality task (study Part 3) was redefined in more detail for this Part 4 task. The additional detail was required for loads and stress analyses to identify External Tank (ET) impacts resulting from the integration of the LO2/LH2 booster into the STS. As a result of the redefinition, the overall length of the LRB is 44 in. longer than the LO2/LH2 booster reported in the Final Report of March 1989. This growth in length is primarily due to a booster structural weight increase as a result of resizing the tank walls to accommodate buckling loads. The increased weight required additional propellants, and therefore a longer vehicle, to satisfy the LRB performance requirement.

Figure 2.1-1 shows the STS with LO2/LH2 boosters. Detail dimensions of tankage and reference stations are shown in Figure 2.1-2. X_T are ET reference stations and X_B are LRB booster reference stations. The overall length of the LRB of 2091 in. is 44 in. longer than the LO2/LH2 booster reported in the Phase I. The added length and tank volumes were the result of updating the configuration to the same level of detail as the LO2/RP-1 booster so that effects on the ET were calculated on a consistent basis. The LO2/LH2 engine used for this LRB analysis is shown in Figure 2.1-3

2.2 MASS PROPERTIES

Table 2.2-1 presents the LO2/LH2 LRB dry weight and center of gravity (cg) data. The LO2/LH2 booster weight is approximately 142,600 lb compared to the LO2/RP-1 dry weight of 123,300. Although the dry weight is higher for the LO2/LH2 booster, because of its increased diameter and length, the liftoff weight of the STS with the hydrogen booster is considerably less due to the low density of the hydrogen fuel. Gross

ET Design Condition	ET Impact	Design Change
Increased Air Loads on LO2 Tank	Load Exceedance on LO2 Tank Pressurization Line, Cable Trays, and Brackets	Extension of Protuberance Airload Ramps 16 ft Potential Redesign of Brackets
	Nose Cone and Intertank Venting Profile Change	Modification of LO2 Tank Pressurization Reference Potential Modification of Intertank Vent Ports
	LO2 Ogive Stability Margin of Safety Reduced to 0.46	None
Increased ET/LRB Forward Fitting "Y" Loads	Intertank Frame at Station 958 Margin of Safety Below Zero at Liftoff	Local Stiffening of Frame 958 Web
Increased Tension Load in LH2 Barrel Panels	Six Barrel Panels Margin of Safety Below Zero	Potential Stiffening of Barrel Panels

Table 1.2-1 ET Impacts Summary

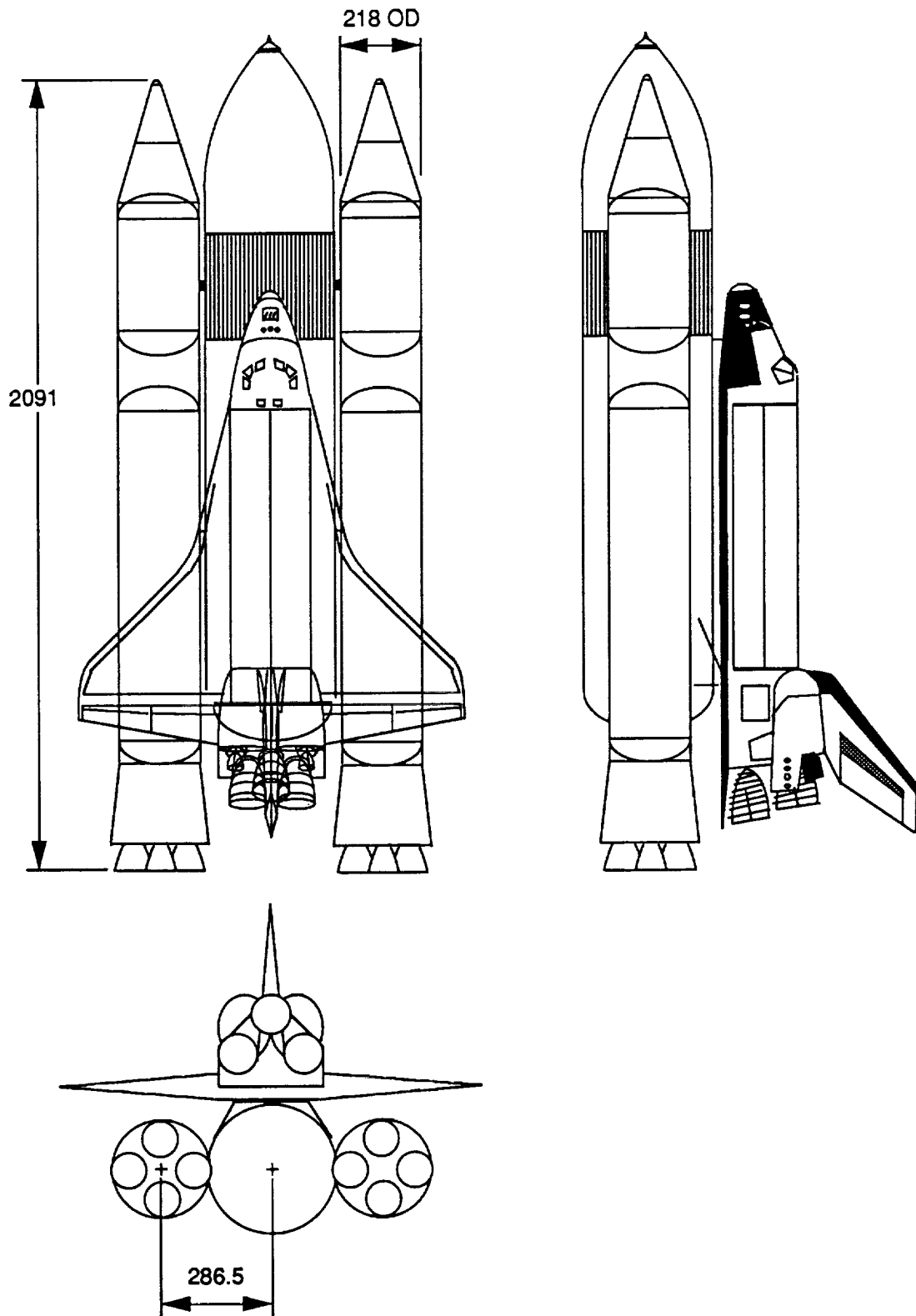
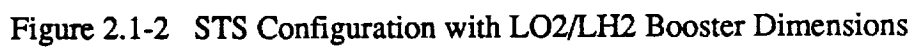


Figure 2.1-1 STS Configuration with LO₂ / LH₂ Boosters



	Booster Engine @	
	NPL	EPL
Mixture Ratio	6	6
Propellant Flow Rate (lbm/sec)	1242	1655
Vacuum Thrust (klbf)	527	644
Sea Level Thrust (klbf)	474	702
Vacuum Isp (sec)	424	420
Sea Level Isp (sec)	380	386
Chamber Pressure (psia)	1855	2473
Area Ratio	25.1	25
Exit Pressure (psia)	7.01	9.35
Weight (lbm)	5755	5755
Throat Diameter (in.)	14.13	14.13
Exit Diameter (in.)	70.8	71
Throttle Range 65-100%		

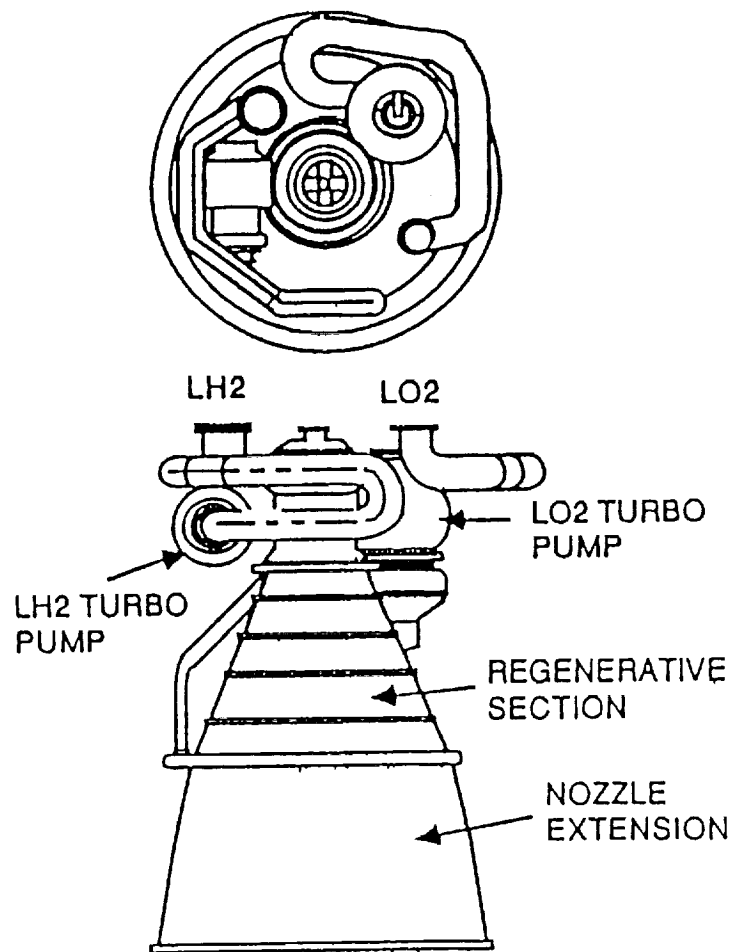


Figure 2.1-3 Pump-Fed Engine LO2/LH2 - Option 2

Item	Weight (lb)	Center of Gravity (in.)		
		X _T	Y	Z
Nose Cone	2,010	641.0	0.0	0.0
Forward Skirt	135	746.7	11.6	0.0
Forward Tank - LO2	15,610	898.3	0.0	0.0
Intertank	6,135	1145.0	0.0	0.0
Aft Tank - LH2	36,870	1724.7	0.4	0.2
Aft Skirt	28,220	2350.0	0.0	0.0
Structure	88,980	1712.0	0.8	0.0
Propulsion System	30,620	2275.0	0.0	0.0
TVC System	720	2440.0	0.0	0.0
Thermal/Acoustical Protection	3,405	1569.0	0.0	0.0
Separation System	1,225	1475.0	0.0	75.8
Avionics	3,180	1620.0	-8.0	8.0
I/F Attach	1,320	1520.0	110.0	0.0
Range Safety	150	1147.0	0.0	0.0
Contingency (10%)	12,960	1838.3	1.6	1.1
Total Dry Weight	142,560	1838.3	1.6	1.1

Table 2.2-1 LO2/LH2 Pump-Fed Dry Weight Mass Properties

liftoff weight (GLOW) for the LO2/LH2 LRB is 3,516,000 lb compared to 4,176,000 lb for the LO2/RP-1 booster. This reduced vehicle GLOW results in a lower overall vehicle thrust requirement and subsequently reduced thrust loads. The increased length of the vehicle and the lower fuel density moves the shuttle cg forward 200 inches at liftoff.

2.3 Vehicle Performance

LO2/LH2 propellant requirements and ascent flight simulation was updated for the redefined booster configuration. The modifications to the trajectory analyses included (1) updated booster weight estimates, (2) increased useable propellants, and (3) updated launch vehicle aerodynamics. Table 2.3-1 presents the LRB reference mission requirements and assumptions.

The POST computer program was used to simulate the STS/LRB ascent trajectory and optimize the amount of payload without exceeding STS trajectory constraints. Table 2.3-2 presents the trajectory and vehicle characteristics for the STS with LO2/LH2 pump-fed LRBs. Although the payload capability of the system is 470 lb below the required 70,500 lb, an additional iteration for propellant requirements was not needed to complete the ET impacts analyses.

3.0 LOADS AND DYNAMICS ANALYSIS

3.1 RIGID BODY ET INTERFACE LOADS - ULTIMATE

Preliminary estimation of launch loads used a simple rigid body loads calculation. Total vehicle mass and inertia matrices were obtained from the component mass and inertia data. This rigid vehicle model was subjected to estimates of vehicle thrust, and the resulting External Tank (ET) interface loads were calculated. Dynamic components of launch transient loads were obtained from prior ET Aft Cargo Carrier (ACC) launch analysis studies (1983). Rigid body loads were factored by 1.25 and the dynamic loads components by 1.4. These components were summed to give the ultimate loads shown in Figure 3.1-1. The factors used are consistent with ET design groundrules. The loads shown in Figure 3.1-1 were used for preliminary sizing of the structure.

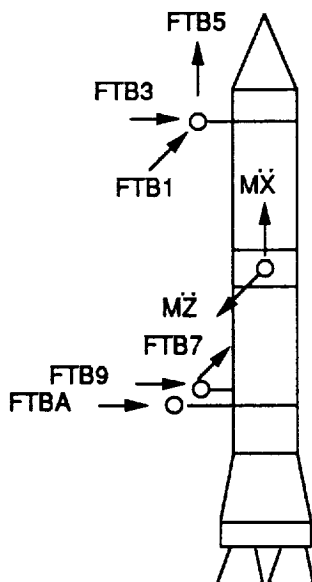
STS/LRB Must Provide 70,500 lb Payload for the Following Mission:	
Launch Site	ETR
Launch Month Mean Winds	Feb
Inclination (deg) (Direct Insertion)	28.5
Altitude (nm)	160
SSME Maximum Power Level (%)	104
Orbiter	OV-103
First Stage Design Criteria	
Dynamic Pressure Limit Dispersed (psf)	819
Dynamic Pressure At Staging Less Than (psf)	75
Q-alpha (psf-deg)	-3000
Maximum Axial acceleration (g)	3.0
Operator (lb)	0
Crew (size/days)	5/4
ET Usable Propellant (lb)	1,590,000
OV 103 MECO Weight (w/o Cargo)	208,229
ET Jettison Weight	74,821

Table 2.3-1 LRB Reference Mission Payload Requirement

Payload	70,029 lb
Manager's Reserve	-471 lb
Thrust / Weight @ T-0 sec	1.389
Gross Lift-Off Weight (GLOW)	3,516,402 lb
Max Dynamic Pressure	704 psf
Burn Time	129.7 sec
Coast Time	2.4 sec
Jettison Weight	297,874 lb
LRB Engine-Out Capability	Make Mission
Sea Level (Vac) Isp @NPL	379.4(424.1)
Useable Propellant Wgt/Booster	637,724 lb
Mixture Ratio	6.0 :1
Engine Exit Area	26.2 ft ²
Booster Lift-off Weight (BLOW)	786,661 lb
Booster Outside Diameter	18.2 ft
Booster Length	174.3 ft

Table 2.3-2 LRB LO2/LH2 Pump-Fed Optimum Performance

FTB	IVBC-3 Loads		Preliminary LRB Study Loads - Rev1								SRB	
			LO2/RP-1 Pump-Fed				LO2/LH2 Pump-Fed				Rigid Body Analysis	
	Max	Min	Max		Min		Max		Min		Max	Min
1	300	-204	3	247.5	3	-172.5	3	259	3	-161	296.3	-123.8
3	282	-107	3	220.0	3	-60.0	3	245	2	-53	225.0	-55.0
5	204	-2113	-	-	5	-2069.0	-	-	5	-2038	-	-
7	368	-273	3	205.5	3	-130.5	3	183	3	-153	172.0	-164.0
9U	414	-369	3	157.0	3	-347.0	3	263	1	-182	154.0	-350.0
A	387	-178	3	197.0	3	-167.0	2	293	3	-297	196.0	-168.0



Loads = Kips (Ult)
 Loads On L.H. Side Of Vehicle Are Shown
 Loads On R.H. Side Are Identical

Load Condition Key:

- 1 - On Pad - Gravity Loads Only
- 2 - On Pad - Gravity & SSMEs - Max Pitchover
- 3 - Lift Off
- 4 - Max Q
- 5 - Ba

Figure 3.1-1 ET Interface Loads - Ultimate

3.2 TRANSIENT RESPONSE ANALYSIS OF LO2/LH2 LRBs

- LRB MODELS

Important details of LRB models generated for transient response and control systems analyses are given below:

- a) Right hand LRB's were modelled as centerline equivalent beam sticks using NASTRAN;
- b) LRB skirts were modelled as plates, reinforced by beams at the holddown pads;
- c) Propellents were represented by elastic axial elements to simulate the approximate primary bulge effects;
- d) Secondary structure, e.g. engines, was modelled as mass elements only;
- e) LRB-ET interface hardware was simulated by NASTRAN multipoint constraints;
- f) LRB model size was 678 degrees of freedom; and
- g) Transient response analysis of the LRB models were reduced to 22 modes and 21 discrete freedoms (the three LO2/LH2 engines, 6 ET attach, 12 MLP interface).

- VEHICLE MODELS

Vehicle models were created from the main STS components, i.e., right and left SRBs/LRBs, empty orbiter model (wt = 202300 lbf), and hydroelastic ET (wt = 1668000 lbf). The empty orbiter is the worst case condition for ET compression loads. Mass and cg data for the three vehicles are given in Table 3.2-1.

The dynamics vehicle models are created relative to the Dynamics Coordinate System. The following orientation defines this system :

- Origin at ET aft LH2 dome;
- +X forward;
- +Y toward the right SRB/LRB; and
- +Z away from the Orbiter.

The following relationships convert dynamics coordinates to ET station numbers :

- ET X STA = 2173.025 - X DYNAMICS
- ET Y STA = Y DYNAMICS; and
- ET Z STA = -Z DYNAMICS.

	LRB (Sta 1157.1)	Vehicle	ET Sta
Weight (lbf)	786,711	3,442,960	
X CG (in.)	1015.92	1112.87	1060.155
Y CG (in.)		0.39	0.39
Z CG (in.)		-18.14	18.14
Vehicle is ~ 1M lb Lighter than STS with SRBs			

Table 3.2-1 Modeled LO2/LH2 Mass and cg

- TRANSIENT RESPONSE ANALYSIS

Although the LRB transient response model was simple due to the level of the LRB design, the transient response analysis was fairly sophisticated. Some of the salient features of the analyses are detailed below:

- 1) ET cryo loads were simulated by applying loads to the external tank which cause the ET to shrink. The model simulates the relief due to ET structural elasticity. Cryo loads were assumed to be the same as for STS with solid rocket boosters.
- 2) A second order force effect, the moment caused by z deflection of the offset cg of the vehicle, was also simulated in the transient analysis.
- 3) Nominal SSME and LRB forcing functions were generated based on the MSFC launch analysis condition L0941 (MSFC generated forcing function database).
- 4) LRB thrust rise curves were developed from the SSME center engine X force by suitable scaling and time shifting. LRB thrust was assumed to be axial only.
- 5) No winds, or thrust mismatch/misalignment were considered. These loads effect booster/acceleration analysis and are not design drivers on interface hardware.
- 6) MLP bolt release was assumed to be instantaneous.
- 7) The four LRB engines were replaced by a single equivalent engine.

- ON-PAD SSME IGNITION RESULTS

The LRBs are bolted to the MLP and support the External Tank and Orbiter. During SSME ignition, the vehicle stack bends producing non-symmetrical loads in the LRB aft skirt and tiedown struts. The resulting base Y bending moments and Z excursions are shown in Figures 3.2-1 and 3.2-2. First bending mode frequencies of the the three vehicles were calculated to be 0.348 Hz for the LO2/LH2 LRB. Release of the vehicle is delayed until the stack is upright and bending moment is minimum.

As shown in Figure 3.2-1, the base Y bending moment curve, the optimum bolt release time for the vehicle was estimated to be at 6.7 sec. Therefore, LRB vehicle bolt release time was assumed to be at the moment bucket (6.7 sec). SSME ignition in all cases was at 1.9 sec., with time t=0 being at SSME ignition command. The maximum cg Z excursion on the pad for the LO2/LH2 LRB is 9 in. as shown in Figure 3.2-2.

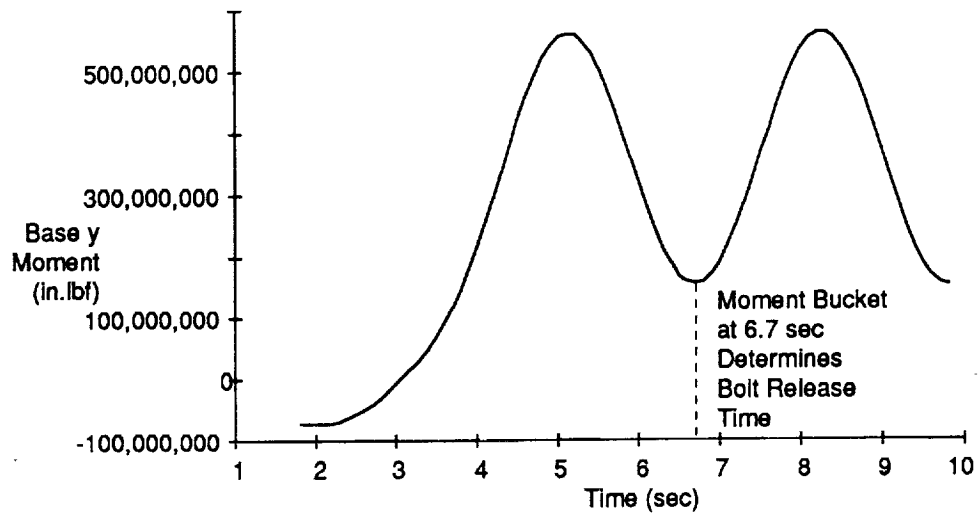


Figure 3.2-1 LO2/LH2 LRB Base Bending Moment

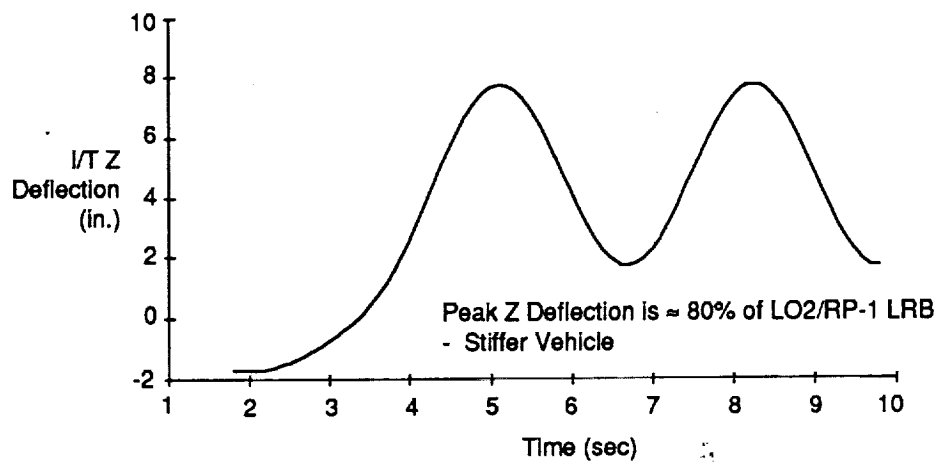


Figure 3.2-2 LO2/LH2 LRB ET cg Z Deflection

-- LRB ENGINE FORCING FUNCTIONS

LRB engine forcing functions were derived from the SSME center engine axial thrust build-up by suitable scaling and time shifting to give a peak thrust of 1885 kips. LRB ignition was at 4.4 sec; peak thrust and bolt release were at 6.7 sec. (the time of the base bending moment bucket).

3.3 TRANSIENT LOADS RESULTS

- ET LOADS DUE TO LAUNCH TRANSIENT

Table 3.3-1 shows the results of launch transient response analyses carried out for LO2/LH2 LRB design. ET loads are shown because the ET interfaces with both the orbiter and LRB, so impacts to the orbiter interface loads would also show up. The loads are max/min, in KIPS, and they are in the dynamics coordinate system. The analysis simulation time from 1.8 sec to 20.0 sec. Loads exceedances from IVBC-3 loads are highlighted.

The LO2/LH2 LRB's have stiffness characteristics similar to the SRB's, as was shown earlier for the on-pad response results. LRB lateral (y) loads are conservative, being obtained from stick models without any radial flexibility. However with LO2/LH2 LRB, there are ET impacts as shown by the exceedances at ET-Orbiter aft linkage loads and at forward ET-LRB Y-loads.

- ET LO2 DOME BOTTOM PRESSURE

Figure 3.3-1 shows the ET LO2 tank aft dome pressure response caused by the transient from the LO2/LH2 LRB vehicle nominal launch. Peak pressure from a launch transient (assuming a 23 psi ullage) is 64 psi, which is similar to the current STS value.

- Z DEFLECTION AT ET1 INTERTANK UMBILICAL

ICD-2-0A002, Section 3.1.3, gives the max allowable -Z deflection at the ET intertank umbilical during SSME ignition and build-up as 23 in. Launch pad positioning tolerance is given in the ICD as 0.9 in. From ACC launch analysis studies (1983), deflection allowance for wind gusts is estimated to be 2 in. This leaves a total allowable deflection during SSME build-up of 20 in.

Fig 3.2-2 shows the z deflection obtained during a nominal SSME ignition sequence (no winds) at the SRB/ET forward fitting (which is 18 in. forward of the umbilical). Maximum deflections for the vehicle stack with a LO2/LH2 LRB was well within the deflection criteria.

Load Description			Max (kips)	Min (kips)
ET/Orb	Fwd Bipod	X	2.4	-8.7
		Y	5.1	-6.8
		Z	102	-2.3
	Aft Link. R	X	499	-105
		Y	52	12
		Z	132	11.2
	Aft Link. L	X	506	-9.9
		Y	-12	-48
		Z	135	11
ET/LRB R	Fwd	X	1044	382
		Y	108	-258
		Z	32	-163
	Aft	X	156	-163
		Y	84	-85
		Z	194	-12
ET/LRB L	Fwd	X	1055	384
		Y	271	-101
		Z	32	-165
	Aft	X	148	-157
		Y	88	-95
		Z	9	-200
Dynamic Loads are an Issue				

Table 3.3-1 ET Loads Due to Launch Transient

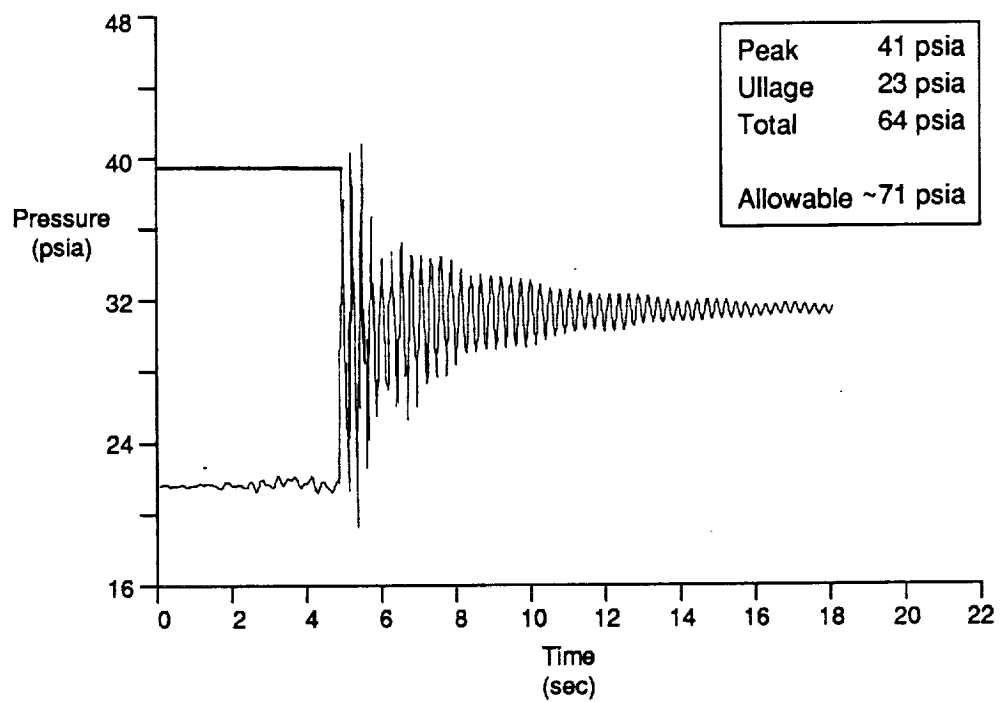


Figure 3.3-1 ET LO2 Tank Bottom Pressure

- CONCLUSIONS

Results from this preliminary analysis indicate that the LO2/LH2 LRB transient response is similar to the SRB baseline vehicle. However, the lateral ET-LRB loads (forward and aft) are higher than for a SRB and are a concern, as are the ET-Orbiter aft linkage loads. A major difference from LO2/RP-1 analyses is that the moment bucket is not as low as before, hence there is more strain energy in the vehicle at launch. The vehicle is stiffer as indicated by the on-pad frequency of the is 0.35 Hz (compared to 0.27 for the SRB, 0.28 for the LO2/RP-1 Pressure-Fed, and 0.29 for the LO2/RP-1 Pump- Fed vehicles). We seem to have crossed some stiffness threshold, i.e., the LO2/LH2 LRBs are too stiff. Both these issues can only be resolved by more detailed shell type models of LRBs which account for radial flexibility

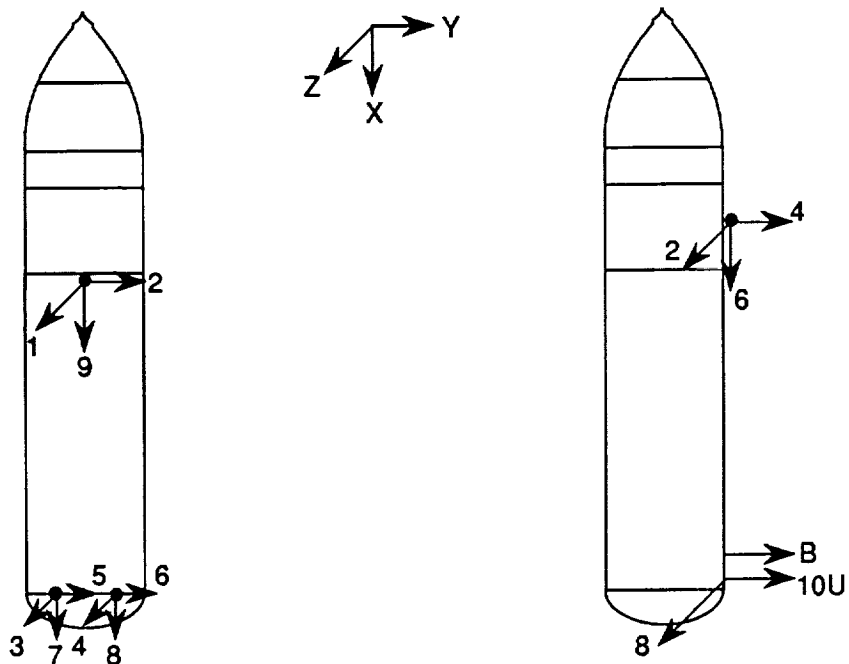
4.0 STRESS ANALYSIS

4.1 ET LOADS

Maximum and minimum ET-LRB interface loads were estimated for prelaunch and maximum booster acceleration conditions based on thrust, mass and inertia using rigid body loads calculations. Dynamic load components were obtained from prior booster launch analysis studies. Interface loads were also developed for liftoff transients using a beam stick model Nastran analysis which, like the rigid body analysis, included no LRB radial flexibility. Also, the loads generated include no winds or load dispersions. ET LO2 dome peak pressure was determined as was the increased aeropressure on the LO2 ogive due to the extended LRB length.

4.2 ASSESSMENT METHODOLOGY

Maximum and minimum ET interface loads for LRB's were compared to maximum and minimum ET loads for SRB's from the most up-to-date STS load set (IVBC-3). Figure 4.2-1 shows the locations and sign conventions for the ET interface loads. Loads for each time regime, i.e., prelaunch, liftoff and maximum booster acceleration, were compared to IVBC-3 loads for the corresponding time regime as well as the overall IVBC-3 maximum and minimum interface loads. Any LRB load exceedances



FTB	Max Loads (Ultimate kips, R.H.)			Min Loads (Ultimate kips, R.H.)		
	LO2/LH2 LRB	IVBC-3 Liftoff	IVBC-3 Summary	LO2/LH2 LRB	IVBC-3 Liftoff	IVBC-3 Summary
1,2	-52	39	300	-52	-132	-204
3,4	-124	-1	107	-124	-136	-282
5,6	-1207	4	204	-1207	-1304	-2113
7,8	52	165	368	52	-42	-273
9U,10U	182	160	369	182	-60	-414
A,B	192	129	387	192	-17	-178

- Boxed LRB Loads Exceed Corresponding IVBC-3 Prelaunch Loads

Figure 4.2-1 ET Interface Loads Convention

over the IVBC-3 set were analyzed in sufficient detail to determine whether the load exceedances impacted external tank structural margins of safety. Margin reduction areas were identified and potential concerns were detailed. Finally, the ET LO2 dome peak pressure and ogive aeropressure were assessed for structural impacts.

4.3 PRELAUNCH ASSESSMENT RESULTS

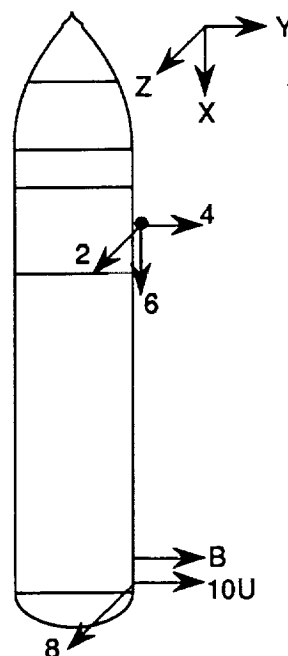
Predicted LRB prelaunch loads are less critical than IVBC-3 prelaunch loads at all locations except the aft attach Y-axis loads or "pinch" loads (FTB9U, FTB1OU, FTBA and FTBB). Figure 4.2-1 shows the comparison between LRB and IVBC-3 prelaunch loads highlighting the pinch load exceedance. A positive pinch load puts the attachment and struts in tension and induces longitudinal compression in the ET LH2 aft dome. Current IVBC-3 prelaunch pinch loads produced a 0.00 margin of safety for aft dome buckling for a condition where the ET is fully loaded and the LH2 tank is unpressurized. Therefore, a pinch load exceedance would be a concern. However, LRB predicted Y-axis loads calculated with the loads stick model, which does not simulate LRB radial flexibility, are conservatively high. Preliminary analyses which include the full LRB flexibility indicate that the LRB aft attachment frame could be designed to maintain the LRB pinch loads within the IVBC-3 pinch loads limits.

More details of this analysis are given in Section 4.8 of this report. As can be seen from Figure 4.2-1, the pinch loads are much larger during flight than during prelaunch. However, the stabilizing LH2 tank ullage pressure is also much larger during flight, and dome stability is not a concern. Also, the ET 2058 frame and fittings are more critical during flight because they are not pressure sensitive. In summary, LRB prelaunch loads will not impact ET structural margins of safety with adequate flexibility designed into the LRB aft attachment frame.

4.4 LIFTOFF ASSESSMENT RESULTS

Predicted LRB booster loads during liftoff are less critical than IVBC-3 liftoff loads at all locations except the forward attach Y-axis loads (FTB3 and FTB4). Figure 4.4-1 shows the comparison between LRB and IVBC-3 liftoff booster loads with the load exceedances highlighted. These loads exceed IVBC-3 loads for both the maximum and minimum conditions indicating that several intertank areas require analysis.

The maximum forward attachment fitting compression case (Max FTB3, Min FTB4) may have an impact on intertank crossbeam stability, crossbeam/dome clearances



FTB	Max Loads (Ultimate kips, R.H.)			Min Loads (Ultimate kips, R.H.)		
	LO2/LH2 LRB	IVBC-3 Liftoff	IVBC-3 Summary	LO2/LH2 LRB	IVBC-3 Liftoff	IVBC-3 Summary
1,2	231	300	300	-45	-204	-204
3,4	151	107	107	-379	-282	-282
5,6	-535	-452	204	-1477	-1833	-2113
7,8	133	252	368	-123	-123	-273
9U,10U	220	369	369	-228	-414	-414
A,B	280	387	387	-17	-178	-178

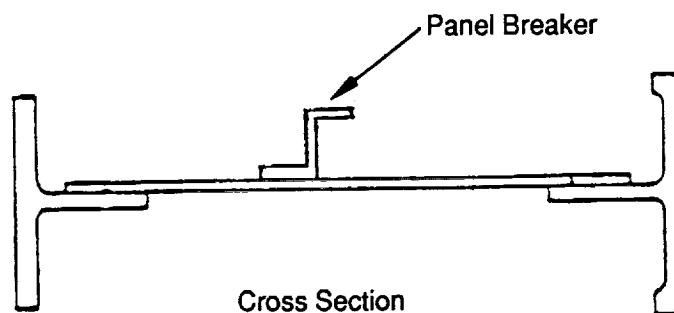
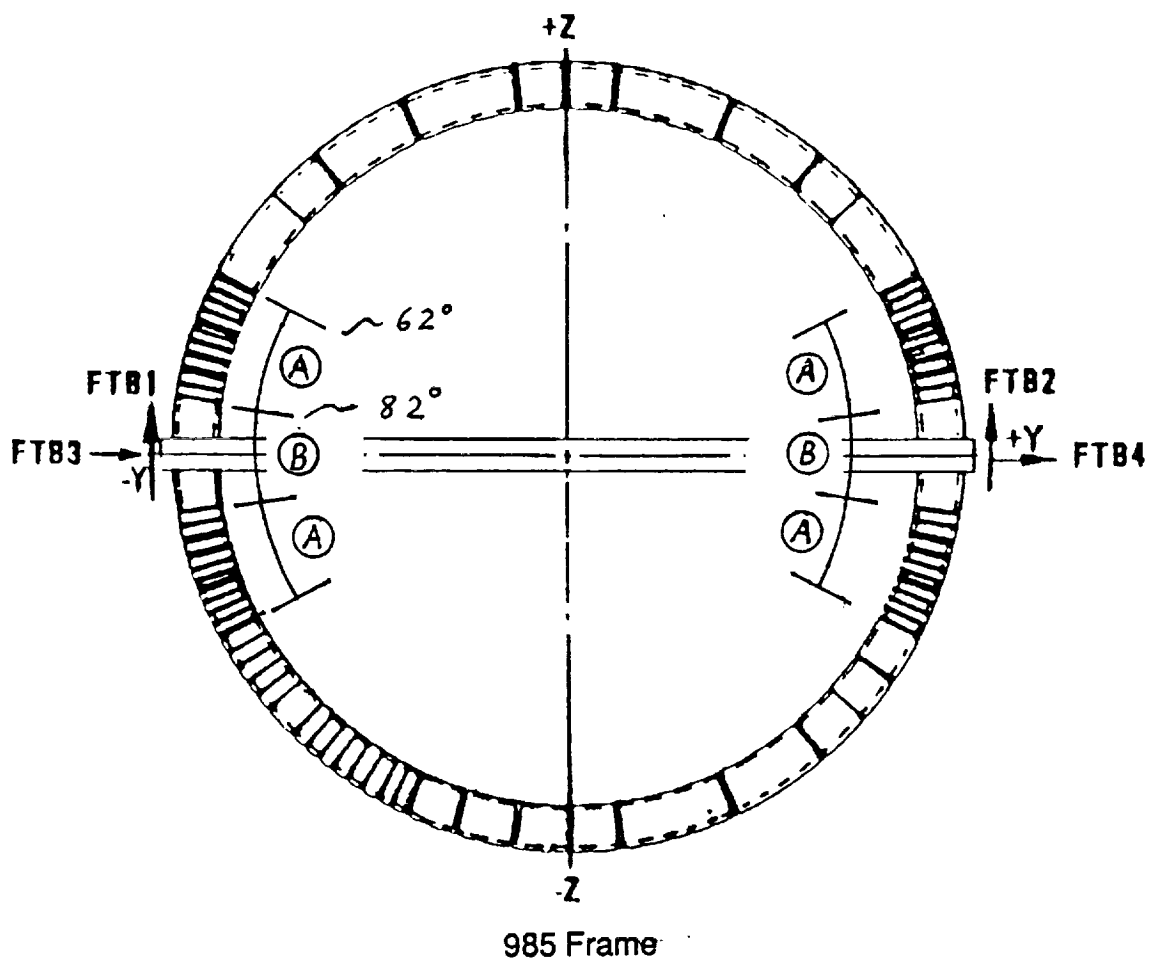
- Boxed LRB Loads Exceed Corresponding IVBC-3 Loads

Figure 4.4-1 Liftoff Booster Loads Comparison

and 985 frame stability. The crossbeam margin of safety program was executed for the Max-Max compression condition and showed that crossbeam stability margins of safety improved over IVBC-3 margins due to the reduced FTB5 and FTB6 thrust loads for LRB. Crossbeam stability is more sensitive to bending induced by FTB5 and FTB6 than to axial compression induced by FTB3 and FTB4. Calculated crossbeam-dome clearances improved over IVBC-3 clearances for both the LO2 dome and LH2 forward dome due to lower LO2 dome pressure and reduced crossbeam bending caused by reduced FTB5 and FTB6 thrust loads. The analysis of the intertank 985 frame, which carries much of the Y-axis compression load, indicates that web shear buckling is a problem. Additional web stiffeners near the attach fittings are required to carry LRB loads. Figure 4.4-2 identifies the type and placement of stiffeners required.

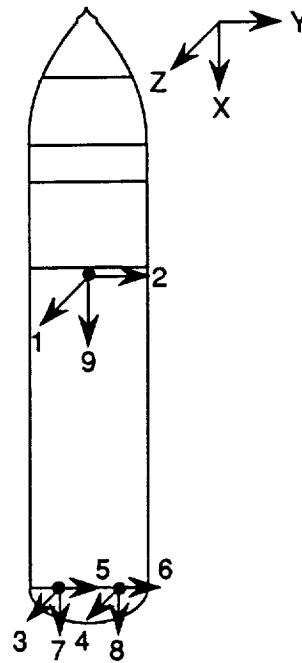
The maximum forward attachment fitting tension case (Min FTB3, Max FTB4) may have an impact on crossbeam lower cap tension and attachment fitting strength. The crossbeam margin of safety program was executed for the Max-Max tension condition and showed that crossbeam tension margins of safety improved over IVBC-3 margins due to the reduced FTB5 and FTB6 loads for LRB. Again, crossbeam tension is more sensitive to bending induced by FTB5 and FTB6 than to axial tension induced by FTB3 and FTB4. Intertank-booster attachment fitting strength margins of safety are driven by FTB1, FTB2, FTB3, and FTB4. Although FTB3 and FTB4 exceeded IVBC-3 values, analysis indicates that the fitting strength margins are unchanged from IVBC-3 margins because FTB1 and FTB2 are reduced from IVBC-3 loads.

Predicted orbiter loads during liftoff are less critical than IVBC-3 liftoff orbiter loads at all locations except the orbiter thrust loads (FT07 and FT08) which produce the maximum compression in the LH2 tank barrel panels. Figure 4.4-3 shows the comparison between LRB and IVBC-3 liftoff orbiter loads with the loads exceedances highlighted. Current IVBC-3 liftoff loads combinations produce a 0.00 margin of safety for LH2 barrel panel buckling. Orbiter thrust loads are larger at booster staging than at liftoff; however, LH2 stabilizing ullage pressure is lower at liftoff. Therefore, the LRB liftoff orbiter thrust loads exceedances pose a potential LH2 barrel panel stability concern. Preliminary analysis based on Max-Max loads indicates that 6 of 32 barrel panels may require additional stiffening material. However, the LH2 barrel loads are a function of orbiter and booster loads as well as overall vehicle acceleration, and a detailed time consistent analysis may show positive margins for barrel panel buckling. LH2 tank thrust struts, fittings and frames, which are not sensitive to tank pressure, are more critical at staging.



- Ⓐ Zones Require Circumferential Panel Breakers as Shown Above
- Ⓑ Zones Require Radial Stiffeners Similar to Those on the Rest of the Frame

Figure 4.4-2 Required 985 Frame Web Stiffeners



FTB	Max Loads (Ultimate kips, R.H.)			Min Loads (Ultimate kips, R.H.)		
	LO2/LH2 LRB	IVBC-3 Liftoff	IVBC-3 Summary	LO2/LH2 LRB	IVBC-3 Liftoff	IVBC-3 Summary
1	32	76	76	-143	-178	-178
2	7	44	93	-10	-41	-83
3	-15	14	447	-189	-275	-426
4	-16	4	386	-185	-310	-491
5	-17	3	148	-67	-88	-141
6	73	125	125	17	-25	-67
7	139	205	205	-708	-677	-892
8	147	204	204	-699	-665	-899
9	12	15	15	-3	-7	-7

- Boxed LRB Loads Exceed Corresponding IVBC-3 Liftoff Loads

Figure 4.4-3 Liftoff Orbiter Loads Comparison

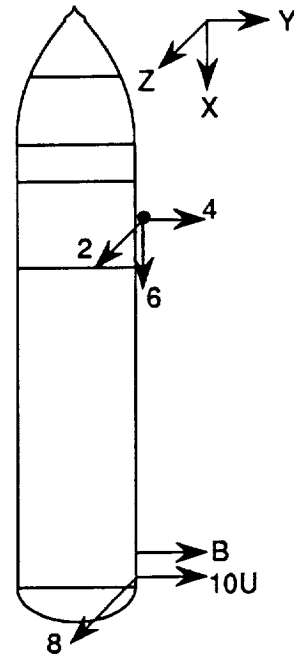
In summary, analyses done for the LRB liftoff condition, based on Max-Max loads, indicate that the 985 frame will require additional web stiffeners and 6 of 32 LH2 barrel panels may require additional stiffening material.

4.5 MAX BOOSTER ACCELERATION ASSESSMENT RESULTS

Predicted LRB Max booster acceleration (BA) loads are less critical than IVBC-3 BA loads at all locations except the ET/LRB Y-axis loads (FTB3, FTB4, FTB9U, FTB10U, FTBA, and FTBB). Figure 4.5-1 shows the comparison between LRB and IVBC-3 BA loads with the load exceedances highlighted. Aft loads are exceeded on the max side-struts in tension. However, these BA loads are still less than the Max IVBC-3 aft Y-axis liftoff loads, and the LH2 aft dome pressure is at a maximum during BA. Therefore, these aft loads exceedances pose no concerns for the aft dome, frame or fittings. The forward ET-booster attach loads exceedance (FTB3 and FTB4) is for compression on the crossbeam and was analyzed for crossbeam stability, crossbeam-dome clearances, and 985 frame stability. The crossbeam margin of safety program was run for the Max-Max compression condition and shows that crossbeam stability margins of safety improved over IVBC-3 margins for BA due to the reduced FTB5 and FTB6 loads for LRB. Calculated crossbeam/dome clearances improved over IVBC-3 clearances for both the LO2 aft dome and the LH2 forward dome due to lower peak LO2 dome pressure and reduced crossbeam bending caused by reduced FTB5 and FTB6 loads. The intertank 985 frame is more critical for liftoff LRB loads than for BA LRB loads because of FTB3 and FTB4 are larger at liftoff than for BA. Therefore, the additional 985 frame web stiffeners required for LRB liftoff loads would be sufficient to show positive margins for LRB BA loads.

4.6 ADDITIONAL ASSESSMENT RESULTS

As a result of the dynamic loads analysis, it was determined that the ET LO2 dome maximum pressure for the LO2/LH2 LRB is 64.0 psig compared to a maximum of 68.6 psig for IVBC-3 conditions. The LRBs extend further forward of the forward attachment point than do the SRBs. During the time of maximum aerodynamic pressure (High Q), the LRB aero flow field imposes 3 psi additional aero pressure on the LO2 ogives. The ogive buckling margin of safety during High Q reduces from 0.51 (IVBC-3) to 0.46 (LO2/LH2 LRB) due to the additional aero pressure.



FTB	Max Loads (Ultimate kips, R.H.)			Min Loads (Ultimate kips, R.H.)		
	LO2/LH2 LRB	IVBC-3 BA	IVBC-3 Summary	LO2/LH2 LRB	IVBC-3 BA	IVBC-3 Summary
1,2	3	29	300	3	-33	-204
3,4	-209	-109	107	-209	-149	-282
5,6	-2038	-1725	204	-2038	-2113	-2113
7,8	22	76	368	22	-30	-273
9U,10U	79	66	369	79	8	-414
A,B	130	108	387	130	46	-178

- Boxed LRB Loads Exceed Corresponding IVBC-3 BA Loads

Figure 4.5-1 Max Booster Acceleration (BA) Loads Comparison

4.7 ET ASSESSMENT CONCLUSIONS

Generally, ET-LRB loads for the LO2/LH2 booster are similar to ET/SRB loads with most LRB loads exceedances over IVBC-3 loads occurring on the Y-axis loads. As stated previously, LRB Y-axis loads are conservative because they were developed on a stick model with no LRB radial flexibility. More accurate loads can only be predicted by more detailed loads models which account for radial flexibility. The other LRB loads exceedance was on the orbiter thrust loads during liftoff, and these loads were developed using an empty orbiter which provides a worst case compression load on the ET LH2 tank barrel panels.

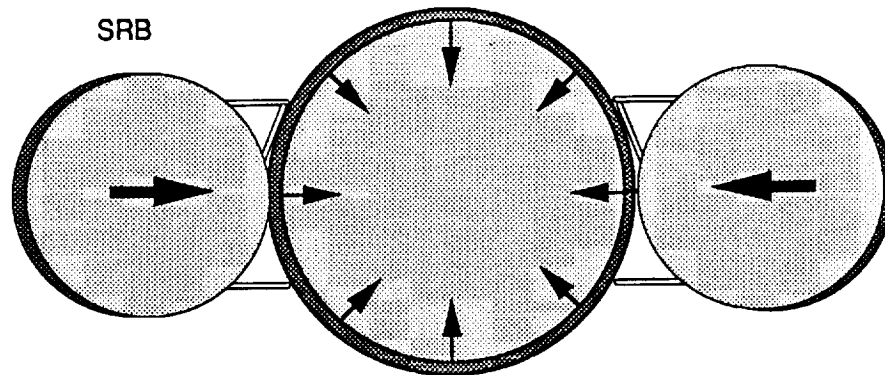
The only significant structural impacts to the external tank identified for the LO2/LH2 LRB are that the intertank 985 frame will require additional web stiffeners as detailed in Figure 4.4-2 and six LH2 barrel panels may require additional stiffening material.

All ET impact analyses were based on Max-Max loads which is a conservative approach. However, time consistent analysis would require an extensive loads database not possible for this preliminary study.

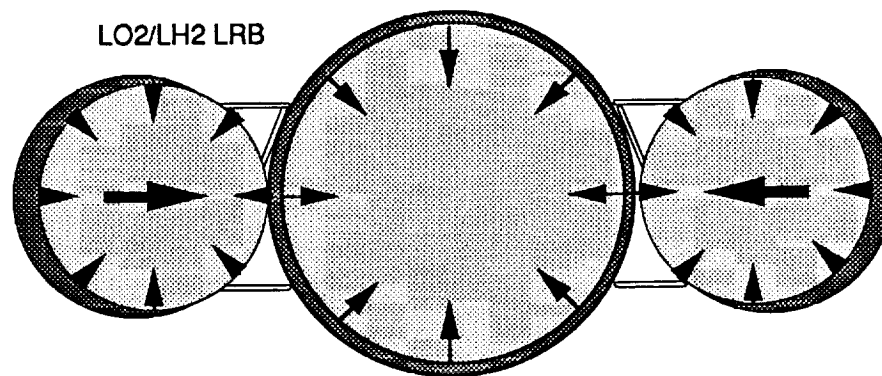
4.8 CRYOGENIC SHRINKAGE AT THE AFT ET ATTACHMENTS

In the previous LRB study phase, cryogenic shrinkage of both the LH2 tank of the ET coupled with shrinkage of an LRB LH2 tank at the aft attach points during filling operations on the launch pad was identified as a major issue in considering LO2/LH2 LRBs. The ET LH2 tank aft dome just below Sta. 2058 and $\pm 90^\circ$ around from the aft SRB attachments is buckling critical during pre-launch because the MLP and SRBs restrict contraction of the ET and result in internal loads with very low stabilizing pressure. It was considered that LRB aft attach loads to the ET would not be able to exceed the present SRB loads during the pre-launch condition. If additional cryo shrinkage was present, Figure 4.8-1, flexibility of the LRB would have to account for the additional displacements. Examinations of the displacements of the ring frame in the LRB at the attach points showed that the frame could not provide the flexibility required without being overstressed. Additional flexibilities in the structures needed to be determined and utilized.

A simple three-dimensional math model of the LO2/LH2 LRB (Figure 4.8-2) was established to account for both radial stiffness at the attach points and overall bending stiffness of the shell, including the aft skirt. Analysis with this model showed that the bending flexibility of the shell, along with the radial flexibility of the aft ring, was more



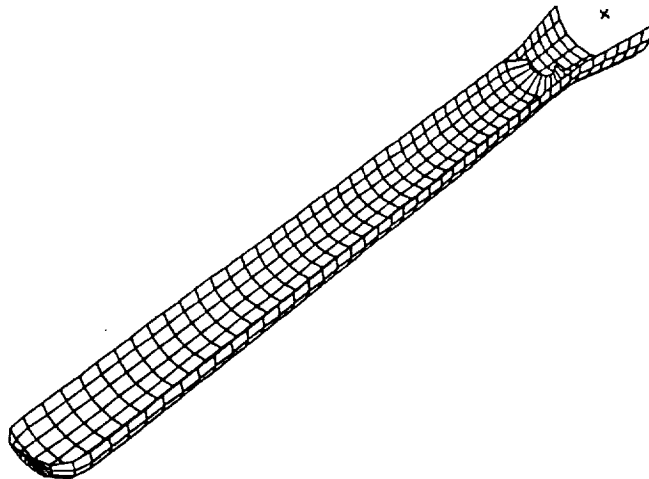
ET Cryo Shrinkage Causes High Interface Loads



ET & LO₂/LH₂ LRB Cryo Shrinkage Causes Higher Loads Unless LRB is More Flexible Than SRB

Figure 4.8-1 ET/LRB Aft Attachment Shrinkage and Interface Loads

	SRB	LO2/LH2 LRB
Radius	72.5	109
Modulus	29e6	10.5e6
Loading	ET Cryo	ET & LRB Cryo
Material	D6AC Steel	Weldalite™049



SRB Finite Element Cutaway View
LRB Finite Element Model Similar

Figure 4.8-2 LRB Math Model and Data

than adequate to allow the additional cryo shrinkage of the LRB without increasing loads above those of the SRB. Stress levels in both the ring and shell were within acceptable levels.

Note that although stress levels were acceptable, it is anticipated that a much finer mesh in the model elements in the ring/shell intersections would identify higher peak stresses than shown by the coarse model. Local tank wall thickness increases could accommodate these higher stresses without changing the overall flexibilities and the resulting interface attach loads.

5.0 AERODYNAMIC IMPACTS

5.1 SHOCKWAVE IMPINGEMENT

An evaluation of pressure increases on the LO2 tank ogive was performed which qualitatively addressed effects on the ET resulting from the forward location of the LO2/LH2 LRB relative to the current SRB. As shown by Figure 5.1-1, the LRB nose cone shock wave was assumed to be identical to SRB nose cone shock patterns. Both the LRB and the SRB have the same cone angle. The LRB nose cone shock wave will impinge further forward on the ET than the SRB nose shock. At Mach 1.46 there will be ET bow and LRB nose shock interference. The maximum pressure increase on the LO2 tank ogive would be expected to occur before ET bow and LRB nose shock interference, i.e., at a Mach number less than 1.46 but greater than 1.25. The ET/SRB shock interactions were traced from Shuttle-C Transonic Wind Tunnel Test (TWT-715) shadowgraphs.

Figure 5.1-2 illustrates the XY plane ET pressure distribution. SRB nose cone shock impingement at Mach 1.4 results in a $\Delta c_p = 0.6$. For a LRB dynamic pressure of 700 psf, the $\Delta c_p = 0.6$ results in a 420 psf pressure increase over 200 inches of the LO2 tank ogive. As shown by Figure 5.1-2 the high pressure SRB shock impingement region is a low pressure nose/cylinder junction flow expansion region for the LRB. Major flow field changes have occurred for the ET LO2 tank and intertank. These major flow field changes will, of course, diminish but not disappear in going from the XY to XZ plane.

LRB nose shock impingement and nose/cylinder junction flow expansion regions on the ET will move forward about 300 and 200 inches respectively. The resulting flow field changes on the LO2 tank and intertank will increase pressures on the LO2 tank ogive and effect location of protuberance airloads (PAL) ramps, protuberance

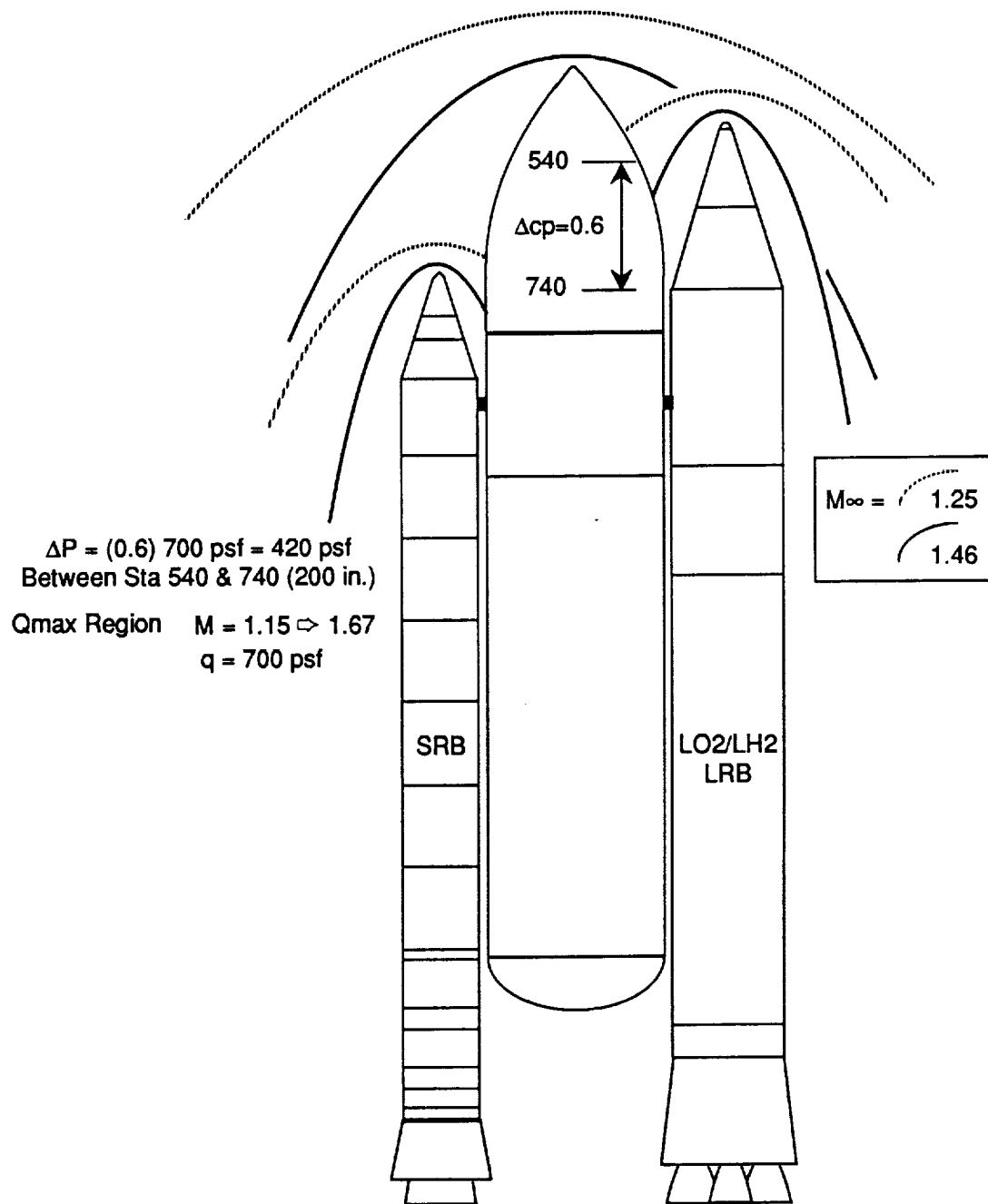


Figure 5.1-1 LO2/LH2 LRB Aerodynamic Impact

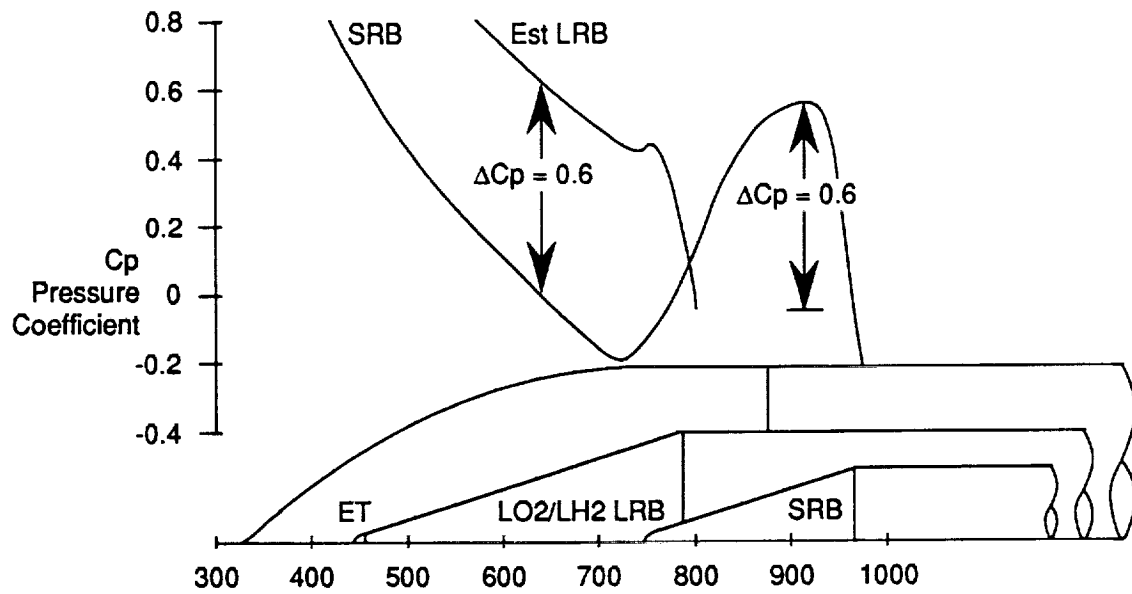


Figure 5.1-2 XY Plane ET Pressure Coefficient Distribution

airloads (cable trays, brackets, LO2 feedline fairing, etc.) cable tray venting, intertank venting, and possibly nose cone venting (LO2 tank ullage reference pressure). Experimental data (pressures, oil flow, shadowgraph, etc.) are required to evaluate these effects. The following ET impacts have been identified as a result of the increased pressure loads:

1. The LO2 tank PAL ramp will need to be extended to about ET station 500
2. Protuberance airloads such as the LO2 tank cable tray/pressure line/brackets will impact hardware.
3. Compartment venting will change, but not impact hardware.
LRB separation motor plume flow field will need to be quantified for both location and strength before ET impacts can be evaluated.

5.2 FUTURE WIND TUNNEL WORK

The following recommendations are submitted for future work:

1. Obtain experimental pressure distribution and flow visualizations in the subsonic, transonic, and supersonic speed regimes.
2. Quantify the location and strength of the LRB separation motor plumes relative to the ET.

6.0 THERMAL IMPACTS ON ET

In Section 5.0, the shock wave from the longer LO2/LH2 LRB was shown to impinge on the ET approximately 25 ft forward of the present SRB design. Determination of the peak heating rates along the ET was accomplished and are shown for both SRB and LRB in Figure 6.0-1. As shown by the curve, there is a higher heating rate for the LRB of approximately 1.2 btu/Ft²-sec starting at Sta. 500 and extending back to Sta. 800.

Comparison to present ET thermal analyses shows that present LO2 tank TPS thicknesses are adequate to protect against this additional heating. At LRB separation, there is considerable LO2 still in the ET which also acts as a large heat sink to any external heating.

7.0 COST IMPACTS

The ET cost impacts effected by the baseline LO2/LH2 booster would be limited to minor, nonrecurring redesign efforts and minimal, recurring materials and labor

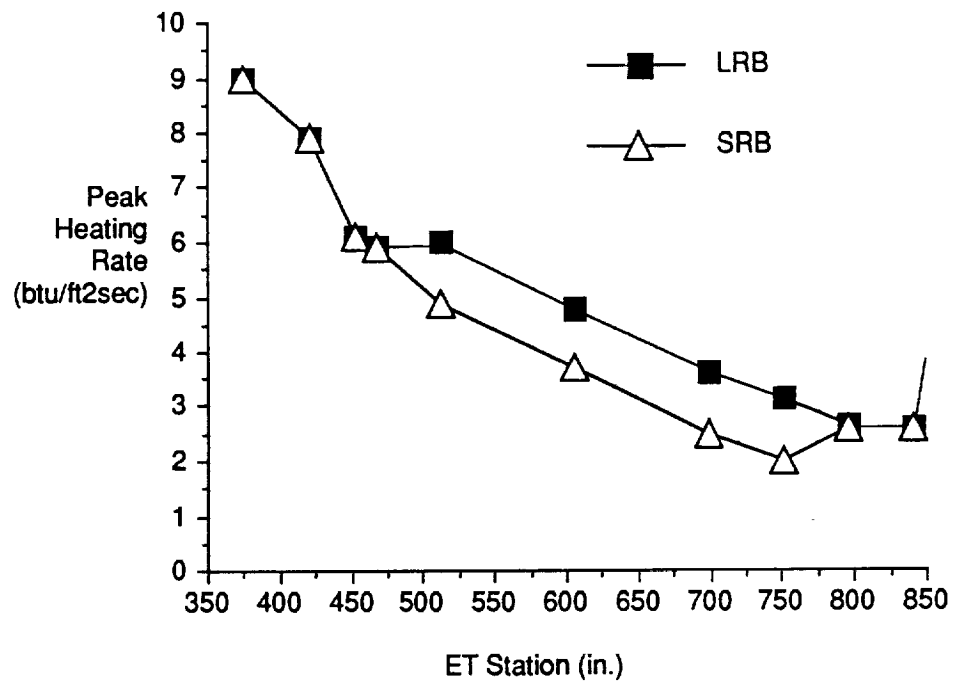


Figure 6.0-1 Comparison of SRB vs LRB Heating

increases. The change requirements can be subdivided into structures (reinforcing the 985 ring frame and adding stiffeners); TPS (extending the LO2 PAL ramp); and electrical (changing the wiring sequence to accommodate the additional LRB data requirements).

The DDT&E cost impacts consist of drawing changes in the affected structures and TPS areas. It is assumed that the existing ET wiring can accommodate the additional LRB data requirements to the Orbiter. Only connector reconfiguration would be required. Engineering analysis efforts and affected manufacturing plans and test procedures would require minimal efforts. Although no discrete estimates were made, past estimates for changes of this magnitude ranged from \$0.5M to \$5.0M.

The recurring cost impacts again follow the structures, TPS, and electrical subsystem impacts indicated above. The changes would require no significant changes in current ET production procedures and only minor materials increases for structures reinforcement and stiffeners, additional TPS, and a new LRB wiring harness. It is assumed that the number and size of the connectors will not change and associated cable trays and other hardware are not impacted. Past estimates for changes of this type were less than \$0.1M per ET once production returned to normal.

VOLUME II ADDEMDUM 1

TASK 2

**RECOVERABLE PROPULSION AVIONICS
MODULE FOR A LO₂/LH₂ LIQUID ROCKET
BOOSTER USING MODIFIED SPACE SHUTTLE
MAIN ENGINES (SSME-35)**

1.0 STUDY OVERVIEW

1.1 BACKGROUND

Cost analyses performed during the Liquid Rocket Booster (LRB) study Part 1, Concept Trades, and Part 2, Concept Definition, indicated that recovery of high cost booster systems could provide life cycle cost (LCC) savings of as much as 7 to 10% over expendable boosters. Uncertainty in non-cost variables including complexity, safety, maintainability and risk overruled the cost results in favor of expendable boosters. The cost analyses used a predicted pump-fed engine unit cost of \$3.6M based on Space Transportation Booster Engine (STBE) study data available in early 1988.

The booster engine costs are a primary driver in the booster recovery trade, and significant increases in engine unit costs could make recovery of the engine systems imperative. Although technology programs are in progress to develop low cost engine designs and manufacturing techniques, pump-fed engine cost predictions have escalated as high as \$12M-\$15M per engine.

As a backup to escalating pump-fed engine costs, the LRB recoverable propulsion avionics (P/A) module study task was performed to develop design concepts, define vehicle performance impacts and develop ROM DDT&E and production costs.

1.2 GROUND RULES AND ASSUMPTIONS

The Space Shuttle Main Engine (SSME) was groundruled for use during this study. Due to their application on a booster vehicle, the engine expansion ratio was assumed to be 35:1. Ocean recovery of the P/A module was also a groundrule and the P/A module shape was assumed to be ballistic

1.3 STUDY RESULTS SUMMARY

A ballistic P/A module design concept was developed that could be integrated into the aft section of a STS LO2/LH2 LRB. The module has excellent aerodynamic trim and static stability characteristics for reentry after separation from the main portion of the LRB and provides sufficient internal volume for the installation of five (5) SSME-35 engines. The shape produces excellent drag which, in conjunction with a decelerator system composed of a drogue and four (4) main ballistic parachutes, reduces the module velocity to 25fps for splashdown. Cost analysis indicate that the LRB P/A module concept

with SSME-35 engines is a viable alternative to an expendable LRB when the LRB engine costs exceed seven million dollars.

2.0 P/A MODULE CONFIGURATION

2.1 GENERAL ARRANGEMENT

The general arrangement of a LRB configured with a P/A module is shown in Figure 2.1-1. Overall dimensions for the aft portion of the LRB with P/A module installed is shown in Figure 2.1-2. The forward diameter of the aft skirt was determined by the maximum diameter of the LO₂/LH₂ LRB. Previous LRB studies determined that approximately 18 feet was the maximum tank diameter that can be flown on the STS without exceeding the orbiter wing load limits. The aft P/A module diameter of 30.6 feet was determined by the minimum mounting plane area for five (5) SSME-35 engines. Longitudinally, a minimum distance of 13.2 feet between the aft skirt forward attach plane and the engine mounting plane was needed to install the P/A module structure, including the nose cap, and package the propulsion system plumbing and disconnects associated with the engines.

The LRB P/A module configuration is shown in Figure 2.1-3. In the forward view, the interface doors, which seal off the fluid and electrical disconnects, are illustrated. The four (4) LRB P/A module structural interface points are also shown. The rear view of the P/A module shows the arrangement of the five (5) SSME-35 engines, as well as the placement of the four (4) cannisters for the main parachutes of the recovery system. Also shown in this illustration are the pertinent overall dimensions associated with the P/A module's ballistic shape. The nose radius of 51.5 feet was developed from drag data associated with large blunt shapes and represents the best shape when considering both the aerothermal aspects of reentry and the structural aspects of ocean impact.

2.2 STRUCTURAL DETAILS

2.2.1 Holddown Loads and Fittings

The major loads applied to the P/A module are the holddown loads to the launch pad, attach loads to the LRB tank sections, thrust loads from the engines, and splashdown loads on the nose cap. Holddown loads design 1) the four longerons and fittings, 2) the

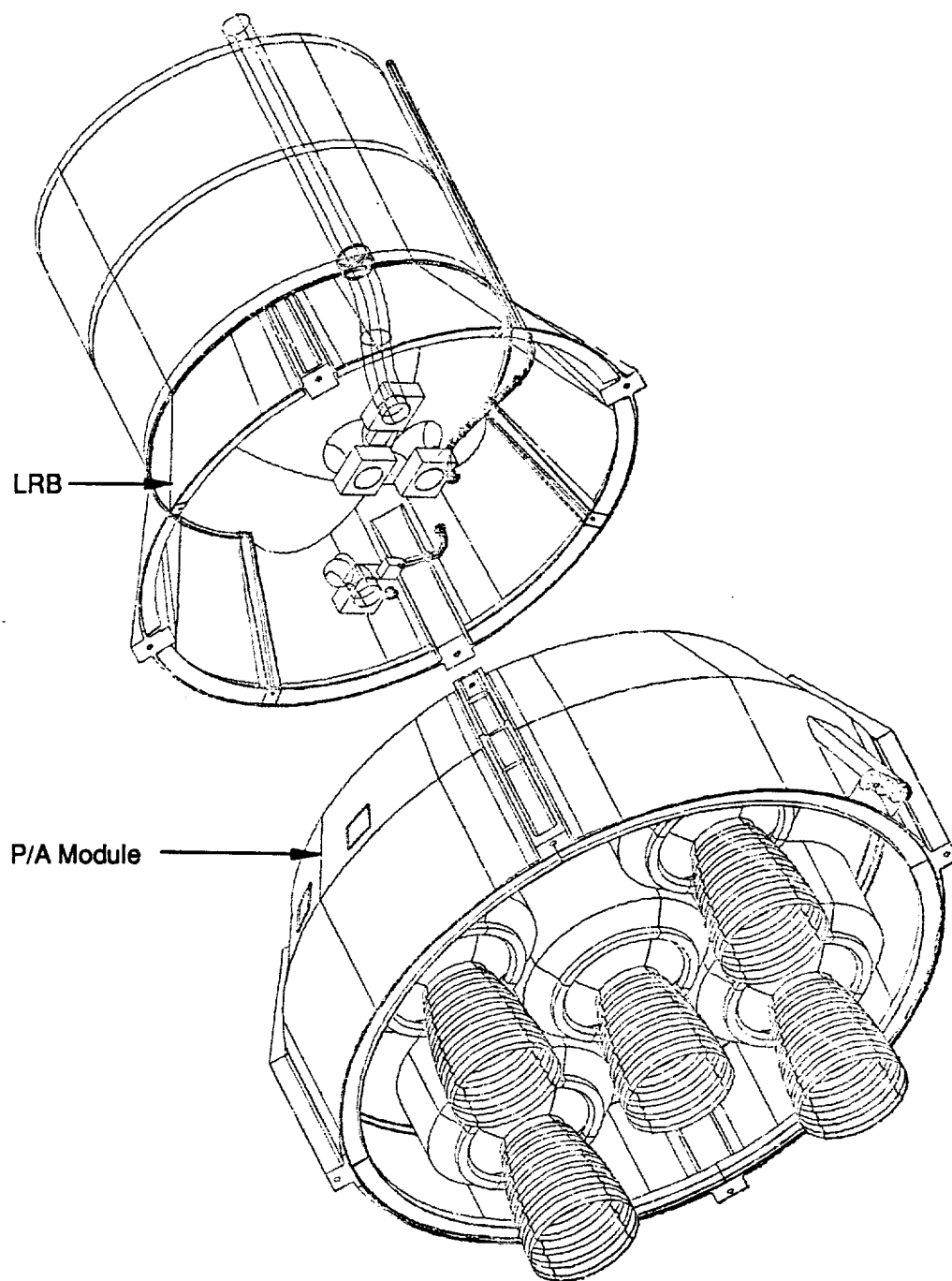


Figure 2.1-1 LRB P/A Module General Arrangement

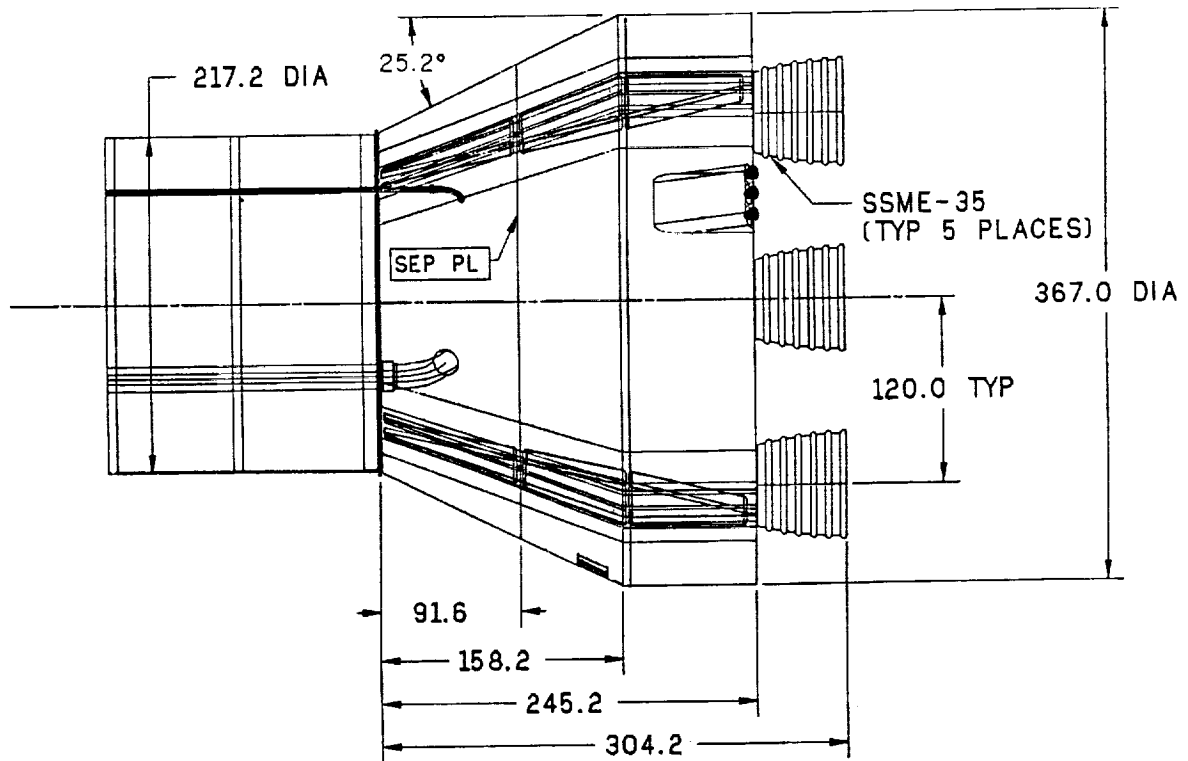


Figure 2.1-2 LRB P/A Module Overall Dimensions

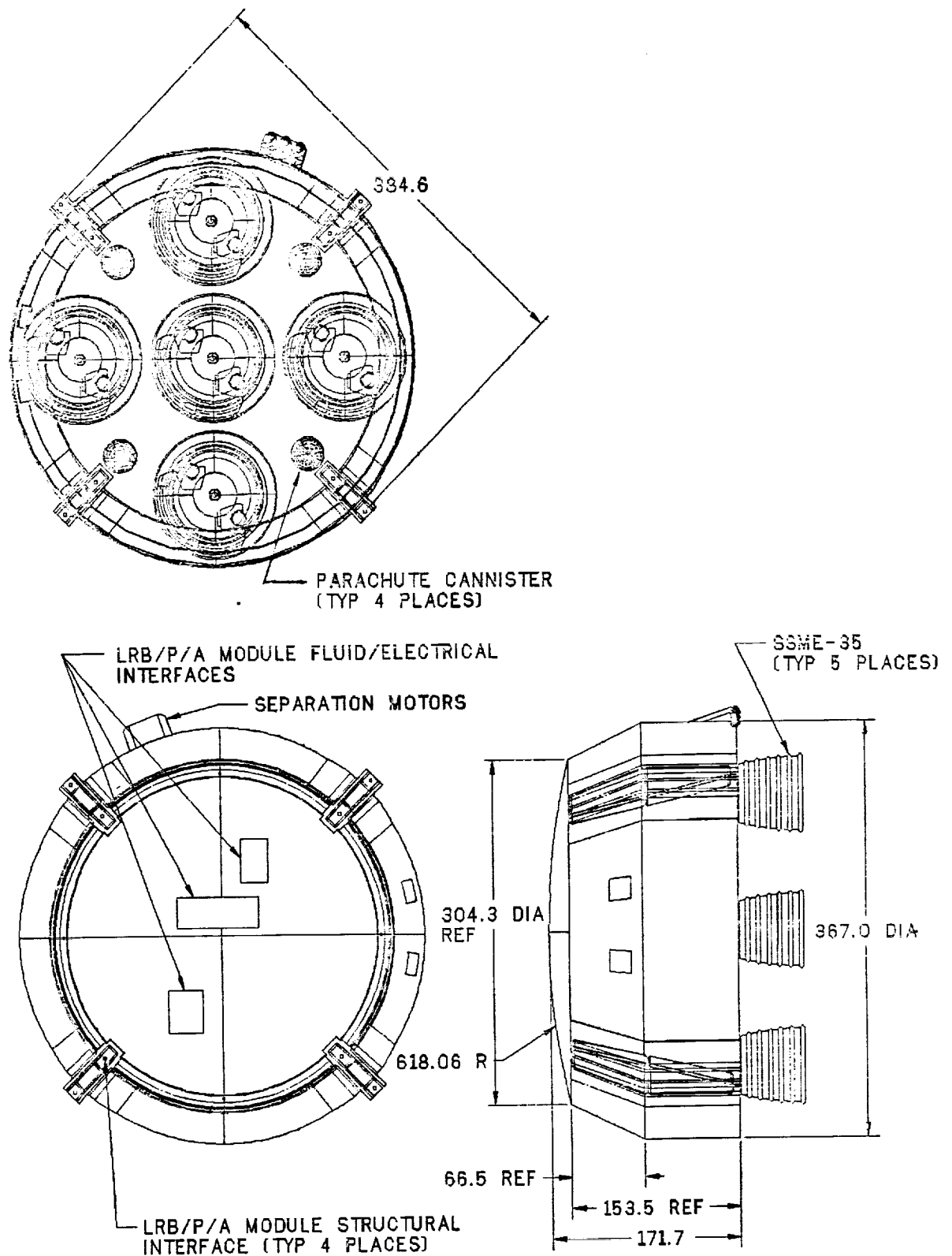


Figure 2.1-3 LRB P/A Module Configuration

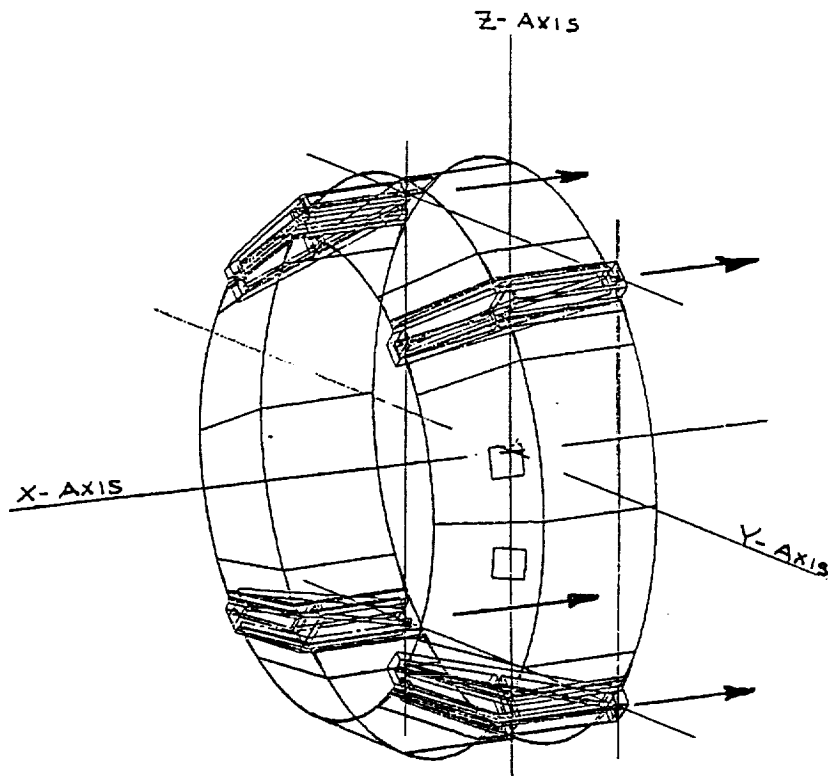
surrounding shell, and 3) the four attachments to the LRB tank section. Figure 2.2.1-1 shows axial (X-axis) holddown loads applied to the longerons. Preliminary design static loads for five on-pad conditions are tabulated. These conditions are: 1) STS empty on-pad, STS fully loaded on-pad with cryogenic shrinkage effects, 2) SSME start to maximum pitch over with static moment, 3) SSME start to maximum pitch over with the dynamic bending moment taken from the transient analysis, and 4) all engines at nominal launch thrust (orbiter SSMEs plus five LRB SSME engines at 88% in each module). Sign convention for the loads is + for compression and - for tension. The max/min loads shown do not occur on all holddown points, but all four longerons and fittings were sized for this peak load in the preliminary design. It is anticipated that a complete dynamic analysis of the module during SSME ignition and liftoff will show that all LRB tie down longerons will experience large shock forces and will require the large cross-sections as shown in Figure 2.2.1-2.

Attachment to the holddown posts on the MLP is made external to the skirt similar to SRB as shown by Section A-A. The upper joint attachment to the LRB skirt at the separation plane consists of four external explosive bolt assemblies which simplify vehicle assembly. Section C-C on the lower longeron side and Section D-D on the skirt side of the joint show that the large forgings are pocketed to allow assembly from the outside. Material for the forgings is Weldalite™ 049.

2.2.2 Thrust Beams

Two engine thrust beams, Figure 2.2.2-1, support the five engines and transfer thrust loads into the shell at points midway between the four holddown longerons. A preferred location for the engine mounting thrust beams, from the shell design standpoint, would have been to connect the thrust beams directly to the longerons instead of 45° around on the shell. To accommodate this preferred design and simplified load path would have resulted in a larger diameter of the aft skirt and further separation of the holddown posts in order to clear the large nozzles on the engines. The location chosen for the engines and thrust beams allows the large longerons to fit between engine nozzles without interference and allows the MLP booster exhaust holes to be smaller.

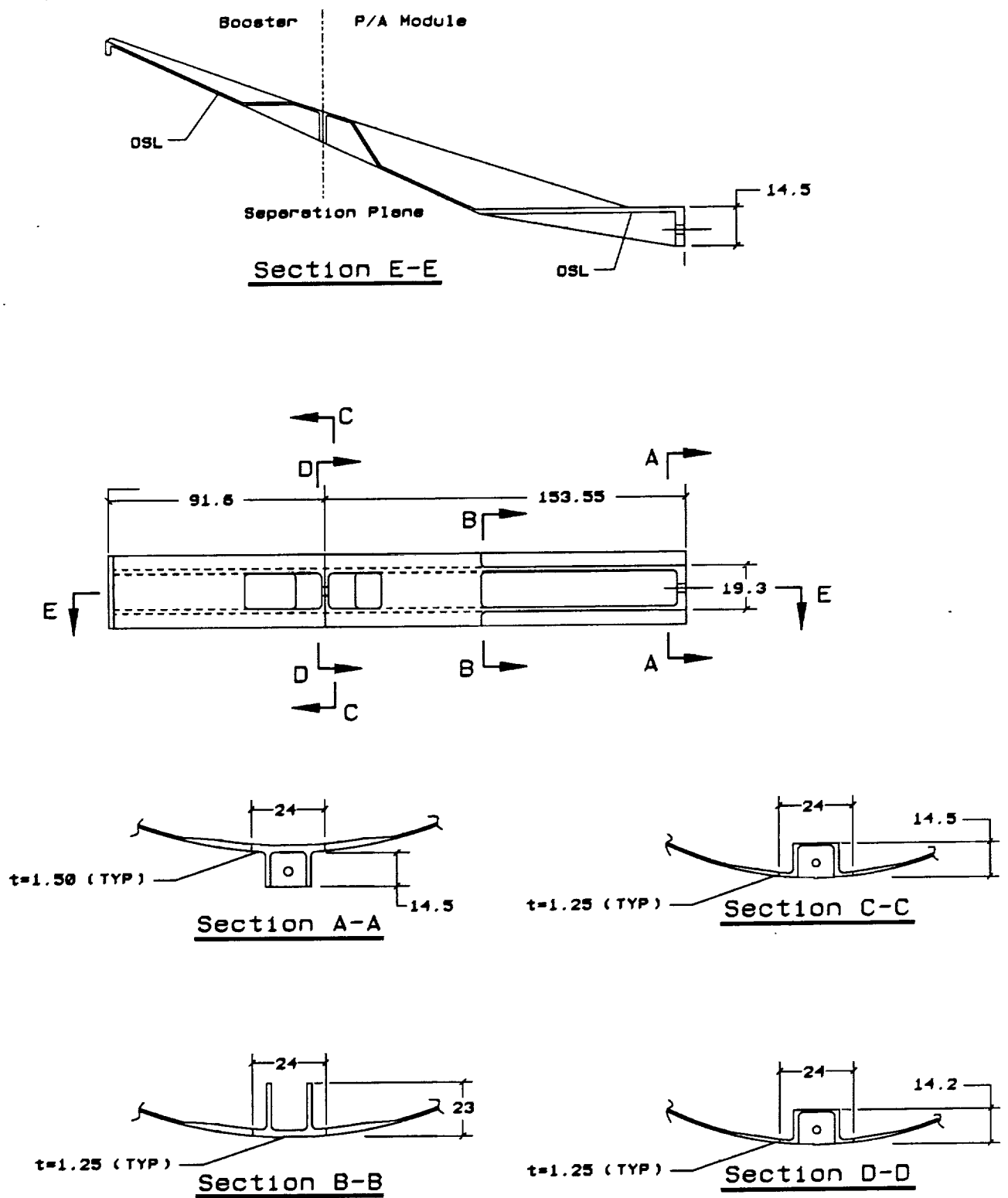
Figure 2.2.2-1 shows the 60 in. deep beams and the design loading conditions. Engine limit loads are shown boxed. The center sections of the beam webs are 2.5 in. deep corrugated webs 0.25 in. thick, and provide structural efficiency at high shear loads. Outboard panels, adjacent to the shell, are 0.60 in. thick plates. Thrust beam caps are



Condition	Max/Min Vertical Loads (kips)
Empty - On Pad	+145 +7
Fully Loaded - On Pad (with Cryo Shrinkage)	+590 +292
SSME Start - Max Pitchover (Static Analysis)	+664 -64
SSME Start - Max Pitchover (Transient Analysis)	+826 -226
All Engines (SSMEs + 5 LRBs @ 88%)	+120 -270

+ Compression Load
- Tension Load

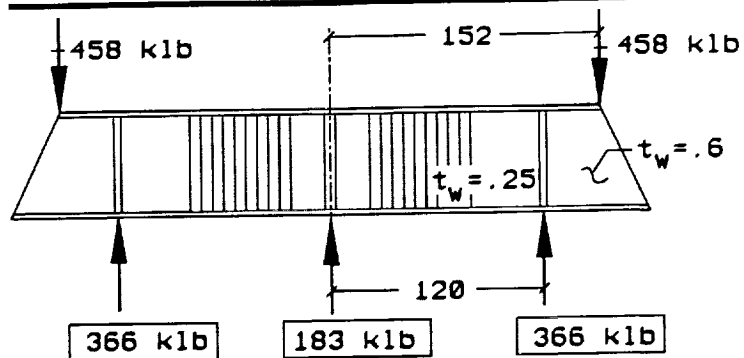
Figure 2.2.1-1 LRB P/A Module X Axis Holddown Loads



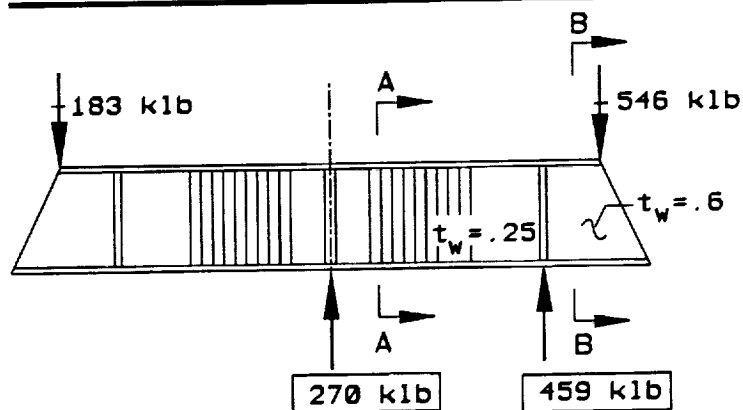
Material: Weldalite 049tm Forgings

Figure 2.2.1-2 LRB-P/A Module Hold Down Longerons

a) All Engines at 88% (416 klb at 100%)

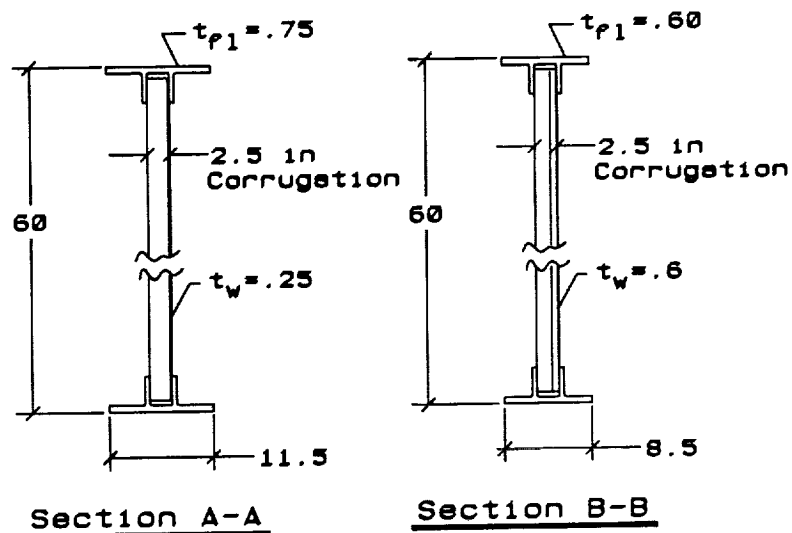


b) One Engine Out - Others at 109%



SSME 109% RPL Thrust=459 klb

Beams are Designed by the
One Engine Out Load Cases



Material: Beam Caps Weldalite 049™ Extrusions
Webs Weldalite 049™ Plate

Figure 2.2.2-1 LRB-P/A Module Thrust Beams

extrusions with flanges on either side of the corrugated webs to accommodate mechanical fasteners. All material for the plate and extrusions is Weldalite™ 049.

2.2.3 Nose Cap

- Water Impact Loads

Water impact pressures used for design of P/A module cap were computed based on an impact velocity of 25 ft/sec. The sea was assumed calm with no wind to cause drift or tilt. Figure 2.2.3-1 shows the mean pressure distribution over the time for the impact.

- Nose Cap Details

Figure 2.2.3-2 shows noscap geometry. The pressure/area relationships for the cap are also shown. The design point used for preliminary design is shown on the curve. This point experiences approximately 50 psi impact pressure over 120 ft² of nose cap area. Impact g levels are noted on the curve and reach a peak of approximately 11 gs.

The noscap cross-section is a 6.0 in. deep honeycomb sandwich with faceplate thicknesses of 0.50 in. in the center and 0.250 in. thick outboard. The faceplates are designed by the bending moment in the cap caused by the pressure, while the core is designed by the shear requirements at the supports and the high local crushing pressure.

A center support to the nose cap, off of the thrust beams, provides much of the support needed and helps to keep noscap bending moments within reasonable limits. This support allows impact pressures to be reacted partially by the beam weight, engine weight, and other equipment mounted to the beams.

Material used to construct the noscap is graphite-epoxy (GR-EP) for the faceplates and internal rings with a Hexcel aluminum 3/16 in. cell, 3.5 lb/ft³ core. Heating rates and duration after LRB separation are low enough to allow for a bare noscap, i.e., no thermal protection.

2.2.4 Shell Details

Figure 2.2.4-1 shows frame and shell plating details for the module. Frames are located at the separation plane of the module and the aft LH2 tank skirt, at the conical and cylindrical intersection of the shell, and at the shell trailing edge. Details of the frames are as presented.

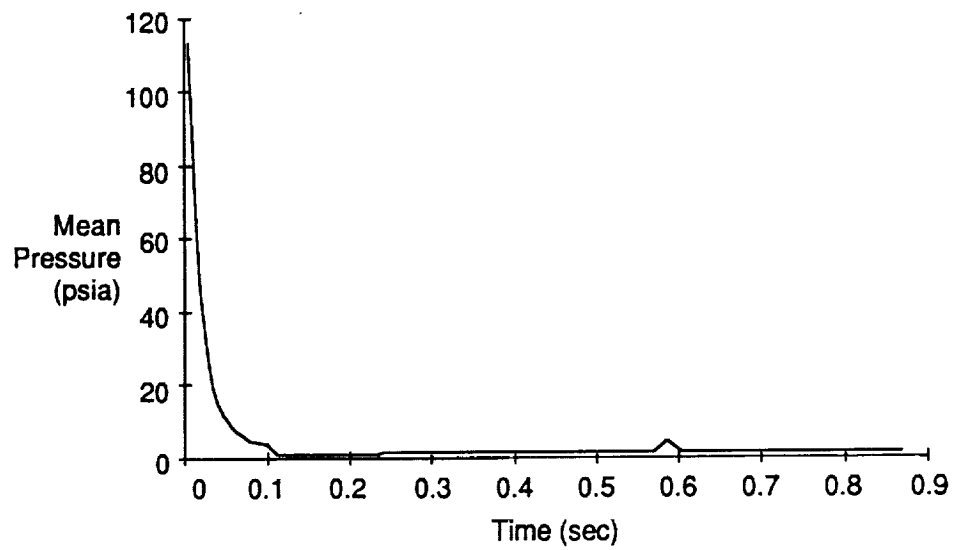
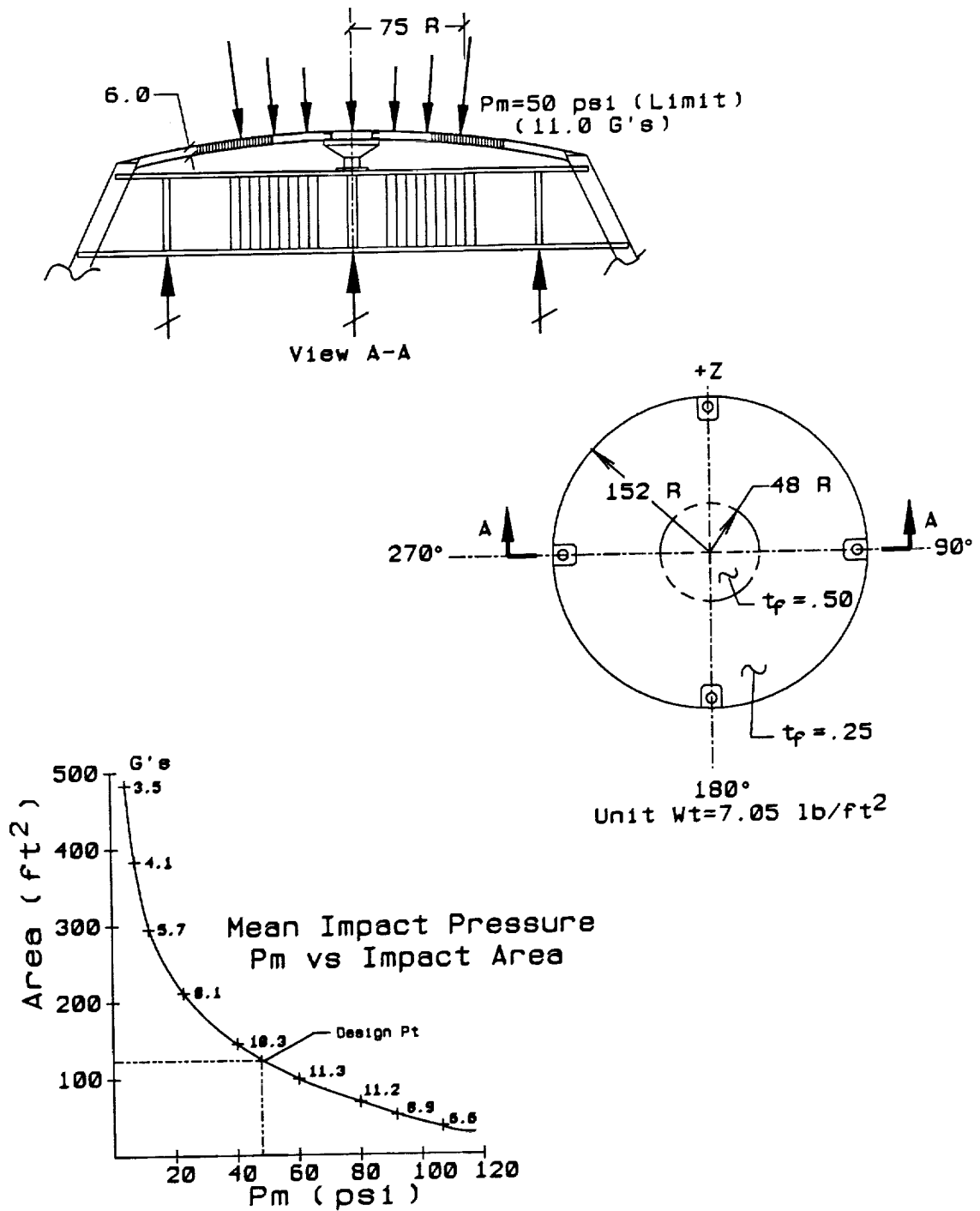


Figure 2.2.3-1 Water Impact Loads



Material: Skins - Graphite/Epoxy
Core - Hexcel 3/16-3.5 lb/ft³ A1
Rings - Graphite/Epoxy

Nose Cap : 6.0 in Thick Sandwich
Designed for Water Impact

Figure 2.2.3-2 LRB-P/A Module Nose Cap Geometry

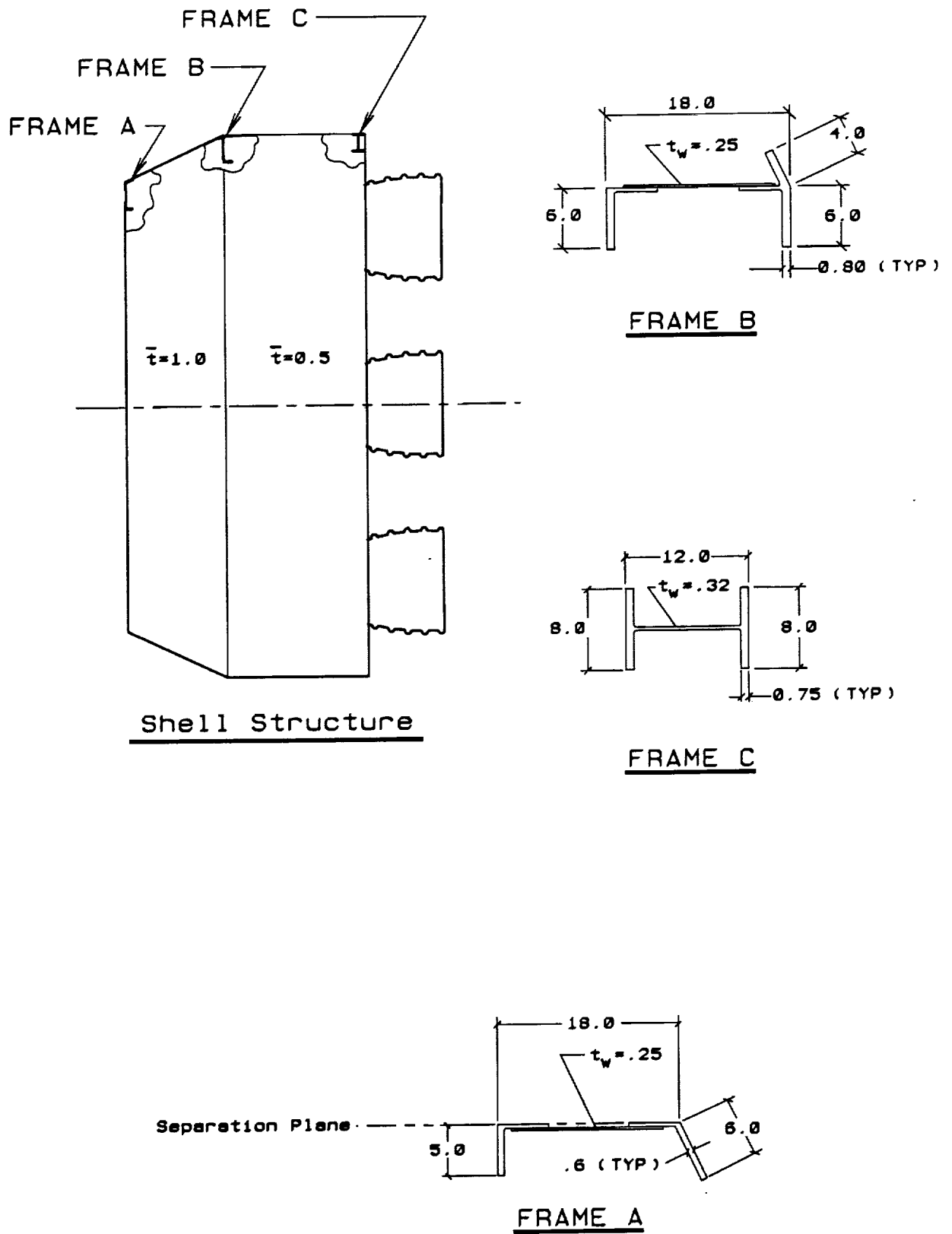


Figure 2.2.4-1 LRB-P/A Module Frame and Shell Details

The majority of the conical section of the shell is slightly less than 1.0 in. thick. At the holddown longerons, shell thicknesses are tapered to accommodate the 1.25 in. thickness of the longeron. Average shell thickness is 1.0 in. In the cylindrical shell section, average shell thickness is .50 in. Material used throughout is Weldalite™ 049.

2.3 P/A MODULE INTERFACES

2.3.1 LRB Interfaces

- Configuration

Maximum utilization of existing Shuttle interface hardware was a goal of the interface study. Only the structural interfaces will require new designed hardware. All other hardware is existing and may be used with some modification. The fluid and electrical disconnects will be mounted on umbilical plates located just under the surface of the heat shield. Access to the umbilicals is through openings with doors in the heat shield (Figure 2.3.1-1). After separation, the doors will be closed for the re-entry phase of flight.

- Structure

Structural interfaces consist of four hard points on the periphery of the P/A module. These interfaces will be held together with an explosive nut thruster, which not only provides mechanical separation, but also imparts some delta velocity to the separated segments. A conceptual design of the nut thruster is illustrated in Figure 2.3.1-2.

- Fluid

-- LO2 and LH2 Feedline Disconnects

The LO2 and LH2 feedline disconnects are identical to the 17 inch diameter disconnects that provide propellant feed capability between the External Tank and the Orbiter. Due to the quantity of propellants required by the five engines on the P/A module, two LO2 and two LH2 disconnects will be required. The disconnects provide the capability to separate and close-off the interconnecting feedlines. With the tank mated to the P/A module, the disconnect halves are held together by the umbilical separation system pyro bolts. After the disconnect halves are mated, the flapper closures located on either side of the interface are actuated open. These closures act as butterfly valves when open, imposing a minimum flow resistance. Prior to umbilical separation, the disconnect closures are pneumatically closed by an actuator in the P/A module. Drive linkages across

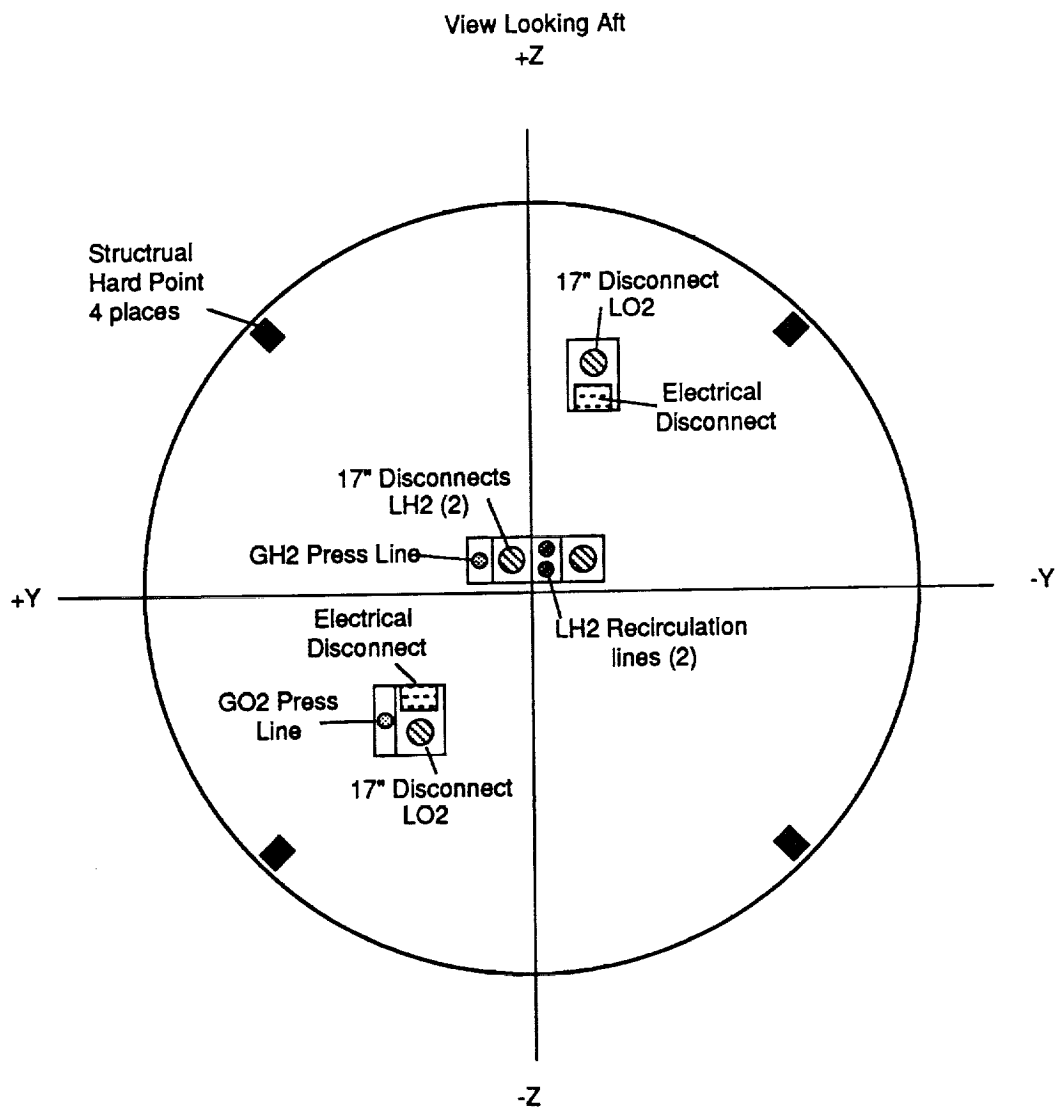
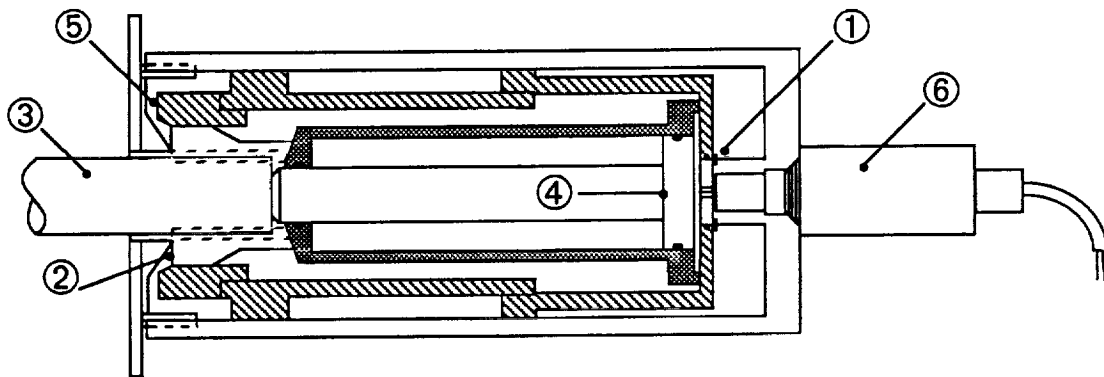


Figure 2.3.1-1 LRB / P/A Module Interfaces



Note: All Similarly Cross Hatched Parts Move As One Piece

- | | |
|-----------------|-------------------------|
| ① Shear Ring | ④ Piston |
| ② Segmented Nut | ⑤ Nut Restraint |
| ③ Bolt | ⑥ Dual Igniter & Charge |

Figure 2.3.1-2 Explosive Nut-Thruster Concept

the interface close the tank half of the disconnect, which in turn drives the closure in the P/A module half. The closures are mechanically driven to the closed position when the P/A module disconnect halves are retracted. This mechanical operation occurs regardless of the pneumatic actuator position. The trapped propellant between the disconnect closures is allowed to dump externally during separation. There are new 14" disconnects under development which have the same flow rates as the current 17" disconnects. These new disconnects will be used when they become available.

-- GO2 and GH2 Pressurization Line Disconnects

The 2 inch pressurization line disconnects are the same types used on the Orbiter and will transmit pressurant flow from the P/A module to the LO2 and LH2 tanks for ullage pressure maintenance. A Naflex seal is provided at the interface. Disconnect halves, once mated, are secured by the umbilical separation system bolts. Interface sealing is accomplished by a metal-to-metal seal. Coaxial poppet valves are contained in both disconnect halves and are forced closed by springs as the umbilicals are retracted.

-- LH2 Recirculation Line Disconnects

The recirculation line disconnects are the same disconnect that is used on the Orbiter. Two of these 4 inch disconnects will be needed to provide the capability to separate and isolate the interconnecting LH2 recirculation and tank replenishment line between the P/A module and the LH2 tank. A Naflex seal is provided at this interface. When mated, the disconnect halves are mounted together by the umbilical separation system. The separation interface is sealed by three compression type seals whose effectiveness is enhanced by media pressure. Swing arm closure disks located in each disconnect half are gear driven, and are capable of pneumatic or mechanical opening and closing. These disks are actuated open by P/A module pneumatic pressure once the disconnect halves are mated. The opening pneumatic pressure is maintained throughout the boost period. After separation P/A module pneumatic pressure is withdrawn actuating both swing arm disks to the closed position. Spring forces on each disk serve as a backup for disk closure. Fluid trapped between the two closed disks is dumped externally as the disconnect sections are disengaged.

-- Electrical Disconnects

The electrical disconnects will be the same as those used on the ET to Orbiter interfaces and will all have shell size 22 receptacles. The connectors are each affixed to a

common cluster plate at the respective umbilical interface and are located approximately on 2 inch centers. Each plate will contain 12 connectors of various configurations of inserts.

2.3.2 Ground Interfaces

The existing launch processing facilities must be modified to accommodate the greater size of the LRB with a P/A module and to provide increased propellant servicing capability at the launch pads. The principal facilities that must be modified are the Mobile Launch Platform (MLP), launch pad, and VAB. Major MLP modifications required will include: a new propellant system, a new or repositioned hold down post and system, and enlarged flame holes for the larger LRB engine plumes. The principal change to the launch pad will be the installation of new propellant storage and transfer systems. The ET GO₂ or ET hydrogen vent arms will have to be modified to enable them to reach the ET around the larger LRB. The principal changes required to the VAB will be modification of interior platforms to accommodate the larger diameter LRB.

2.4 RECOVERY SYSTEM

The recovery system consisted of the following elements: 1) ballistic P/A module; 2) drogue parachute; 3) four main parachutes; and 4) flotation bags. The recovery method is parachuting into the ocean. Following LRB separation from the ET, the P/A module separates from the LRB. The remaining part of the LRB (nose cone, LO₂ tank, intertank, and LH₂ tank) is expendable. Figure 2.4-1 provides the recovery system arrangement. The parachutes characteristics are presented in Table 2.4-1.

Prior to impact, four flotation bags are deployed to provide positive flotation (Figure 2.4-2). Each bag is 8 ft in diameter and 22 ft long.

3.0 VEHICLE ANALYSIS

3.1 AERODYNAMIC ANALYSIS

3.1.1 Aerodynamic Characteristics

High drag and good stability are desirable aerodynamic characteristics for a ballistic reentry configuration. A nose radius to nose diameter ratio of two contributes to both high drag (97% disk drag) and good stability where the nose center of pressure (C_p)

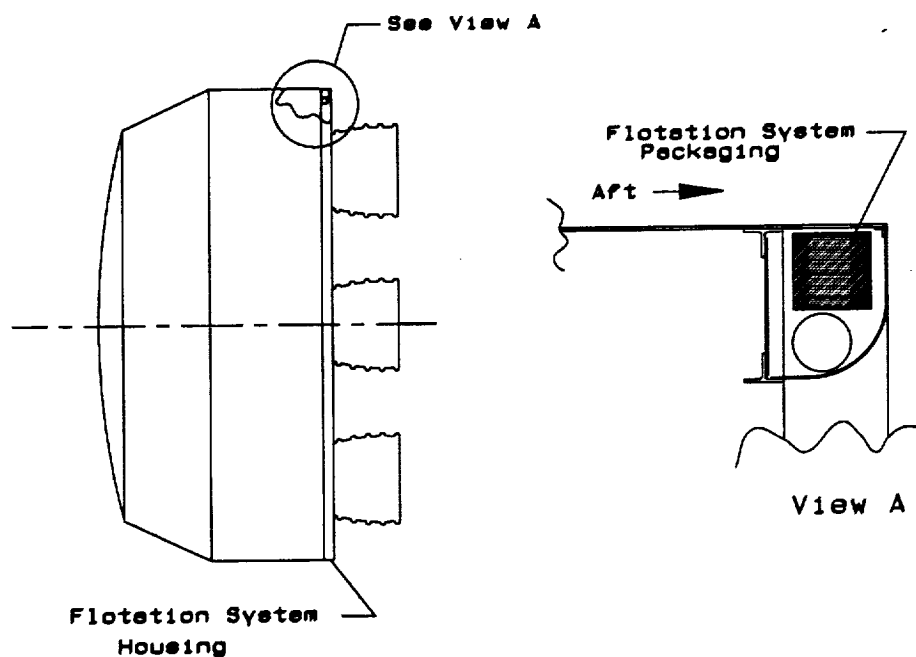
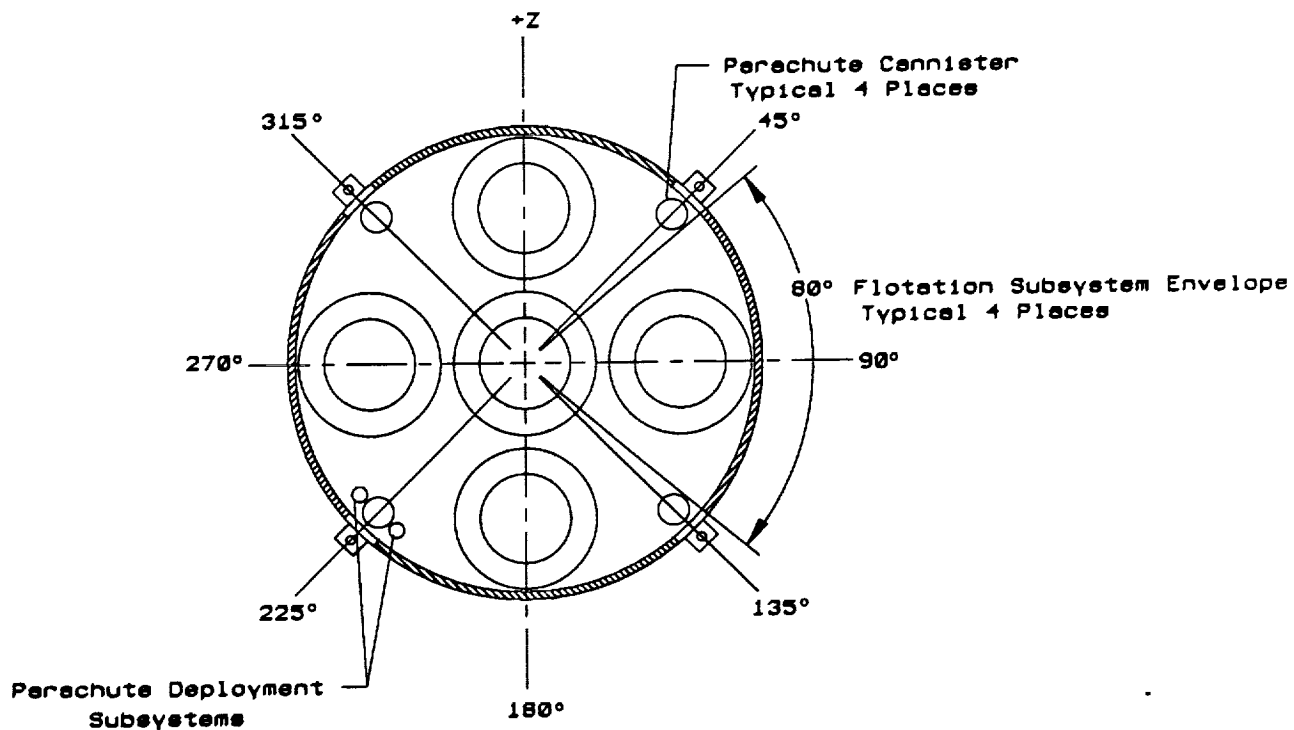


Figure 2.4-1 LRB-P/A Module Recovery System Arrangement

Description	Number	Size (ft)	Fill Time (sec)
Drogue Parachute	1	46	7.5
Main Parachute	4	225	40
Flotation Bag	4	8X22	

Note: Drag Coefficient per Main Parachute of 0.85
Parachute Cluster Efficiency of 0.85
Calm Seas
No Wind at Splashdown

Table 2.4-1 Recovery System Characteristics

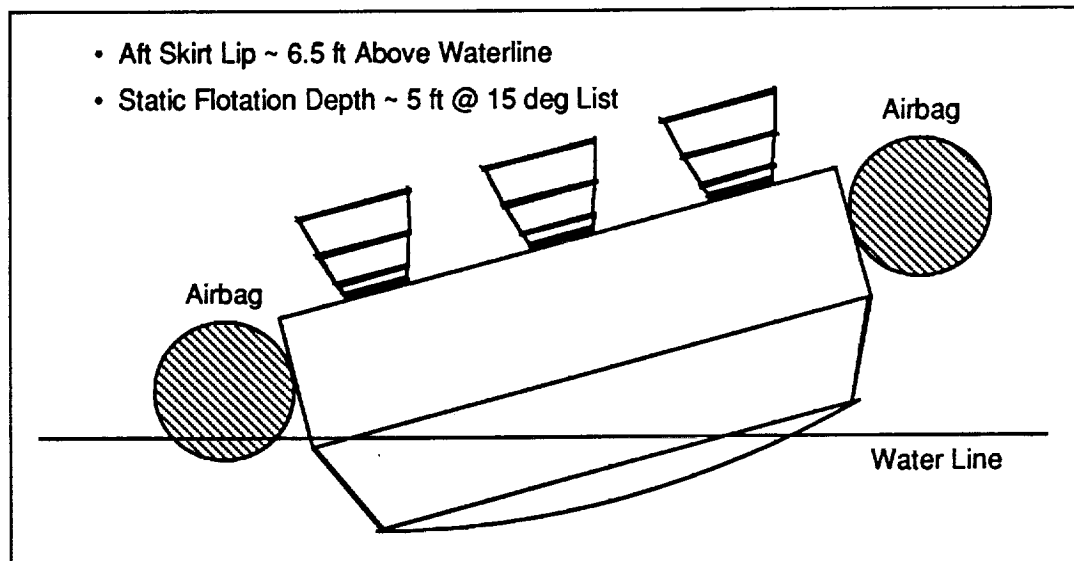


Figure 2.4-2 Flotation Bags

is located at the nose radius origin. The 25.2° cone frustrum also contributes to the aerodynamic stability.

The Hypersonic Arbitrary Body Program (HABP) with the modified Newtonian and Prandtl-Meyer expansion options at mach number five was used for computing the LRB/P/A vehicle aerodynamic coefficients. As shown by the stability margin and trim condition charts (Figure 3.1.1-1), the vehicle exhibits good "stability margins" of 20% to 10% for longitudinal cg locations at 80 to 125 inches aft of the nose cap (Sta 0). The stability margin is the distance between the longitudinal cg and the aerodynamic C_p expressed as a percentage of the vehicle diameter. The stability margin is 14.6% for a longitudinal cg = 108.3 inches and is independent of the vehicle angle of attack and offset cg. In addition, the vehicle will trim at about five degrees angle of attack for reasonable offset cgs of 3.0 to 1.5 inches and longitudinal cgs of 80 to 125 inches.

As shown by the aerodynamic characteristics (Figures 3.1.1-2 through 3.1.1-5), the normal force, pitching moment coefficient and lift to drag ratios are linear with angle of attack. For low angles of attack ($\approx 10^\circ$), the axial force is equal to the drag force and decreases about 1% of maximum drag for each five degree change in angle of attack. The lift to drag ratio is small ($\approx .001$ per degree alpha) and decreases for an increase in angle of attack.

The LRB/P/A ballistic shape has been configured for high drag, low L/D, and good stability such that reasonable offset cgs and changes/shifts in the longitudinal cg may be accommodated.

3.1.2 Aerodynamic Loads

The LRB/P/A module nose cap, cone frustrum, and cylinder pressure distributions were computed at the maximum reentry dynamic pressure of 367 psf at Mach 2.97 employing the modified Newtonian and Prandtl-Meyer expansion theories. Referenced to ambient pressure, the maximum wall pressure is about 4.5 psig. This data is depicted in Figure 3.1.2-1.

3.2 AEROTHERMAL ANALYSIS

Both ascent and reentry aeroheating rates for key P/A module body points were generated using the LANMIN computer code. These rates were computed assuming a cold wall temperature of 0° F. Heating rate plots for each of the body points are shown in Figures 3.2-1 through 3.2-4. Body point No.1 shows no initial heating since the location

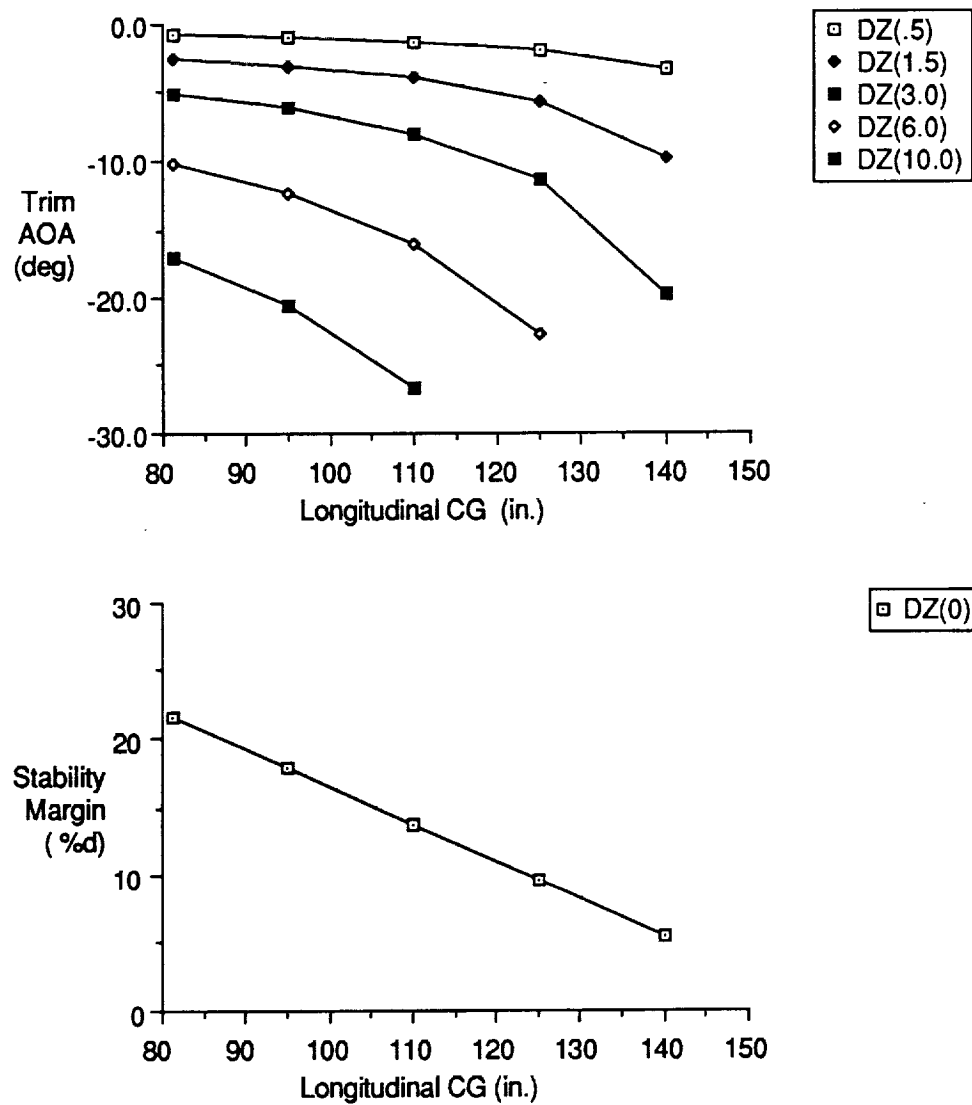


Figure 3.1.1-1 Stability Margin and Trim Conditions

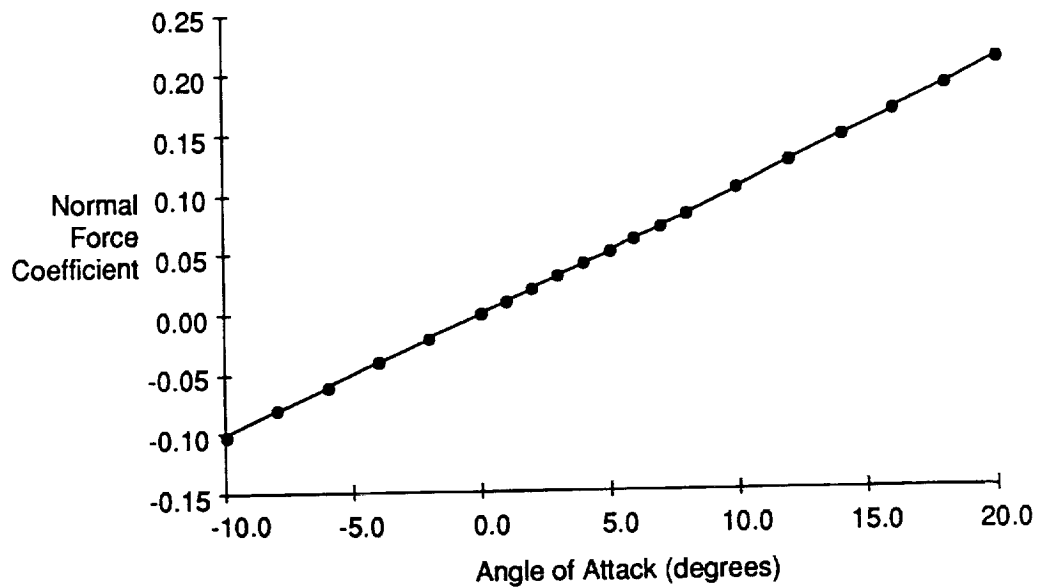


Figure 3.1.1-2 Aerodynamic Characteristics - Normal Force

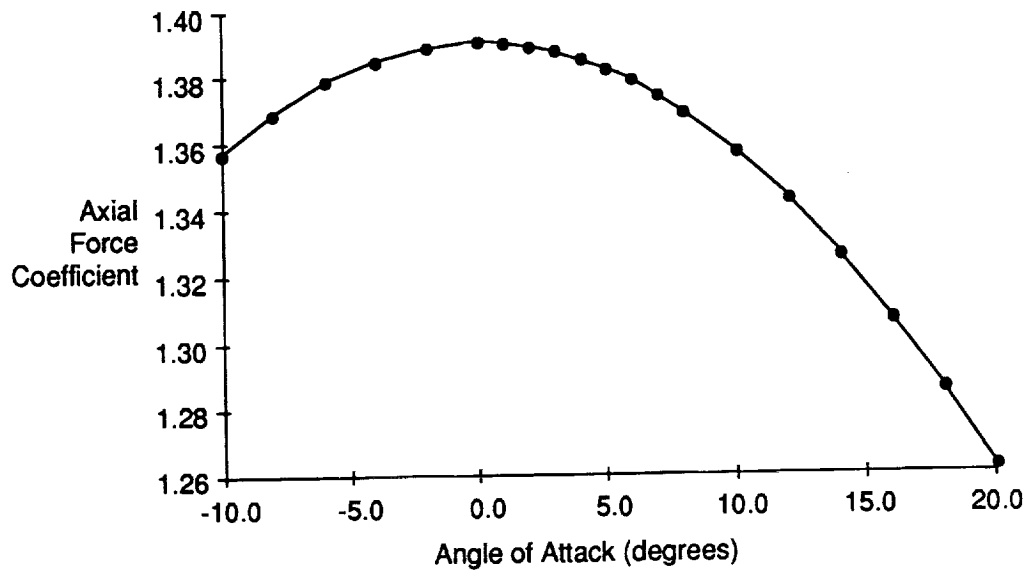


Figure 3.1.1-3 Aerodynamic Characteristics - Axial Force

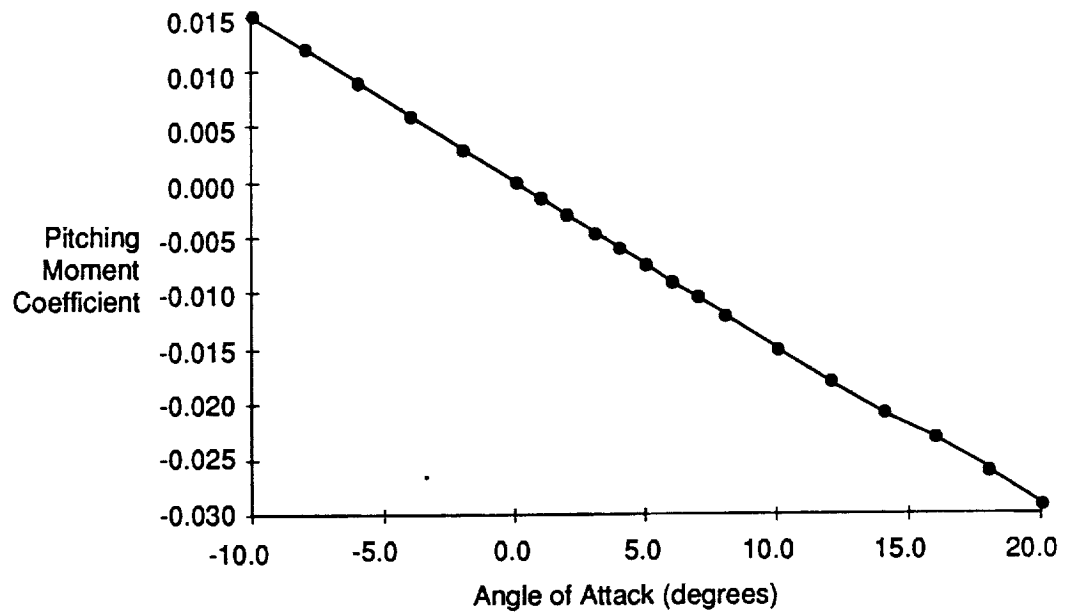


Figure 3.1.1-4 Aerodynamic Characteristics - Pitching Moment

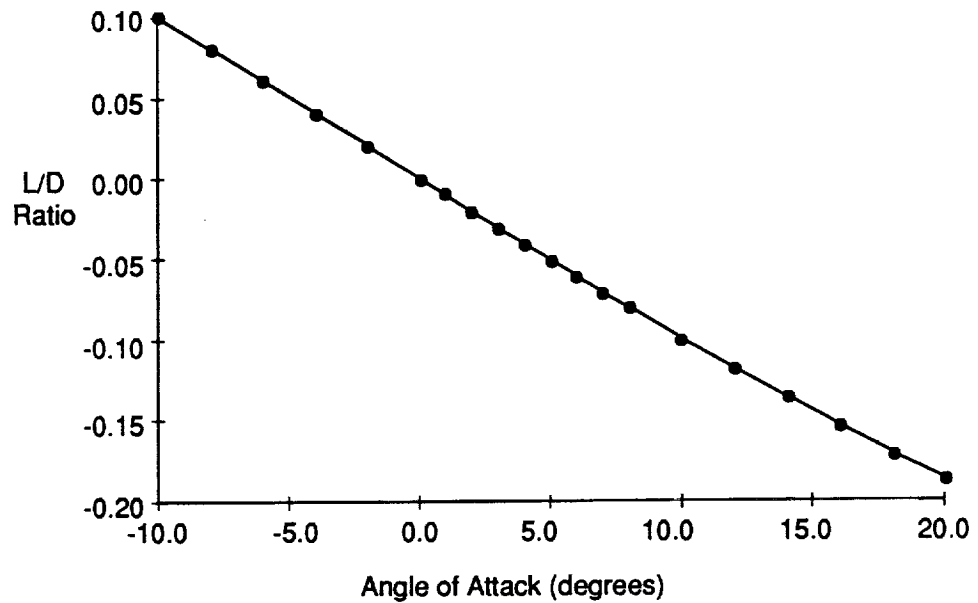


Figure 3.1.1-5 Aerodynamic Characteristics - L/D Ratio

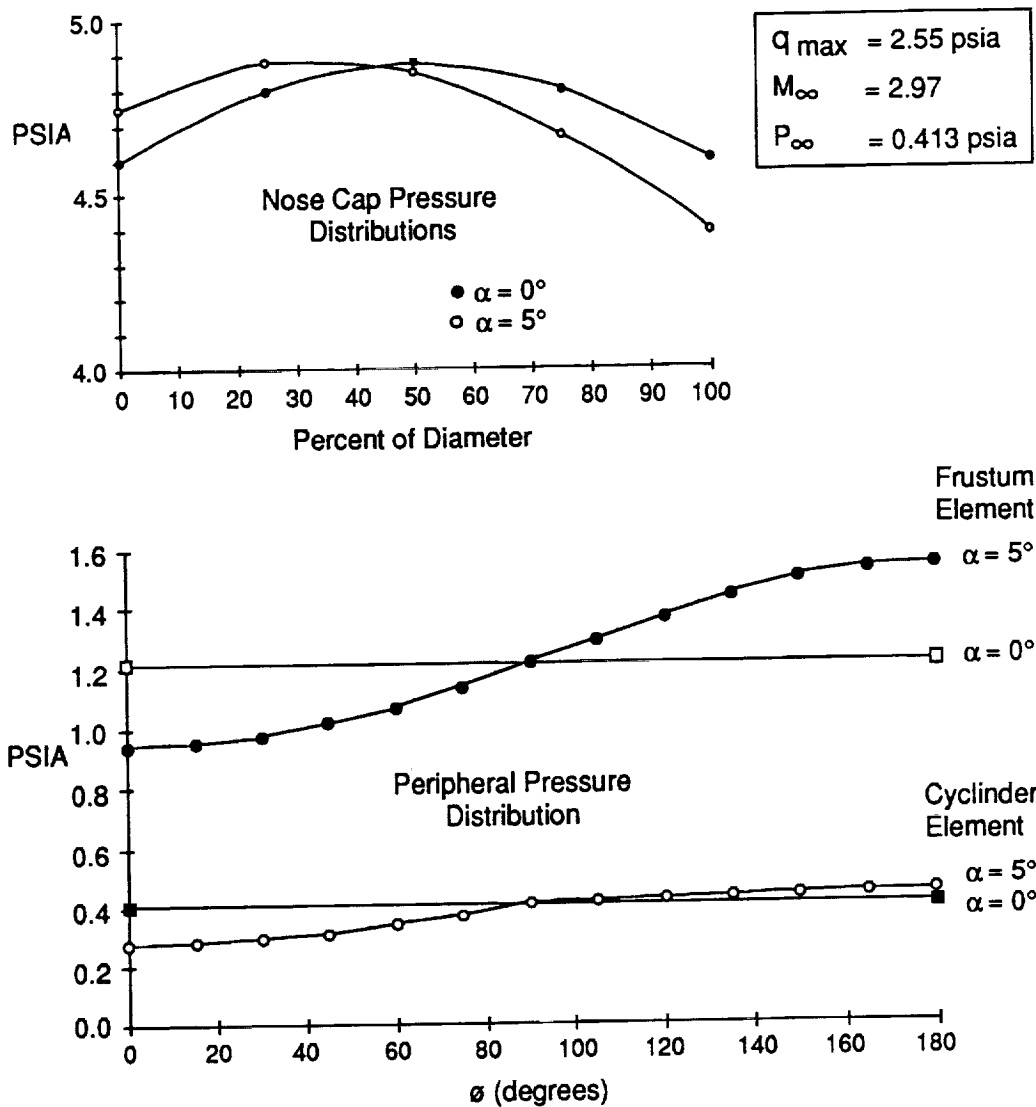


Figure 3.1.2-1 Aerodynamic Loads

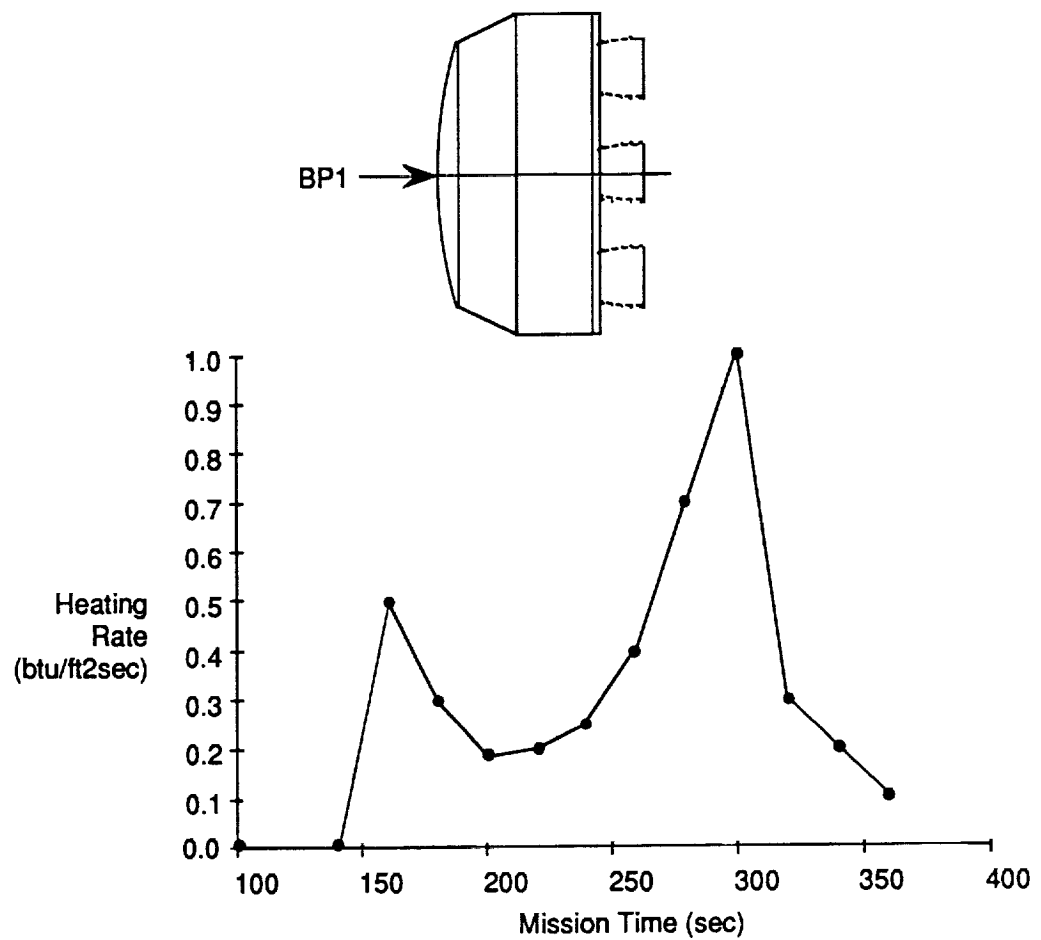


Figure 3.2-1 Ascent and Recovery Heating Rates - BP1

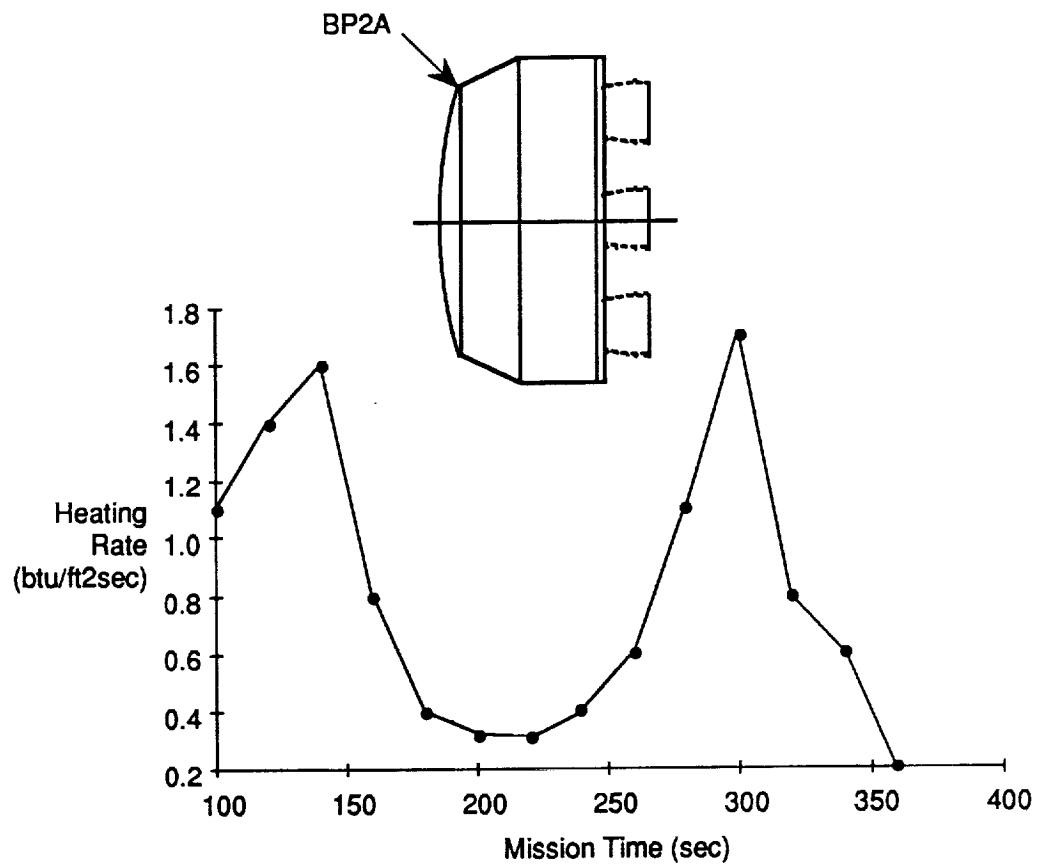


Figure 3.2-2 Ascent and Recovery Heating Rates - BP2A

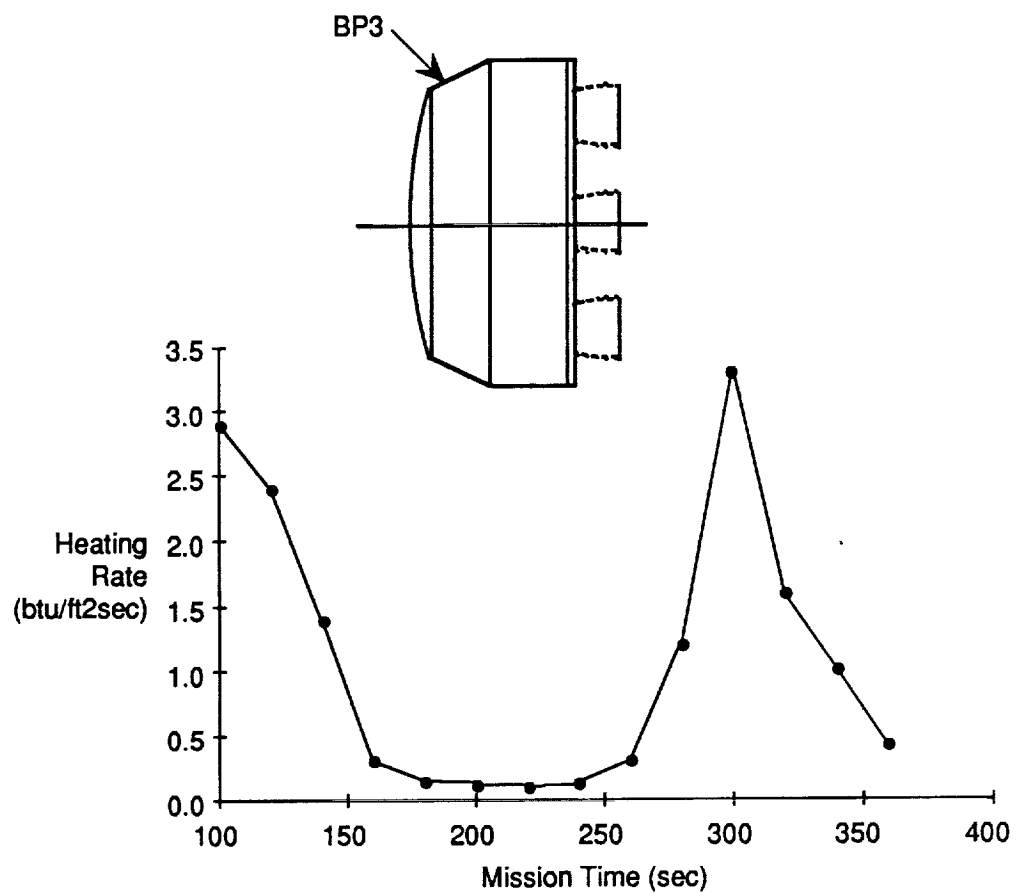


Figure 3.2-3 Ascent and Recovery Heating Rates - BP3

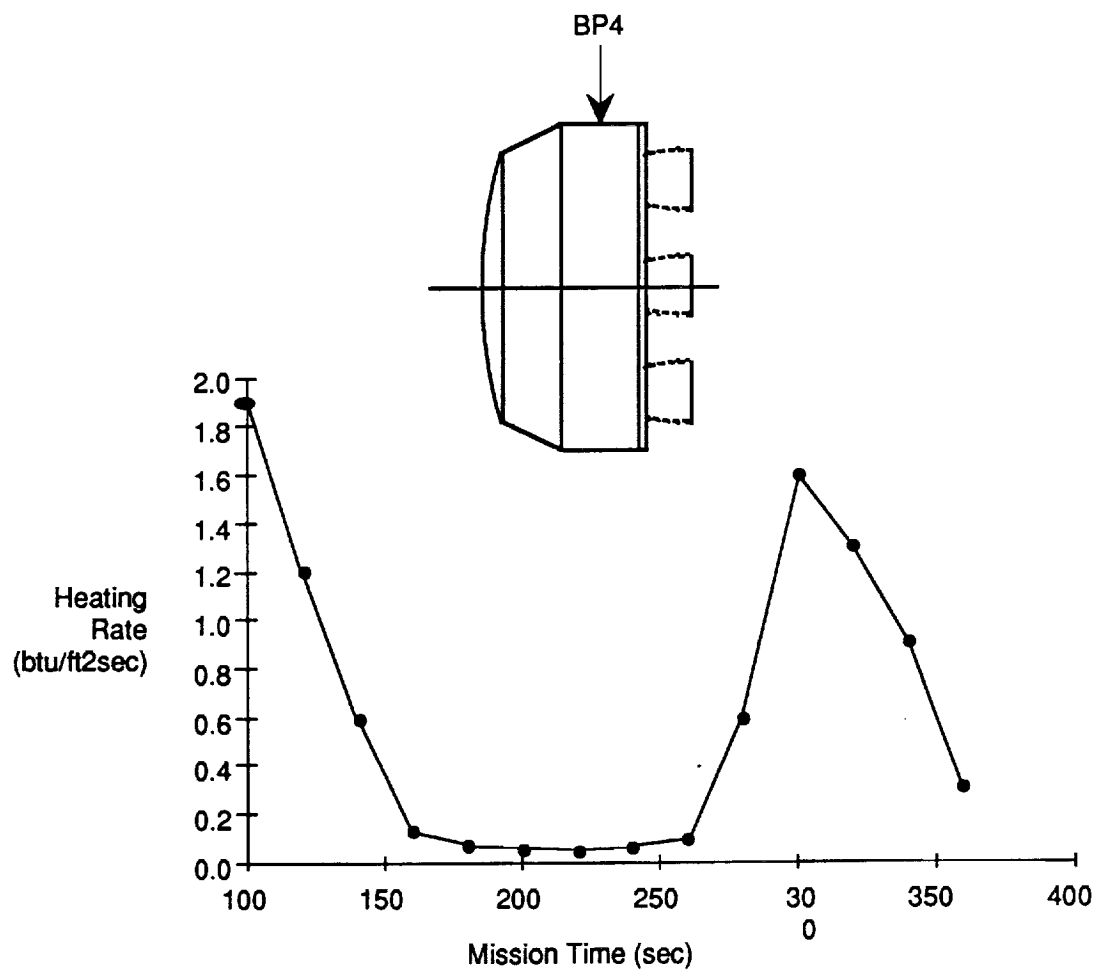


Figure 3.2-4 Ascent and Recovery Heating Rates - BP4

is not exposed during the ascent portion of the flight. Total heat loads produced by these rates ranged from ~35 btu/ft² at BP#4 to ~80 btu/ft² at BP#3.

3.3 THERMAL ANALYSIS

Thermal analyses were performed to size the TPS and structure required to maintain the LRB P/A module structural temperature equal to or less than 350°F from lift-off to splashdown. Results for structural parametric sizing are presented in Figure 3.3-1 and TPS (NCFI) thickness requirements are shown in Figure 3.3-2.

The P/A module nose cap, BP1, is not exposed to aeroheating until after LRB separation because the nose is covered during first stage flight. The forward skirt, BP2a and BP3 experiences aeroheating throughout the flight, but no plume radiation is experienced because its surface is turned to a view away from the SSME engine plumes. The aft skirt, BP4, was exposed to aeroheating throughout flight and is also assumed to be exposed to SSME radiation.

3.4 RECOVERY

Several reentry trajectory simulations were performed to support this study. The POST computer program was used for these simulations. The recovery system consisted of the following elements: 1) ballistic Propulsion Avionics module; 2) drogue parachute; 3) four main parachutes; and 4) flotation bags. Recovery was from the ocean.

LO2/LH2 booster propellant was designated. SSMEs were used for engines. Each had an expansion ratio of 35 and are designated as SSME35s. These engine characteristics and booster weight estimates, including recovery system weight, were used in the booster sizing analysis. The booster reference mission which resulted from the original LRB contract was used. It specified that the STS/LRB ascent launch vehicle provide at least 70,500 lb of payload to a 160 NM orbit without violating any STS constraints. Each booster has five SSME35 engines. For the nominal mission these engines are operated at 87.2 percent of rated thrust. This provides mission completion capability for single booster engine failure or shut down at any time during booster flight.

An important objective of this reentry study was to size the main parachutes so that the descent velocity at water impact was 25 ft/sec or less. Predicted reentry performance of the final recovery system configuration also provided flight profile data to

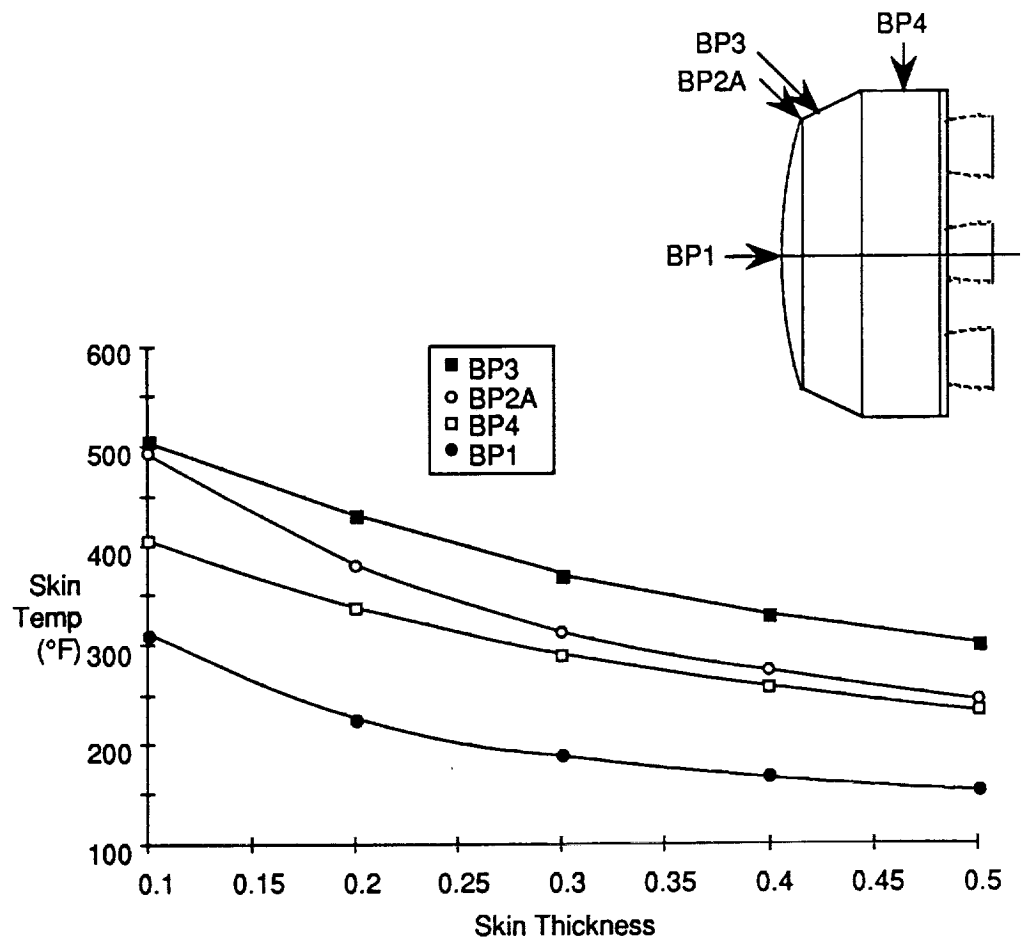


Figure 3.3-1 Structural Parametric Sizing

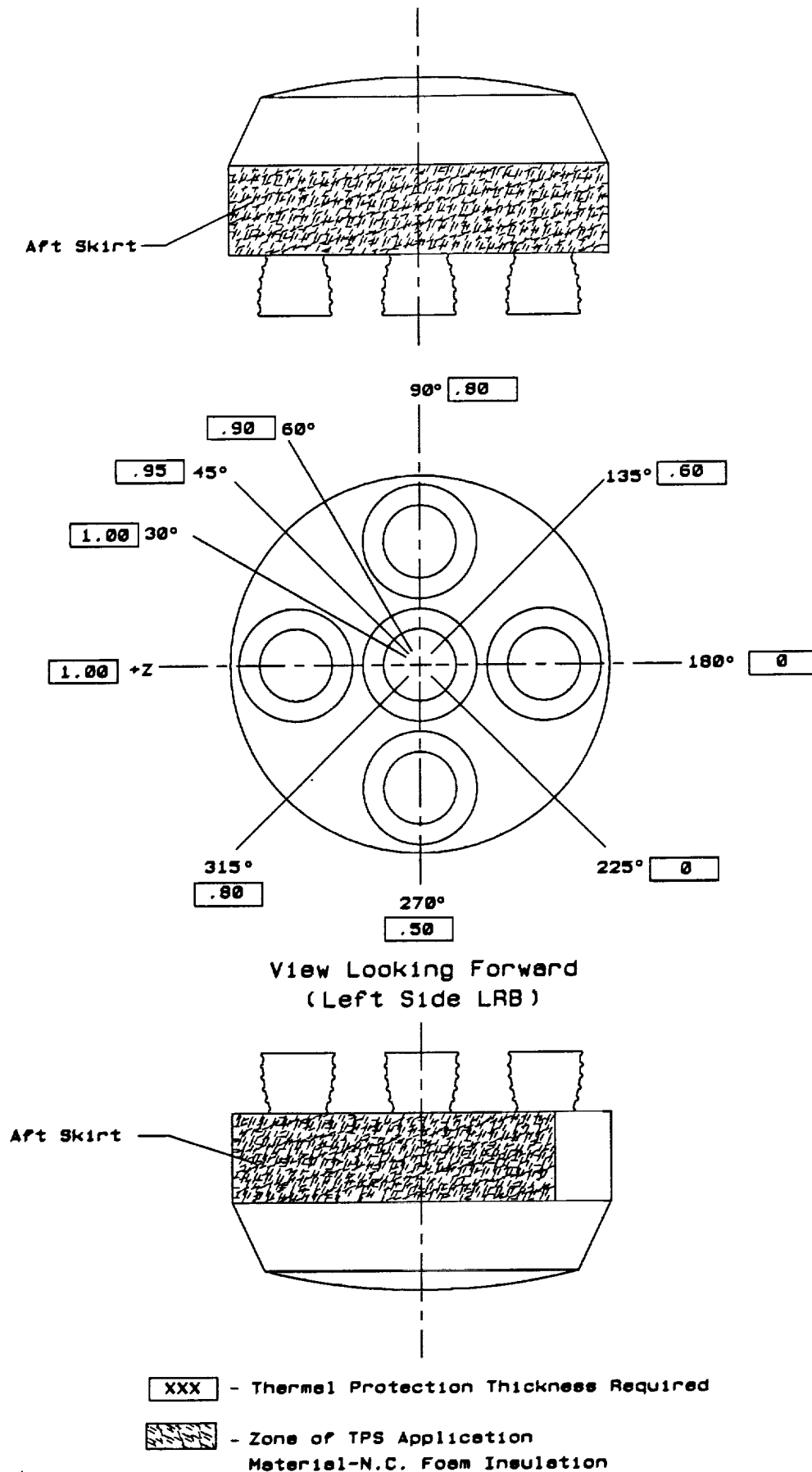


Figure 3.3-2 LRB-P/A Module TPS Thickness Requirement

support computation of 1) ballistic P/A module reentry air loads; 2) rigid body parachute inflation loads (no line stretch); 3) acceleration loads, and 4) reentry heating.

Parachute drag coefficient estimates were obtained from a parachute technology study made by Pioneer Parachute Company. The level of detail required to provide parachute reefing schedules could not be provided within the scope of this study. Inflation factors similar to existing parachute systems were used. It is felt that the parachute fill times are reasonable and could easily be accomplished with realistic reefing schedules.

A summary of the recovery events sequence is provided in Figure 3.4-1.

An estimated P/A module CdA of 1014 ft sq was used in the recovery system simulation. It was assumed that there are no appreciable tip-off attitude rates and that the angle of attack remained zero during the ballistic phase of the reentry trajectory. Using the P/A module weight of 81,557 lb and the CdA of 1014 ft sq a ballistic coefficient of 80.4 psf is obtained. Both maximum dynamic pressure and maximum acceleration occur in the ballistic portion of the reentry trajectory.

Results of the main chute sizing indicated that a cluster of four parachutes, each having a diameter of 225 feet, was required to limit the descent velocity to less 25 ft/s. The maximum dynamic pressure, 334 psf, occurred at 312 seconds flight time (flight time is referenced to liftoff of the ascent launch vehicle). Maximum parachute inflation loads were 135,840 lb and 132,078 lb for the drogue chute and main cluster respectively. The maximum acceleration load is predicted to be 4.26 gs. The above data represent the maximum values experienced during the nominal reentry trajectory and do not include any effects of possible dispersions.

3.5 MASS PROPERTIES

3.5.1 LRB P/A Module Weight Statement

The ballistic P/A module weight was calculated with information detailed in both design layouts and analysis results. The structural members weights were calculated in one of three ways depending on the level of information available. The nose cap frame, nose cap support and longerons properties were calculated using cross sectional areas. The forward and aft skirt shell properties were calculated using average thicknesses. The bulkhead, bulkhead frame, aft frame and thrust beam properties were based on specific dimensions. The nose cap properties were based on the calculated surface area.

Thermal protection system calculations used current STS properties data. The result of this analysis called for protection in the aft skirt area due to engine plume heating.

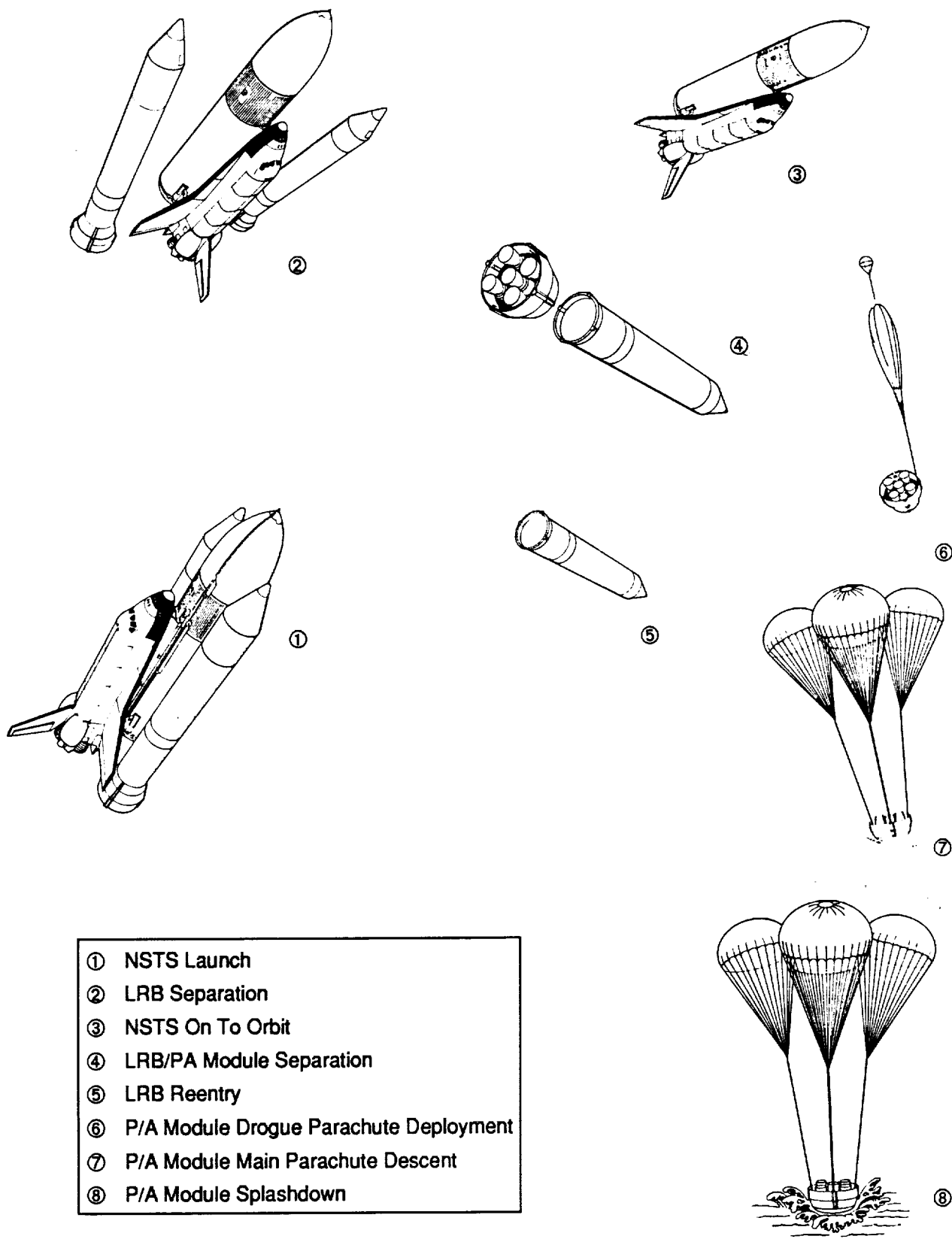


Figure 3.4-1 Recovery Events Sequence

The drogue and main parachute weights were based on Pioneers' Advanced Recovery System (ARS) study. A segmented toroidal bag formed the flotation device and was sized to maintain the floating P/A module at a list angle below 15°.

The propulsion system weight included a vendor weight for SSME -35 engines, weight from existing feed line disconnects, standard straight and flexible feed lines, and corresponding prevalves. The manifold weight was calculated from a layout drawing.

The thrust vector control system, separation motors, avionics and range safety system as well as items not mentioned above remained unchanged from previous LRB studies.

3.5.2 LRB Weight Impact

The recoverable P/A module was compared to a corresponding aft section of an expendable booster with five STBE engines and a tank diameter of 18.1 ft. The difference in weight was due to differences of structure, propulsion systems and the landing and recovery systems on the P/A module.

The structural weight penalties for the P/A module were a result of the landing (splashdown) loads, different diameter and shape of the skirt shell, and the integration of landing and recovery hardware.

The P/A module skirt shell was larger in diameter and had a higher average thickness. Due to the larger diameter, the overall bending loads decreased. The size and weight of the longeron fittings decreased for they are designed in part by these loads. The larger skirt was responsible for increases in the bulkhead area, the bulkhead and aft frame diameter, and the thrust beam length. The weight for each of these items increased.

Items which were part of the P/A module but not required in the expendable booster were the nose cap, the nose cap frame, nose cap support, and all landing and recovery related hardware. Table 3.5.2-1 presents the LRB with a P/A module weight summary.

3.6 FLIGHT PERFORMANCE

The reference mission used for the LRB/P/A module ascent simulation evolved during the initial LRB contract. It is a combination of the original STS BRM-1 and performance characteristics from STS-26 trajectory design data package (TDDP). Once this reference mission was defined, it has not changed. The trajectory details are provided in Table 3.6-1. These parameters accurately reflect current STS characteristics. The

Item	Weight (lb)
Structure	24,612
TPS	101
Landing & Recovery	5,273
Propulsion System	39,526
Thrust Vector Control System	1,280
Separation System	456
Avionics	2,744
Range Safety System	150
Growth	7,414
Total	81,557
Center of Gravity	inches
x (forward point of nose cap)	104.0
y (vehicle center line)	0.1
z (vehicle center line)	0.1

Table 3.5.2-1 LRB P/A Module Weight Summary

STS/LRB Must Provide 70,500 lb Payload for the Following Mission:	
Launch Site	ETR
Launch Month Mean Winds	Feb
Inclination (deg) (Direct Insertion)	28.5
Altitude (nm)	160
SSME Maximum Power Level (%)	104
Orbiter	OV-103
First Stage Design Criteria	
Dynamic Pressure Limit Dispersed (psf)	819
Dynamic Pressure At Staging Less Than (psf)	75
Q-alpha (psf-deg)	-3000
Maximum Axial acceleration (g)	3.0
Operator (lb)	0
Crew (size/days)	5/4
ET Usable Propellant (lb)	1,590,000
OV 103 MECO Weight (w/o Cargo)	208,229
ET Jettison Weight	74,821

Table 3.6-1 LRB Reference Mission Payload Requirement

vehicle payload capability represents an increase of about 20,000 lb over the present STS/RSRB. Another of the LRB contract requirements was that the vehicle had to be able to perform a safe intact abort with one booster engine out. Martin Marietta has additionally established as a mission goal that pump-fed LRB be able to complete the mission with one booster failed or shut down at any time. This is provided by running each of the five booster engines at 87% power level. Should a booster engine failure occur, the other four engines are throttled to the maximum power level of 109%. The resulting power level then matches the power level of the opposite booster with five engines operating.

The objective of the booster sizing and ascent flight simulation was to provide a recoverable LRB that would meet the payload requirement without violating any of the current STS ascent flight constraints. Previous LO2/LH2 LRBs that have been defined were expendable. The approach was to start with the expendable LO2/LH2 LRB and apply these changes: 1) Add the recovery system; 2) Make customer directed engine change; and 3) Update launch vehicle aerodynamics.

By adjusting the usable propellant, a recoverable LRB that provides 71,600 lb of payload for the booster reference mission (BRM) was obtained. The booster separation flight conditions were used to start the reentry flight simulations. Table 3.6-2 presents the results of the LRB/P/A module performance analysis.

4.0 COST ANALYSIS

4.1 GROUND RULES, ASSUMPTIONS, AND RESULTS

The programmatic groundrules are consistent with the earlier LRB studies and conform to the groundrules set by NASA. The NASA groundrules defined the flight rates and the support, reserve, and fee factors in order to establish consistency throughout the program cost estimates. The flight rate was set at 14 per year after an initial ramp rate of 4, 8, and 12 in the first three years. The LCC estimates are based on a 10 year program for a total of 122 shuttle flights (i.e., 244 boosters). The groundrules used in this analysis require all cost estimates in undiscounted 1987 dollars. The 40% government wraparound factor includes a 5% government support factor, a 25% management reserve factor, and a 10% contractor fee factor. It is important to note that we have included this 40% factor in all cost estimates except when noted. Table 4.1-1 identifies all of the groundrules and assumptions.

In addition to the programmatic groundrules and assumptions, the issue of reusability requires further definition of key variables. Table 4.1-2 identifies the baseline

Payload	71,660 lb
Manager's Reserve	1,160 lb
Thrust / Weight @ T-0 sec	1.31
Gross Lift-Off Weight (GLOW)	3,557,678 lb
Max Dynamic Pressure	703.3 psf
Throttle Schedule	constant 88% RPL
Burn Time	143.0 sec
Coast Time	2.4 sec
Jettison Weight	318,474 lb
LRB Engine-Out Capability	T-0 sec & Make Mission
Sea Level (Vac) Isp @ 100% RPL	390.33 (438.8) sec
Useable Propellant Wt/Booster	647,247 lb
Mixture Ratio	6.0 :1
Engine Exit Area	20.715 sq ft
Booster Lift-off Weight (BLOW)	806,484 lb

Table 3.6-2 LO2/LH2 LRB Performance Summary with P/A Module

Program Phase	Groundrules and Assumptions
General	<p>All Costs are in Constant 1987 Dollars</p> <p>Government Factors Included</p> <ul style="list-style-type: none"> - Government Support 5% - Management Reserve 25% - Contractor Fee 10% <p>No Discounting Used</p> <p>No SRB Transition Cost Impacts Included</p> <p>No SRB Flights Delayed or Cancelled</p>
DDT&E	<p>Ground Test Hardware Includes GVTA, STA, MPTA, SETA, and Shock and Acoustic Test Articles</p> <p>Orbiter Mass Simulated for GVTA</p> <p>Engine's Mass Simulated for Shock and Acoustic Tests</p>
Production	<p>Capability Sized for Steady State of 28 Boosters per year</p> <p>Separate Learning Curves Identified for Specific Hardware Items</p> <p>Expendable Production Spares</p> <ul style="list-style-type: none"> - Engines 10% - Other Subsystems 6%
Operations	<p>10 Year Operational Program</p> <p>Ramp Rate 4,8,12,14 Launches; then 14 per Year</p> <p>122 Flights Total (244 Boosters)</p> <p>KSC and JSC Operations Excluded (Expendable)</p> <p>KSC Impacts Included for Recovery Operations</p>
Facilities	<p>Sized for Steady State of 14 Flights per Year</p> <p>Booster Manufacturing Facilities Reflect MAF Shared Facility Costs</p> <p>MPTA, SETA, and Engine Component Tests at Stennis</p> <p>STA, GVTA, and Modal, Shock, and Acoustic Tests at MSFC</p> <p>KSC Facilities Included</p>

Table 4.1-1 Programmatic Cost Groundrules and Assumptions

	Expendable STE	Partially Reusable STE	Partially Reusable SSME-35
Attrition (% of Reusable Hdw.)	-	0	0
Production Learning % (Engines)	85	95	95
Refurb. Learning	-	90	90
Refurb. Factor (% of New)			
-Engines	-	30	25 *
-Avionics, MPS, Structures	-	33	33
Initial Spares (%)			
-Engine	5	10	*
-Other	6	10	10
Aft Section Recovery %			
-Engine	-	100	100
-Structure	-	100	100
-MPS	-	100	100
-Avionics	-	100	100
-Chutes	-	0	0
Service Life (Flights)			
-Engine	1	15	10
-Other (Reusable Hdw.)	1	15	15
Engine Quantity	976	65	120
DDT&E Reusable Impacts (%)			
-Engines	-	3	N/A
-Structures (Reusable)	-	8	8
-MPS (Reuseable)	-	10	10
-Avionics (Reusable)	-	10	10

* SSME-35 Spares Are Included In Refurbishment Factor

Table 4.1-2 LH2 LRB P/A Module Recovery Assumptions

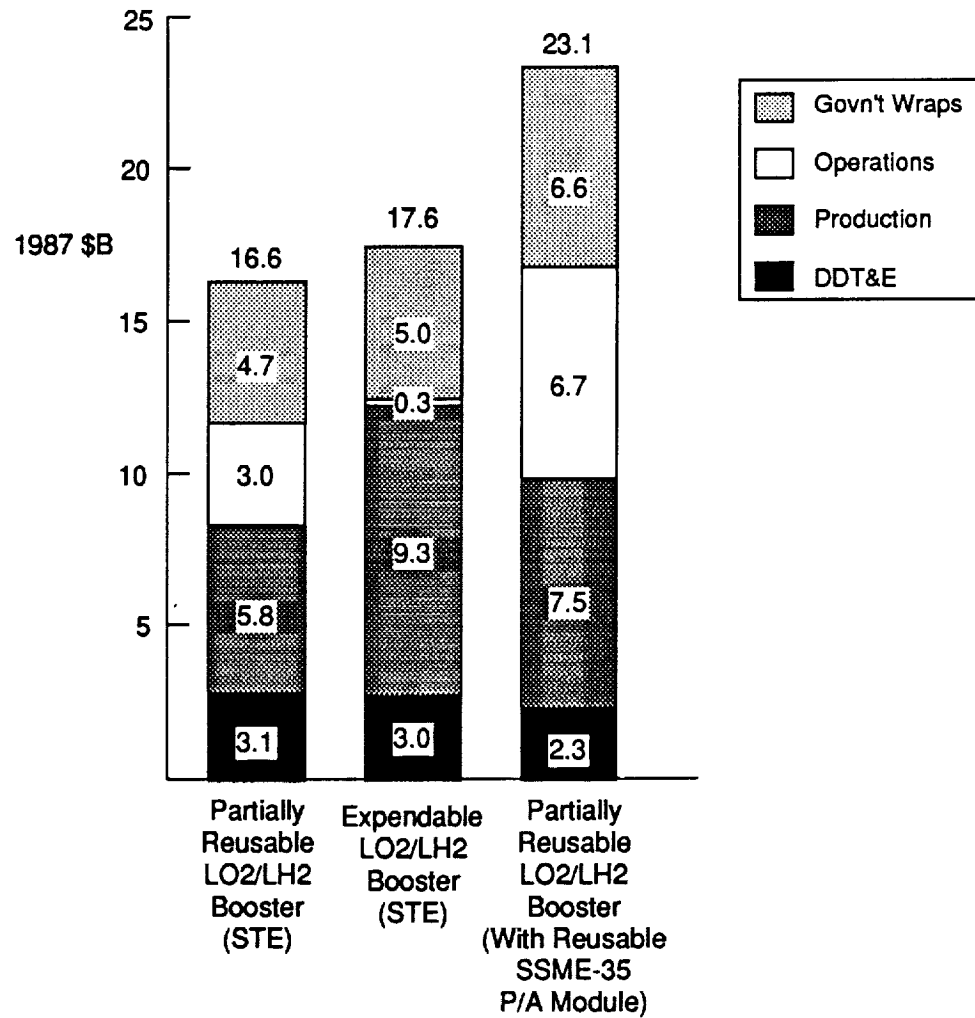
values for each variable used in evaluating both the expendable and reusable LO2/LH2 LRBs. The baseline values for the reusable STE and SSME-35 equipped boosters are the same except in the engine refurbishment and service life factors. The primary discriminators between the engines is that there is a large experience base for the SSME engines whereas the STE engines lack that experience based data. With an indefinite engine concept, many of the parameters can still be defined, hence the engine contractor inputs for the STE values are different than the SSME-35.

The recovery assumptions provide the framework to begin analyzing recoverable booster concepts. Sensitivities to the key assumptions are provided after the results section. The sensitivities allow the impacts of alternate assumptions to be understood. As much as possible, each of the variables were defined in a discrete fashion. But, the major problem is that there is a limited amount of historical data by which the variables can be substantiated. Because of a limited reusable historical database, our assessment may be conservative. To date, the effects of water impact loads and saltwater corrosion on the engines and other hardware are not well understood. Further analysis or testing is required to determine the condition of the hardware after recovery before one can substantiate the assumptions used in this analysis. Other assumptions can be made to improve or degrade the attractiveness of recovery and reuse. The sensitivities data that follow the discussion of results are aimed at assisting reevaluation when alternate assumptions deviate from our baseline assumptions.

In comparing similarly equipped boosters, the total LCC (Figure 4.1-1) savings provided by the STE reusable booster is \$1.0B constant year dollars (approximately 6% of the LCC). Comparing an expendable STE and reusable SSME-35 engine puts the recovery analysis on an unequal footing by comparing known engine costs with predicted engine costs. However, the analysis is valuable in assessing recovery of more expensive engines. As latter sensitivities will show, if expendable and reusable STE estimates grow at the same rate, reusable systems become more advantageous. Additionally, if STE estimates double, the SSME-35 P/A module is economically viable. While this analysis only included pump-fed boosters, it is believed that the pressure-fed booster could provide more reusable systems than the pump-fed booster. In addition to recovery and reuse of the propulsion and avionics systems, the thickness of the pressure-fed structures offers significant potential for total booster reuse which will amount to additional LCC savings. A recoverable pressure-fed booster may provide the lowest cost system at minimum risk.

The baseline expendable LO2/LH2 booster was evaluated against two reusable P/A module vehicle concepts that differed in engine type (STE and SSME). Due to the low probability of reusing pump-fed LRB hardware forward of the aft booster skirt, the P/A

- LCC Represented For Three Point Designs
- SSME-35 Engine Costs Account For The Difference Between Reusable Boosters



Reusable LCC is Less Than Expendable For Comparably Equipped Boosters

Figure 4.1-1 LRB LH2 Booster LCC

module concept was developed by outfitting the expendable booster with an aft skirt recovery system. A separation system at the aft skirt/fuel tank assembly was added to allow recovery of the aft booster section which houses the engines and parts of the main propulsion, power, and avionics systems. The remainder of the booster, including the tankage and forward structures is expended. This P/A module approach to recovery provides three desirable benefits. First it allows a reduction in the size of the deceleration system when compared to complete booster deceleration. Second, it minimizes saltwater corrosion by bringing the recovered aft section (propulsion/avionics module) on board the recovery ship to receive an immediate fresh water wash. And third, the approach minimizes the handling and disposal of non-reusable hardware. The recovered aft section is returned to the launch site for disassembly, component packaging, and shipment to the hardware component's refurbishment depot. Refurbished parts reenter the booster manufacturing cycle in a fashion similar to new parts.

As mentioned above, P/A module reusability for two different engines was examined. The first is a conceptual space transportation engine (STE) and the other is the SSME-35, a derivative of the space shuttle main engine (SSME). The STE assessment shows the same trends found during the LO2/RP-1 booster reusability trade study performed in 1988. There is a 6%-10% LCC benefit for comparably equipped reusable systems. For the SSME-35, a reusable system becomes attractive if current STE cost estimates double. The SSME-35 P/A module is an interesting design point because the SSME costs are based on actuals, whereas the STE costs are based on estimates.

Although earlier recovery trades showed the same 6% to 10% cost savings, expendable boosters were selected based on the relatively small magnitude of the savings and the risks associated with the maintainability, safety, reliability, and the validity of reusable assumptions. Key recovery/reusability assumptions included: production and refurbishment learning rates, refurbishment cost as a percentage of unit cost, service life, and attrition.

The average unit cost per flight (exclusive of the 40% program wraps) is detailed in Table 4.1-3. The P/A module concepts are titled 'partially reusable' to emphasize that the tankage and forward part of the boosters are expended each flight. For the partially reusable concepts, all reusable hardware is amortized over 15 flights except the SSME-35s which are amortized over 10 flights (SSME groundrules). The production and operations costs for each concept are represented to quantify the refurbishment effort. Recovery operations at KSC are also included in the estimates.

The unit cost for the STE is based on Aerojet inputs to the LRB phase II study. The SSME-35 unit cost is based on current SSME costs projected into the 1995-2000 time-

	Expendable STE	Partially Reusable STE	Partially Reusable SSME-35
Amortized Production Cost (Per Booster Flight)	244 Units	24 Units	24 Units
Structures/TPS	5.9	4.6	4.8
Propulsion	3.0	2.5	2.6
Power	1.2	1.2	1.2
Avionics	6.4	2.3	2.7
Engines (4 STE, 5 SSME-35)	15.1	3.6	9.6*
Recovery	0.0	0.9	0.9
Assy. & Check Out	1.7	2.2	2.6
Program Support	5.0	6.5	5.9
Total	38.3	23.8	30.3
Operations Cost † (Per Booster Flight)			
GSE	0.3	0.3	0.3
Propellant	0.3	0.3	0.3
Structure Refurb.	0.0	0.5	0.5
Propulsion Refurb.	0.0	0.3	0.3
Power Refurb.	0.0	0.0	0.0
Avionics Refurb.	0.0	1.9	1.9
Engine Refurb.	0.0	7.1	22.4
Recovery Ops.	0.0	0.2	0.2
Disassembly Ops.	0.0	1.6	1.8
Total	0.6	12.2	27.7
Avg. Unit Cost Booster/Flight (\$M)	38.9	36.0	58.0

* Amortized Over 10 Flights

† At 14 Recovery Cycles Per Year
(28 P/A Modules Per Year)

Table 4.1-3 LH2 LRB P/A Module Average Unit Cost Per Flight

frame. SSME-35 average unit cost without the LRB Program is estimated at \$26M. The additional engines required for the LRB program would drive unit costs to \$19M. SSME refurbishment is based on current actuals - approximately \$5M per engine flight (9 refurbishment cycles per engine). An important distinction between the booster concepts is that the STE booster has only 4 engines whereas the SSME-35 booster has 5 engines. Also the STE engine service life is 15 and the SSME-35 is only 10. Should the SSME service life increase to 15, the LCC estimates for this concept would be further reduced.

The technical definition of our reusable boosters attempted to minimize acquisition costs by limiting the hardware additions to the recovery and separation systems (i.e., no retro rockets). Additionally, we assumed maximum utilization of existing SRB recovery facilities and support equipment. This accounts for the minor DDT&E impact for the reusable booster concepts. The SSME-35 P/A module realizes the lowest DDT&E estimates because of the small magnitude of the engine development costs (roughly 25% of new engine development). The nozzle of the current SSME must be redesigned in the SSME-35 for an alternate expansion ratio to optimize for sea-level operation. Other DDT&E impacts include an 8% additional cost for development and testing of reusable structural hardware, 10% more for both avionics and propulsion hardware, and 3% greater costs for reusable STE development.

4.2 RECOVERY COST SENSITIVITIES

The recovery cost sensitivities are included to point out that any number of changes to the baseline assumptions can have a significant impact in the outcome of the recovery analysis. These sensitivity analyses show crossover points where the selection of an alternate assumption changes the attractiveness of reusability. These sensitivities are not exhaustive, but indicate the potential for the recoverable cost estimate to vary with respect to the expendable booster estimates when the values of key variables change.

4.2.1 STE Cost Growth Sensitivity

Figure 4.2.1-1 identifies the cost trend for increases in the Space Transportation Engine (STE) estimates. As engine cost estimates increase at a constant rate, the trend between expendable and reusable STE equipped boosters is in favor of reusable boosters. As STE estimates quadruple, the potential savings increase from the baseline 6% to 10%. The SSME-35 estimates are based on a known engine cost and past performance. The estimates for that engine are assumed constant. The STE equipped boosters exhibit a greater LCC than the SSME equipped boosters at approximately two times the current STE

- Recoverable SSME-35 P/A Module Concept Is Economically Viable If New STE Estimates Double
- Recoverable STE P/A Module Booster LCC Is 6-10% Less Than A Comparable Expendable Booster

Booster Configurations (244 Boosters)	
Expendable STE	
4-Engines/Booster	
976 Engines	
Reusable STE	
4-Engines/Booster	
65 Engines	
(STE Service Life 15)	
Reusable SSME-35	
5-Engines/Booster	
120 Engines	
(SSME-35 Service Life 10)	
(SSME-35 Cost	
\$6.9M/Engine/Flight)	

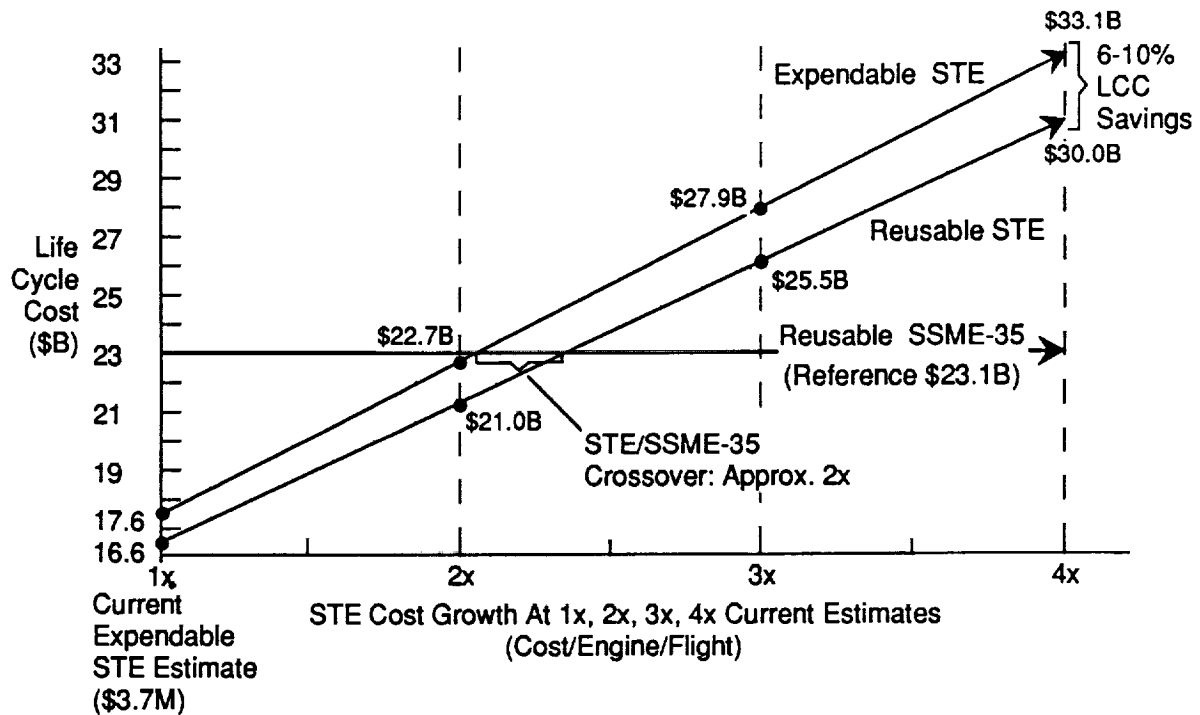


Figure 4.2.1-1 LRB LH2 Booster Expendable vs. Reusable LCC

estimates. This analysis indicates that the SSME-35 P/A module may be an economically viable concept if STE estimates double.

4.2.2 LCC Sensitivity Service Life

Figure 4.2.2-1 highlights the sensitivity of the reusable STE LRB estimates to booster service life (i.e. the number of times a P/A module can be refurbished and reused). The expected service life will determine the number of reusable elements required to service a finite number of uses by refurbished elements. Reusability becomes more attractive than expendability at 7 or 8 reuses. The analysis demonstrates that under the groundrules and assumptions of the LRB study, a service life of 20 to 25 flights is adequate and that further improvements in service life provide diminishing cost benefits.

4.2.3 LCC Sensitivity: Refurbishment Factors

The refurbishment requirements of an LRB include the recovery of the boosters, disassembly, inspection, refurbishment and reassembly. The amount and condition of the hardware recovered determine the advantages of reusing the element. An airline mission offers a fairly benign recovery method and thus very little flight to flight refurbishment is required. The P/A module experiences a fairly severe recovery environment with the combination of water impact loads and salt water corrosion. The sensitivity analysis of LRB LCC to the amount of refurbishment shows the breakeven point for reusable systems at 40% of initial unit cost (Figure 4.2.3-1). Any improvement in the refurbishment profiles would obviously further enhance the attractiveness of reusable LRB concepts. The baseline estimates for the STE booster recovery analysis were made based on 33% for avionics, structures, and propulsion ; and 30% for engines.

4.2.4 Attrition Sensitivity

It is important to clarify the definition of attrition as it is used here. Attrition is irreparable damage to hardware that is anticipated for later reuse. For both P/A module concepts, only the aft end is anticipated to be reused. The entire forward part of the booster is completely expended including: tanks; skirts; TPS; and portions of avionics, power, and propulsion systems. Therefore, the forward part of the booster is not considered attrition hardware but is expendable hardware.

In addition to defining attrition, it is important to distinguish it from recovery probability. The terminology is sometimes misunderstood. The term recovery probability

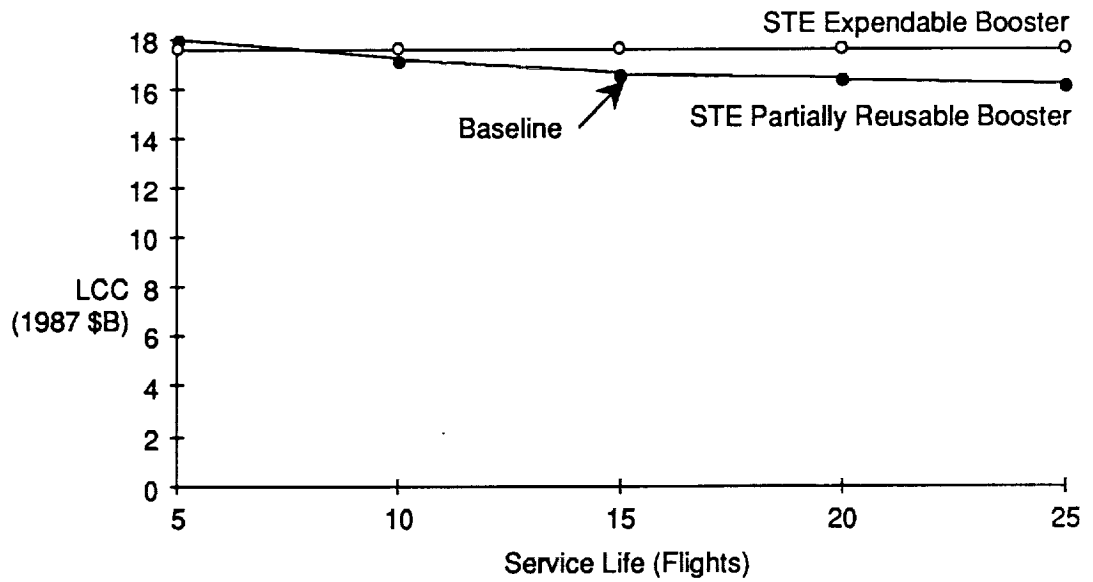


Figure 4.2.2-1 Service Life

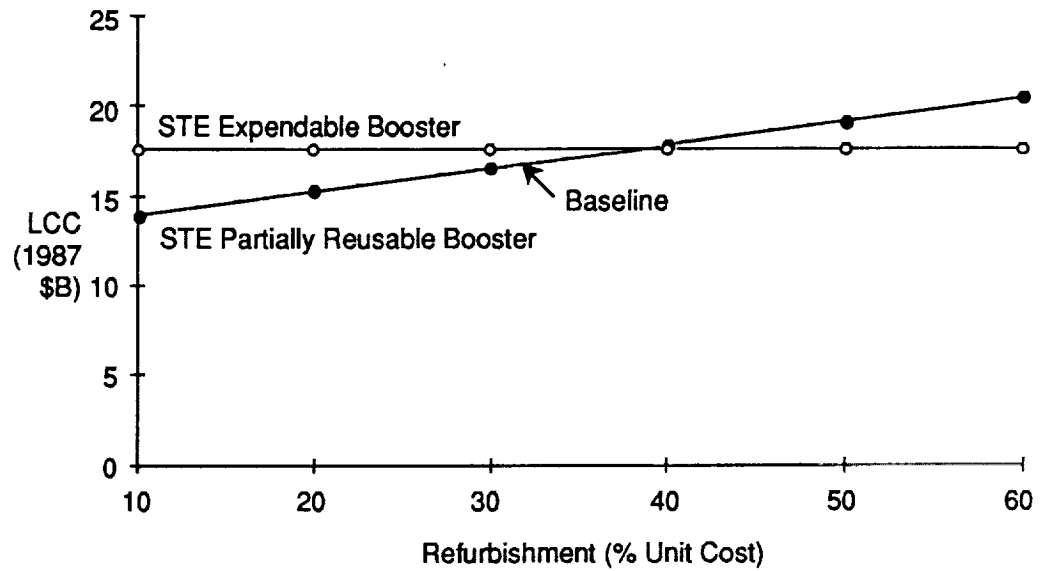


Figure 4.2.3-1 Refurbishment

cannot be equated to attrition. The following example will distinguish the two terms and the resulting differences. The example below simplifies the analysis by not considering on which specific mission an engine is lost (i.e., on its first or last mission). It emphasizes the point that widely different hardware quantities result depending on the methodology employed. For this example, 72 engines are required considering 10% 'attrition' of reusable hardware (7 attrition units) and 165 engines are required if 90% recovery probability is assumed (100 engines lost).

EXAMPLE:

- **Attrition = 10% of reusable hardware.**
 - Assuming no attrition and 15 flights / engine, 65 engines are required to make 975 engine flights.
 - With 10% reusable hardware attrition 6.5 engines are or not reusable.
($65 \times 10\% = 6.5$)
 - When rounded up, this equates to a loss of 7 engines
 - Total engines requirement is 72 units. ($65 + 7 = 72$)
- **Recovery = 90% Probability**
 - This assumes that 10% of the 244 booster are not recovered (or reusable)
 - This says that 24.4 P/A modules are not recovered.
($244 \times 10\% = 24.4$)
 - When rounded up, this equates to loss of 100 engines
($25 \times 4 \text{ engines/P/A module} = 100$)
 - Total engine requirement is 165 units. ($65 + 100 = 165$)

Figure 4.2.4-1 shows that even at a 20% hardware attrition rate, the LCC for the reusable concept is lower than the expendable concept. The crossover point is reached between 25 and 30%. The 30% hardware attrition rate increases the engine requirements from 65 to 85 units. Should one consider the recovery probability at 90%, over 165 engines would be required. Thus calling into question the attractiveness of reusability.

4.3 COST SUMMARY

Recovery offers a 6%-10% LCC savings over comparably equipped (STE engines) boosters, using the current groundrules and assumptions. Further testing and

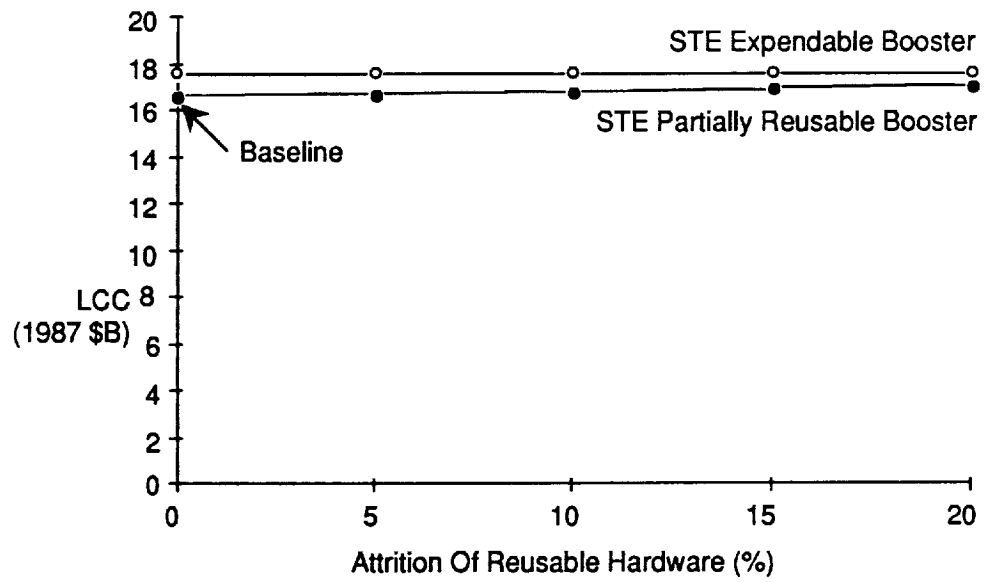


Figure 4.2.4-1 Attrition of Reusable Hardware

evaluation must be performed to substantiate the assumptions since small changes in the reusability assumptions can alter the outcome of the analysis. The assumptions regarding the water impacts and subsequent reusability are poorly understood at this time and should be verified through testing.

While this recovery analysis only covered pump-fed boosters, it is believed that the pressure-fed booster could provide more inherently reusable systems than the pump-fed booster. In addition to recovery and reuse of the propulsion and avionics systems, the thickness of the pressure-fed structures offers significant potential for total vehicle reuse which will amount to additional LCC savings. A recoverable pressure-fed booster may provide the lowest cost system at minimum risk.

In examining the new engine cost parameters, we found that the benefits of reusability tend to grow as engine costs increase. The SSME-35 P/A module concept is based on an existing engine and is an economically viable alternative to a new STE P/A module if current STE estimates double (to approximately \$7.4M per unit). The SSME-35 engine requires the lowest development effort (and cost) and could offer a near term reusable LRB engine option if schedules demand.